Rendering Spatiotemporal Mid-Air Tactile Patterns

William Thierry Alain Frier
PhD
University of Sussex

2015-2019

Acknowledegments

I would like to thank the numerous people who have supported me through my PhD studies. The present manuscript would never have been possible without you all. The following list may not be exhaustive, and I apologise to the people I will miss.

In particular, I would like to thank my supervisor, Professor Sriram Subramanian. I am honoured to have worked with Sri and feel that in his presence I have developed as many personal skills as I have research skills. He helped me see through the numerous obstacles I encountered during my studies, but most of all, he entrusted me and gave me the freedom necessary to grow.

In addition to Sriram, I am in debt to Thomas Carter and Steve Cliffe. All three were crazy enough to bet on me and helped me through starting the PhD adventure.

I am gratefull to my colleagues at Ultrahaptics: SueAnn Seah, Benjamin Long and Orestis Georgiou. I have looked up to you over the years and will still be doing so many years from now. This thesis would have probably never existed if I had not had the chance to benefit from our regular exchanges and your frequent feedback.

I am thankful to my wonderful lab mates at the Interact Lab, as well as to the members of the Schilab, with whom I spend my days (and more during the deadlines). Working would not have been as much fun without you all.

I would also like to say a special thank you to Damien Ablart, fellow PhD student, flatmate and above all, friend. The PhD experience would have not been what it was without you. Whether it was at university or at the maquis, it was an absolute pleasure to share my PhD years with you.

I would like to thank my friends, new and old. There are too many names to cite here, but all of you have contributed to some extent to this thesis. No one can go through life without a good laugh, so thank you for keeping me smiling over the years.

Finally, I am grateful to my family, who I would like to thank in my mother tongue. Lise, continue comme tu es, la meilleure des soeurs. Papa, Maman, je sais que je suis loin de la maison, et que parfois ce n'est pas facile, mais il n'y aucun

doute que si aujourd'hui je suis qui je suis, c'est grâce à vous. Si je n'avais qu'une chose à vous dire ce serait "Merci !".

UNIVERISTY OF SUSSEX

PHD DEGREE

RENDERING SPATIALLY DISTRIBUTED MID-AIR HAPTICS PATTERNS

SUMMARY

Mid-air haptics is a recent field concerned with conveying haptic feedback in mid-air to complement 3D interfaces which are already integrating gesture tracking or volumetric displays. While the community has mainly spent the last decade focusing on the technical challenges of developing a mid-air haptic display, little attention has been spent on haptic pattern-rendering techniques. The work presented here targets this last consideration and investigates the perceptual implications of varying the parameters of a recently developed rendering technique called spatiotemporal modulation.

The technique aims at producing spatially distributed mid-air haptic patterns, by rapidly and repeatedly moving a tactile point along a given pattern path. However, it is unclear how the rendering parameters affect skin deformation and haptic perception. In addition, especially when two parameters are interdependent, it is unclear which should be optimised.

In the first study, I used vibrometry to compare the effects of pattern-rendering speed (i.e. the speed at which the tactile point moves along the pattern) and rendering rate (i.e. the rate at which a given pattern is repeated) on skin displacement. The study highlights the importance of rendering speed over rendering rate in maximising the skin displacement. A user study showed later that rendering speed also maximised pattern perceived strength, corroborating that increased displacement leads to increased perceived strength.

A second user study investigated the importance of the pattern sampling rate (i.e. the sampling position number along a pattern) while rendering a given mid-air haptic pattern. The results show that decreasing the sampling rate enhanced the

pattern strength, especially for patterns rendered at a rate of under 20 Hz. These results also allow the unlocking of low rate stimuli that could not be perceived with the traditional sampling approach.

In each of these studies, the discoveries are summarised in comprehensive guidelines, so designers can benefit through an implementation of my results in their design of mid-air haptic patterns.

Contents

List of Figures

List of Tables

Chapter 1

Introduction

For a long time, human-computer interactions (HCI) was synonymous with bulky mechanical controls such as buttons, sliders and knobs. With the spread of personal computing, these controls have evolved into user-friendly interfaces such as keyboards, computer mice and, more recently, touch screens. The development of these new interfaces has always been aimed at making the interaction with a computer more natural and intuitive to the user. Ultimately, such interfaces are proxies for interacting with virtual content. Free-hand interaction is one that is natural and intuitive, in other words, an interaction through which the user can use their bare hand to touch and manipulate content. The recent progress in gesture tracking technologies (e.g. Kinect, Leap Motion) and three-dimensional displays (Konrad and Halle [2007], Holliman et al. [2011], Geng [2013]) enables such interactions. Taken together, gesture tracking and three-dimensional displays, have brought today's interfaces one step closer to the ultimate display, Sutherland envisaged in the 1960s. Now, interaction can take place entirely in mid-air as it is depicted in science fiction movies such as Iron Man or Minority Report.

Still, interactive three-dimensional displays and Sutherland's ultimate display differ on a major point: the ability to feel the virtual elements one is touching. To overcome this issue and make the new generation of interfaces completely natural and intuitive to the user, haptic feedback is required. Across a whole range of interactions, from complex tasks like laser microsurgery (Fichera et al. [2016]) to simpler tasks such as text entry (Lee and Zhai [2009], Ma et al. [2015]), haptic feedback has been shown to improve user performances. With this fact in mind, researchers have strived to develop a device capable of conveying the sense of touch in mid-air. For a while wearable devices (Pacchierotti et al. [2017]) were used as a compromise. However, requiring users to be augmented with some form of apparatus goes against the principle of free-hand gesture and was seen as a drawback. This

pushed researchers to renew their effort in developing entirely contactless haptic displays.

Their investigations lead to the development of a plethora of mid-air haptic display technologies. Among them ultrasonic phased arrays (UPAs) stand out and are becoming the prevailing technology in the field. The reason for this growing popularity is the relatively small extent of the feedback (under 1 cm) and the high time resolution (update rate of up to 40 kHz), as well as the ability to create multi-point feedback. However, ultrasonic frequencies are greater than the frequency relevant to touch, and therefore the tactile point produced with UPAs needs to be modulated. This can be achieved by using various modulation techniques. Two of these techniques - amplitude modulation (AM) (Hoshi et al. [2010]) and lateral modulation (LM) (Takahashi et al. [2018]) - share a common parameter space. Amplitude modulation and lateral modulation perceptual space have been investigated through numerous user studies (e.g. Obrist et al. [2013]). These modulation techniques show common points with vibrotactile stimuli as they produce localised stimuli. To convey distributed patterns, one needs to produce several mid-air tactile points, which can lead to power issues for higher numbers of points (Long et al. [2014]). More recently, spatiotemporal modulation (STM) has extended the advantages of ultrasonic mid-air haptics with the ability to produce spatiotemporal stimuli (Kappus and Long [2018]). This new technique overcomes the drawbacks of previous techniques in rendering distributed patterns and hence offers a paradigm shift compared to traditional vibrotactile stimuli, with a completely new and un-investigated parameter space. It is the aim of this thesis to explore this space and provide useful haptic design considerations and insights.

To understand the extent of ultrasonic mid-air haptics perceptual space, and use it in interactive 3D-displays, one needs to rely on perceptual research on mid-air haptics. However, like haptics in general, mid-air haptics is a young field spanning across many research domains and involving extensive knowledge in each one of them. Despite the recent progress in the field, little is known about the perception of mid-air haptics, even less than about haptics, which has slowed the adoption of the technology in HCI aimed at the general public. For the wider field of haptics, Schneider et al. [2017] have highlighted this lack of knowledge as a real challenge for haptic experience designers (HaXDs). As stressed in their study, the multidisciplinary nature of haptics makes the relation between device output and users' perception opaque to the designers. Indeed, haptic perception involves the common effort of at least three domains of research: 1) biomechanics, 2)neuroscience and 3) psychophysics. Each of these domains is involved at different stages of human haptic

information processing. First, biomechanics describes how the skin, and each of its layers, became deformed in the presence of a tactile stimulus. Then, neuroscience determines how human touch receptors, referred to as low threshold mechanoreceptors (LTMRs), encode and process skin deformation and by extension, tactile information. This encoding is made through spike trains travelling along the nerve from the LTMR to the central nervous system (CNS). Finally, psychophysics studies the relation between tactile stimulus and one's perception of this stimulus. Mid-air haptics adds non-linear acoustic to the picture, increasing one notch further the multidisciplinary complexity of mid-air haptic perception. Given these intricacies, HaXDs rely on clear guidelines to tailor mid-air haptic feedback to the interaction. However, the field is not mature yet, and the guidelines for HaXDs are too sparse, and many studies on mid-air haptics perception are still needed. This last fact limits the integration of ultrasonic mid-air haptic displays to current HCI applications targeted at the general public.

This motivated the current thesis, which aims at being one of the pioneering works on ultrasonic mid-air haptic perception, and especially on the perception of spatiotemporal patterns. In other words, the work presented here investigates the relationship between ultrasonic mid-air haptics parameter space and its corresponding perceptual space. It is divided into five distinct chapters articulated as follows.

First, in Chapter 2, we present the current understanding of touch. Hence, the chapter includes a comprehensive review of the scientific community knowledge on tactile perception. The review starts with a brief introduction to the sense of touch and how it can be divided into different components such as proprioception (one's perception of movement), tactile perception (one's perception of skin deformation) and thermoception (one's perception of temperature), as well as the different common usage of our sense of touch. Due to the nature of the interaction of tactile perception with ultrasonic mid-air haptic displays, the rest of the chapter mainly focusses on tactile perception. Finally, the chapter details the different stages of tactile perception, from skin deformation after a tactile stimulus occurrs to the interpretation the brain makes of this stimulus. We refer to the former as Tactile Sensation and the latter as Tactile Perception, and discuss them further into two distinct sections. The information developed in this chapter is notably relevant to better understanding the extent of the haptic perceptual space, and will be essential, when applied to mid-air haptics, as well as the rest of the work reported in this thesis.

In Chapter 3, we assess the stimulation capabilities of the current state-of-the-art mid-air haptic displays. As stated previously, there is a plethora of displays, from air-

based displays, to laser-based displays and going through electrical-based displays. We describe each technology and compare one to another in section 3.1. From this comparison, we determine that the UPA is the most appropriate technology for our purpose. Due to this, the chapter then goes into further detail about the working principles of UPAs. In addition to presenting the approach to creating a tactile point in mid-air using ultrasound, the corresponding sections describe the distinction between various modulation techniques that are commonly used to produce mid-air haptics stimuli. These techniques can be divided into two kinds, one localised and similar to vibrotactile stimuli (i.e. AM and LM), and one distributed based on spatiotemporal stimuli (i.e. STM). In the following section, we define mid-air haptic patterns as being the combination of a shape (i.e. geometry) and a sensation (i.e. feelings), and review related work on both rendering mid-air haptic shape and mid-air haptic sensation. This review helps us to focus our efforts on shape rendering using STM and especially on maximising the perceived strength of these shapes. Furthermore, drawing on Plaisier et al. [2009]'s results, which showed that shape recognition relies mainly on edges and vertices, we will focus only on rendering shape outlines. Finally, at the end of the chapter, we discuss the different approaches to evaluating ultrasonic mid-air haptics rendering capabilities and the perceived strength of the rendered patterns.

These first two chapters paint a picture of mid-air haptics perception, from the input specified by the designers (i.e. parameter space) to the tactile perception experienced by the user (i.e. perceptual space). The different stages and components of the process are depicted in Figure 1.1 alongside reference numbers to the corresponding chapters and sections in which we discussed them into more details.

Chapter 4 presents our first study on mid-air tactile parameter space, in which we explore the effect of tactile point speed when rendering mid-air tactile patterns with STM. Traditionally, mid-air haptics patterns have been described based on the frequency parameters due to their connection with vibrotactile stimuli. However, in the case of STM, a pattern could be both described by a frequency parameter and a speed parameter. The former represents the number of times a pattern is repeated per second, while the latter represents the speed at which the tactile point moves along the patterns. Furthermore, we noted that both parameters were dependent as proportional to each other with the pattern size as a coefficient of proportionality. Using first vibrometry data and then user study data, we determined that mid-air haptic point speed could be optimised, independently of the pattern size, in order to maximise the pattern perceived strength. The user study pointed towards an optimal speed of around $7\,\mathrm{m\,s^{-1}}$. The entire results of this study have been

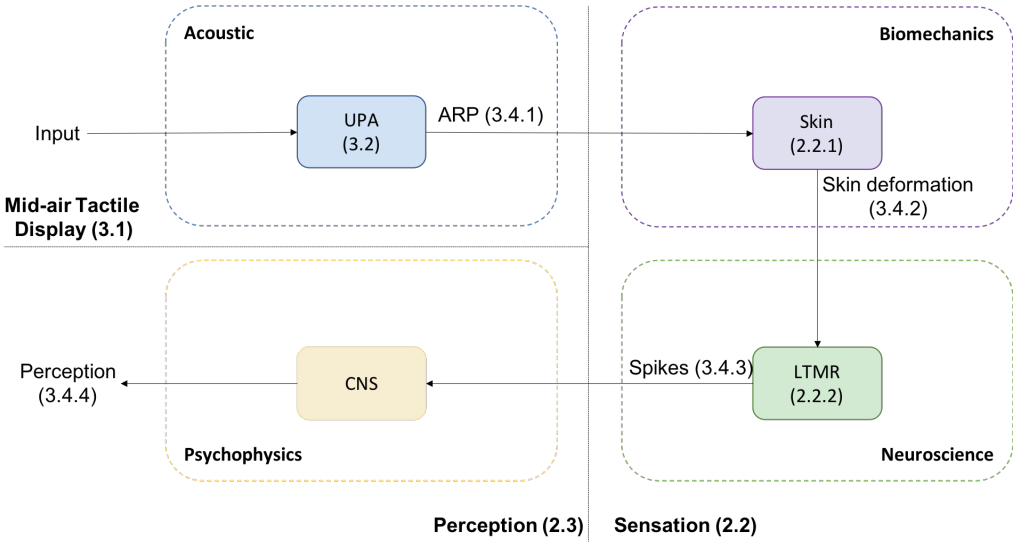

Figure 1.1: Mid-air tactile information processing can be divided into four steps, each relying on a different domain of research. Details about each of them can be found in the corresponding section.

presented at Eurohaptics 2018, DOI:10.1007/978-3-319-93445-7_24.

In Chapter 5 we investigate further the Spatiotemporal Parameter space. Based on the statement that all mid-air haptics stimuli are discrete rather than continuous, we investigated the effect of the sampling rate on users' perception. Surprisingly, we found that in some contexts, a lower sampling rate as opposed to a higher sampling rate helped users to perceive the pattern more strongly, while having no effects in other contexts. The contexts in which the sampling rate impinged on mid-air haptic perception were the instances where patterns were rendered at a low frequency (i.e. below 20 Hz). These observations were obtained from two distinct user studies in which the pattern's frequency, size and sampling rate were varied. While the studies did not point towards optimal sampling rate values that worked for each case, general guidelines were extracted to choose an appropriate sampling rate. Those guidelines, as well as the details of the results were presented at CHI2019, DOI:10.1145/3290605.3300351.

From these two previous chapters, and especially Chapter 5, the paradigm shifting nature of STM begins to unfold. Spatiotemporal patterns cannot be expressed using a similar parameter space as with vibrotactile stimuli. Therefore, in Chapter 6, we develop a new framework of research for mid-air haptic patterns. This new framework looks more closely into the physical quantities at play when the mid-air haptic point moves across the skin surface. For instance, it looks at the pressure applied to the skin and skin deformation over time, as well as the Fourier transform of those quantities. In the same chapter, initial measurements and results are pre-

sented and analysed using this new framework of research. Finally we define the next step to finishing the investigations initiated in the previous chapter.

Finally, in Chapter 7, we summarise the contributions and limitations of our work.

Chapter 2

The Sense of Touch

One perceives one's surroundings through one's senses. Traditionally, five senses have been defined: sight, hearing, touch, smell and taste. While touch is the only sense that puts one immediately in contact with one's world, it is largely understudied compared to sight and hearing. Nonetheless, touch has been the object of a growing interest in the scientific community over the past decades. Many studies have continuously expanded the knowledge about the sense of touch and have shown a light on the versatility and complexity of tactile perception mechanisms. In this first chapter, we briefly present the sense of touch and what makes it so complex. We further discuss the steps involved in tactile information processing from sensation (i.e. stimulus input) to perception (i.e. interpretation output).

2.1 The Sense of Touch

Touch is part of the five traditional human senses. However, it is more complex than one usually thinks. A simple action like grasping and lifting, a cup of tea is an excellent example to illustrate this complexity.

Through the pressure perceived at the fingertips, one knows when one's hand is ready to grasp and lift the cup. Through the shear forces perceived at the fingertips, one knows whether the grasp is stable and that the cup is not slipping through one's fingers. These same shear forces, being indirectly related to the cup's weight, will automatically let one know whether the cup is full or empty. Through thermal exchange between the cup and the skin, one will also be able to determine whether the tea is still too hot or good to drink. All this information results from simple contact between a cup and one's fingertips and the performance of one's sense of touch. But touch is also responsible for one's ability to distinguish between wood and laminate from a simple stroke, as well as one's ability to determine whether a

fruit is ripe enough to eat from a gentle squeeze. Being able to gather such a wide variety of information in a brief instant definitely proves both the importance and the complexity of the sense of touch.

In this section, we review the main attributes relative to tactile perception, and expose some mechanisms involved from the sensation to the perception of tactile information. A better understanding of these mechanisms is essential for the work reported here later on.

2.1.1 Touch is Part of the Somatosensory System

It has been shown that the sense of touch is actually part of a larger group of senses, referred to as the somatosensory system, and includes for instance itching and balance. What is commonly referred to as touch is also further divided into various components namely, tactile perception, proprioception, thermoception and nociception.

Tactile perception, also referred to cutaneous perception, is the part of touch concerned with skin deformations, either under normal force or under lateral stretch. Tactile perception, for instance, evokes sensations such as contact being made with the skin, but also processes information such as surface roughness and hardness.

Proprioception, or kinaesthesia, refers to one's ability to perceive the motion and the position of one's limbs. Proprioception is particularly solicited when manipulating objects, but can also determine information such as weight and stiffness.

Thermoception refers to one's ability to perceive temperature. Aside from determining temperature itself, thermoception involves differentiating between objects' surfaces (e.g. at room temperature metal feels colder than wood).

Nociception refers to one's ability to feel pain. Nociceptive information can come from both harmful contact such as a strong blow, or harmful temperature such as burning or freezing.

Each of these aspects of touch relies on a different set of receptors and perception mechanisms. Hence, studying touch as a whole is a complex endeavour and researchers usually concentrate their investigations on a single aspect of touch. Similarly, the work contained in this thesis focuses only on tactile perception.

2.1.2 Active and Passive Touch

Tactile perception is concerned with the perception of contact between the skin and its surroundings. Tactile perception is mainly used in two different ways: an active way where one's sense of touch is stimulated through one's own actions - *I'm*

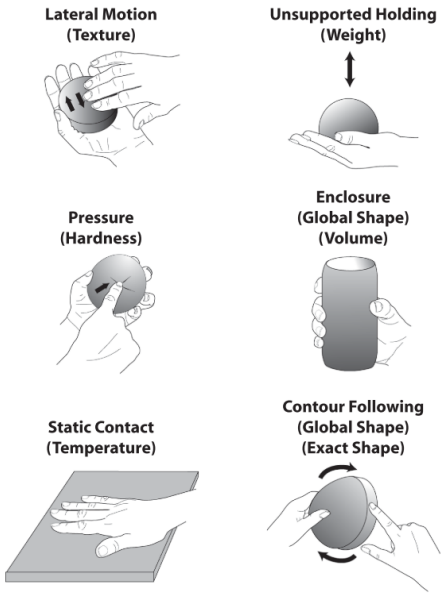

Figure 2.1: To extract tactile information, one uses up to six exploratory procedures (Lederman and Klatzky [2009])

touching this surface; I'm grasping that object. - and a passive way, in which one's sense of touch is stimulated unexpectedly - *something is touching me.*

The active way represents a scenario in which one interacts with surfaces or manipulates objects, while extracting tactile information about these surfaces and objects. The tactile information hereby extracted varies in nature, and includes for instance roughness, hardness and temperature. However, the nature of the various forms of tactile information being intrinsically different to one another, they are also extracted according to different strategies. For instance, to perceive a surface's roughness, one may rub one's fingers repeatedly across this surface, but when perceiving its temperature one may keep one's palm still against the surface. These different strategies have been studied and categorised by (Lederman and Klatzky [1987]). In their study, the authors showed that these strategies, referred to exploratory procedures, are common across people. They identified six exploratory procedures, namely lateral motion, pressure, static contact, unsupported holding, enclosure and contour following (Figure 2.1).

In the passive way, on the other hand, the surface (or object) touches one without one having any control over the nature and properties of the contact (e.g. applied load, motion speed). In active perception, this information arises from the proprioception aspect of the sense of touch. The lack of proprioceptive information in passive perception has been thought to impinge on perceptual performance. In other words, if one was rubbing a given surface on someone else's fingertips, the second person's ability to distinguish the surface is altered compared to if this per-

son were free to rub their fingers on the surface as they pleased. Some studies have investigated the differences in perceptual performances in the two scenarios. Even though these results seems to lean towards the formulated hypothesis, none of them significantly confirm that touch performances is lower in the passive condition (Lederman [1981], Yıldız et al. [2015]). This is particularly releavant to mid-air haptics studies, as it means mid-air haptic stimuli can be studied in either conditions and results apply to both conditions.

2.1.3 Discriminative and Affective Touch

Tactile perception is not limited to the ability to perceive the difference between contact or no-contact. Through a simple contact between the skin and a surface, our tactile sense is able to extract significant information about this surface, such as its roughness and hardness. One's ability to infer physical properties and to distinguish between them upon a simple contact is often referred to as discriminative touch. For example, discriminative touch is one's capacity to differentiate between a sturdy and rough plank of wood and a soft and fluffy blanket.

The hand, and especially the fingertips, is dense with low threshold mechanoreceptors (LTMRs; i.e. touch sensors embedded under the skin), which makes it the most acute organ, able to resolves spatial features as small as a millimeter (Gibson and Craig [2005]). Through complex perceptual mechanisms, the LTMRs can encode various information (see section 2.3.2). After an extensive literature review, Okamoto et al. [2012] concluded that the information touch process can be categorised according to four main dimensions: roughness, hardness, temperature and frictions. Knowing how these LTMRs encode information is crucial when one wants to reproduce these sensations and embed them in a virtual tactile feedback such as mid-air tactile patterns. Some of these mechanisms are described later in this thesis (see section 2.2.2). However, temperature perception is omitted as it relies on different receptors than cannot be stimulated through the current technology of mid-air haptic displays (see section 3.1).

The sense of touch is not limited to discriminative touch, and is also extensively used in social interactions for non-verbal communication between individuals. A gentle stroke or hard squeeze can often say more than words. This ability that touch has to convey emotional content is what one may refer to as affective touch. Affective touch is essential to human social development and the lack of touch in the early stage of development can lead in the future to antisocial behaviour. Affective touch perception rely mostly on nerve endings present on hairy skin (i.e. the whole body except the palm and sole). These receptors are mainly sensitive to motion and

temperature (McGlone et al. [2014]). Nonetheless, as affective stimuli are learned since the early stages of development, some of them can still be perceived on glabrous skin using discriminative touch mechanisms. This is particularly relevant to mid-air haptics as it means that mid-air tactile patterns, targeted to the palm, can potentially be augmented with emotional cues.

Even though discriminative and affective touch rely on different perceptual mechanisms, understanding their mechanisms is crucial to designing adapted rendering algorithms for mid-air tactile patterns.

2.1.4 Sensation and Perception

Tactile information processing happens in a succession of different steps. These steps can be divided into two distinct groups. On the one side, there is sensation, the physical phenomenon which yields to touch perception. On the other side, there is the perception, the interpretation the central neural system (CNS) makes of the sensation. Sensation and perception rely on complex mechanisms. Not all sensations are perceived, and two similar sensations can lead to different perceptions. Both aspect have been studied either together or separately. The next part of this chapter further detailsthe mechanisms involved both at the sensation stage and perception stage.

2.2 Tactile Sensation

Touch is capable of extracting a wide range of information. Understanding how the sense of touch actually processes tactile information will provide insights on designing appropriate mid-air tactile patterns. A tactile stimulus, or tactile sensation, arises from the skin deforming when it makes contact with a given surface. Upon contact, the skin deforms differently, depending on the surface's properties. This deformation then stimulates LTMRs embedded under the skin, which encode the tactile information (i.e. deformation) into electrical activity (i.e. spikes) that travel on nerve afferents in the direction of the CNS..

In this section, we discuss how skin deformation can be predicted, and how LTMRs encode tactile information.

2.2.1 Skin Mechanics

When touching a surface, the skin deforms due to the load applied at the contact location. However, the skin being a complex viscoelastic medium, made of several

layers, predicting how the skin deforms in a given scenario is a difficult task. Researchers have long sought a relation between a surface's physical properties and skin deformation.

To approach the problem, researchers have first undertaken to characterise the skin's mechanical properties, and then to develop equations or models predicting skin deformation in increasingly complex scenarios.

Skin properties

Before trying to predict skin deformation in a given scenario, it is important to understand the skin properties.

First, the skin is composed of two different layers. The first layer, the epidermis, is about 0.104 mm thick at the fingertips, while the second layer, the dermis, is about 1.157 mm thick at the fingertips (Wagner et al. [2008]) It is important to note, that the skin is bounded to the bone, often represented as a third rigid layer. The epidermis and dermis are viscoelastic, but posses different viscoelastic properties.

Overall the skin acts as a viscoelastic medium. Wiertlweski determined that the skin presents a dominant elastic behavior for vibratory stimuli of up to 100Hz but that above this frequency, the viscous part dominates (Wiertlewski and Hayward [2012]). Due to its viscosity the skin takes time to deform and therefore the contact area with a surface grows over time, even long after the contact has been made. Such observations have been measured by Dzidek et al., who also discuss the influence of such phenomena on friction perception (Dzidek et al. [2016]). Similarly, skin viscous properties also affect skin relaxation time (Wang and Hayward [2007]). Table 2.1 presents some estimates of the skin's mechanical properties for the fingertips. However, even though the skin's properties have been measured repeatedly, results range widely due to variance between individuals. Such variance has been explained according to different factors such as age, sex and occupation.

Although the skin is often assumed to be homogeneous and isotropic to simplify computations, the presence of many organs, tendons, fat and so on, makes the skin a medium far from homogeneous. Additionally, it has been shown that the skin is not isotropic, and therefore deforms differently according to the direction in which the load is applied. We refer the reader to Derler and Gerhardt [2012] for more details on skin tribology.

Continuum mechanics and numerical analysis

To estimate the skin deformation according to the force applied, one can use Hooke's law.

Table 2.1: Skin viscoelastic properties at the fingertip

Skin properties	**Averange-Range**
Stiffness (Wiertlewski and Hayward [2012])	$0.6\,\mathrm{kN\,m^{-1}}$ to $2\,\mathrm{kN\,m^{-1}}$
Elasticity (Young modulus) (Dandekar et al. [2003])	0.18 MPa (epidermis)
	0.018 MPa (dermis)
Viscosity (Wiertlewski and Hayward [2012])	0.75 - $2.38\,\mathrm{N\,s\,m^{-1}}$
Poisson's ratio (Wu et al. [2004])	0.4
Friction coefficient (Zhang and Mak [1999])	0.46

$$\sigma = E\epsilon \tag{2.1}$$

where σ is the static force, or stress, applied to the surface, E the medium Young's modulus and ϵ the resulting deformation, or strain produced.

However, skin deformation extends beyond the immediate location on which the load is applied and the Hertzian theory of contact captures how the skin deforms beyond the contact area.

Using both Hooke's law and Hertzian theory, as well as skin properties, one approach to predicting skin deformation is to use the laws of continuum mechanics and solve them analytically. Sripati et al. [2006] used this approach and applied it to the whole fingertip, enabling them to predict deformation induced by a given static load pattern. However, such an approach cannot be extended to dynamic load, due to the skin viscosity part becoming predominant, especially above 100 Hz (Wiertlewski and Hayward [2012]). The literature is abundant in models characterising viscoelastic behaviour (e.g. maxwell, kelvin Voigt, Standard linear solid model). However, such models are complex to solve across a whole surface, especially when the model needs to account for phenomena such as surface waves propagating on the skin surface (Manfredi et al. [2012], Shao et al. [2016]). This has pushed researchers to move from an analytical solution to numerical analysis approaches, such as the finite element model (FEM) and finite boundary element model (FBEM). For instance, Wu et al. [2004] have applied FEM to fingertip skin deformation. The authors' model describes the geometry of the fingertip (i.e. shape) as well as its 3-layers composition (i.e. epidermis, dermis and bones) and their relative mechanical properties. The model is then able to predict deformation under different scenarios.

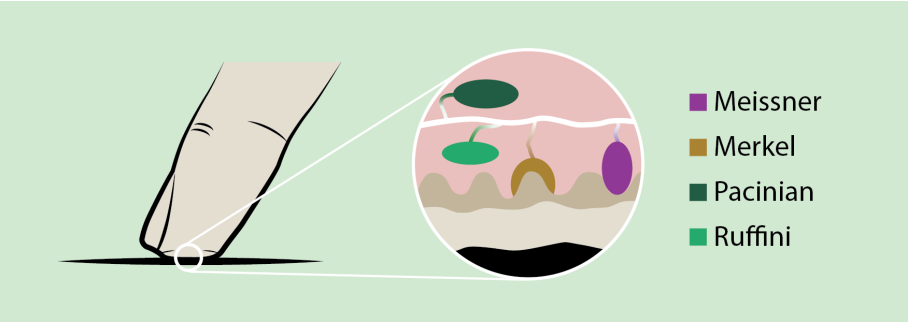

Figure 2.2: Mechanoreceptors are localised in the dermis, under the epidermis

Cell	Channel	Density	Receptive field	Sensitivity
Meissner	RA	$140\,\mathrm{cm}^{-2}$	12.6 mm	Vibrations 5-50 Hz Spatial deformation
Merkel	SAI	$70\,\mathrm{cm}^{-2}$	11 mm	Constant pressure Vibrations lower than 5 Hz Spatial deformation
Pacinian	PC	$20\,\mathrm{cm}^{-2}$	101 mm	Vibration 50-500 Hz Spatial deformation
Rufinni	SAII	$20\,\mathrm{cm}^{-2}$	59 mm	Constant pressure Lateral stretch

Table 2.2: Mechanoreceptors Properties at the fingertip

2.2.2 Mechanotransduction

It is worth noting that skin deformation does not always evoke a tactile perception. For perception to occur, the sensation (i.e. skin deformation) needs to reach the LTMRs embedded in the skin. There are different kinds of mechanoreceptors, which all have different properties, such as density, acuity, and response characteristics. These mechanoreceptors properties are presented in further detail in this section.

Low threshold mechanoreceptors

As depicted in Figure 2.2, there are four kinds of LTMRs in the glabrous skin, the hairless skin covering human palms and soles. Because each type of mechanoreceptors encodes the deformation information, or strain, differently, mechanoreceptors are often associated to a tactile channel describing the mechanoreceptor sensitivity and its corresponding signal on the nerve afferents. There are two slowly adaptive channels, referred to as SA1 and SA2, which depict the behaviour of the Merkel cells

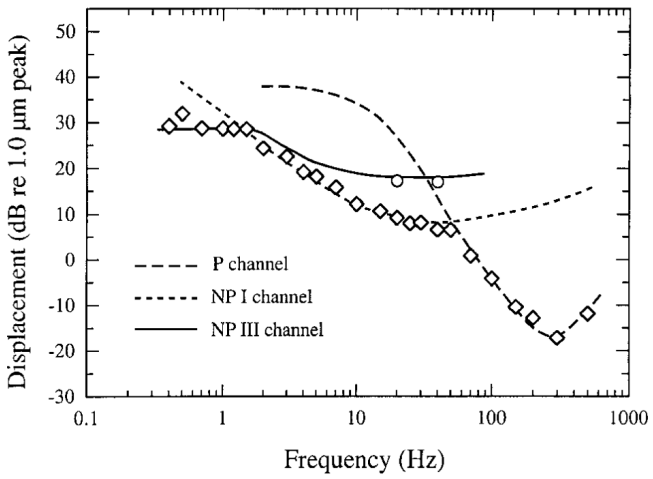

Figure 2.3: Channel threshold as a function of frequency (Gescheider et al. [2002]). P, NPI and NPII are old terminology for PC, RA and SA1 channel, repectively.

and the Ruffini endings, respectively. There are two rapidly adaptive channels, one depicting the Meissner cells behavior, which is referred to as RA (or alternatively, FA, for fast adaptive) and a second one depicting the Pacinian corpuscle behavior, which is referred to as PC.

The repetition of the same spatiotemporal strain pattern, will trigger the same nerve activity on each of the mechanoreceptors' nerve afferent (Hayward et al. [2014]). However, each mechanoreceptor encodes the spatiotemporal strain pattern differently (Johansson and Vallbo [1983]). The RA channel encodes vibrations from 5 to 50 Hz and is mostly sensitive to the rate of change in the spatial deformation. The PC channel encodes vibrations from 50 to 500 Hz. The SA1 channel is sensitive mostly to constant pressure and vibrations below 5 Hz. The SA2 channel responds also to constant force, as well as responding to skin stretch.

In addition to being sensitive to different frequency ranges, mechanoreceptors have also a different thresholds of perception according to the frequency of the stimulation. Indeed, according to the frequency of the input stimulus, oscillation will need to occur with a greater or lower amplitude to be perceived. This phenomenon can be summarised in the frequency sensitivity curves represented in Figure 2.3 (Gescheider et al. [2004]). For instance, to be perceived oscillation around 200 Hz requires lower amplitude than oscillation at 10 Hz. In the case of the PC channel, this sensitivity will further depend on the area of the contactor (Verrillo [1963]) and stimulation duration. These properties of the PC channel are referred to as spatial and temporal summation, respectively (Gescheider et al. [2002]). Spatial summation means that at equivalent amplitude, oscillations over a greater contact surface are perceived as stronger than those over a smaller contact surface. Similarly, temporal

summation means that at equivalent amplitude, oscillations shorter in duration are perceived as weaker than those longer in duration.

Mechanoreceptors not only react differently to strain, but also vary in distribution and receptive fields sizes. Meissner and Merkel cells are the most numerous with 140 and 70 units per square centimeters, respectively and have the smallest receptive field at 12.6 mm^2 and 11 mm^2, respectively. The Pacinian corpuscle and Ruffini endings are the least numerous with 20 units per squared centimeter each and have bigger receptive fields of 101 mm^2 and 59 mm^2 respectively Johansson [1978], Johansson and Vallbo [1979]. These values, summarised in Table 2.2, are relative to the fingertips and are different on other body parts. Hence, spatial acuity and threshold of perception might be found to be lower at other body locations.

Mechanotransduction

The process mechanoreceptors undergo to transform mechanical stimuli into electrical spikes is referred to as mechanotransduction. In the same way that researchers have attempted to model skin deformation, they have tried to model mechanotransduction. The first attempts started in the 1980s, and models drew analogies with electrical circuits (Freeman and Johnson [1982]). The idea behind such models was to represent a mechanoreceptor as a system converting deformation into electrical potential. Once the potential reaches a given value (i.e threshold), a spike is emitted and the potential is reset to its resting value. However, mechanoreceptors are more complex and later electrical-inspired models had to include various phenomena such as the *refractory state*, *hyper-excitability period*, *absolute threshold*, *entertainment threshold*, and so on, to capture the complete mechanoreceptor behaviour. For further details on these phenomena, we refer the reader to Freeman and Johnson [1982]. We just wanted to stress here that instead of adding ad hoc modifications to electrical-inspired models, a new paradigm was required.

This new paradigm appeared recently with Dong et al. [2013], who proposed to separate mechanical transduction and spike emission into two parts. On the one side, instantaneous displacement, as well as displacement velocity and acceleration, is added through a weighted sum and then run through a saturation filter. The resulting signal represents the *potential*, which is then used as input for an integrate-and-fire neuron model (Mihalaş and Niebur [2009]). The neuron model is accounting for all mechanoreceptors behaviours described previously. After training their model based on microneurography measurements, the authors were able to accurately predict spike emission. Future iterations of the model were then developed by the same research group. To this day, the most complete model is from Saal

et al. [2017]. This model captures mechanotransduction on the whole hand as well as three kinds of mechanoreceptors, both for static and dynamic input patterns.

Electrical spikes emitted by the mechanoreceptors then travel on afferent nerves up to the central nervous system, where tactile information is processed. Little is known about how the tactile information is treated once it arrives in the primary sensory cortex. However, the resulting interpreted information, or perception, has been studied through psychophysical techniques. The next part covers tactile perception in further details.

2.3 Tactile Perception

As described at the beginning of the chapter, tactile perception encompasses many physical quantities, such as roughness or hardness. Those different physical quantities can be seen as the different dimensions of touch. Beyond detecting a physical quantity, the sense of touch can discriminate between different amplitudes of the same quantity, as well as recognising a given amplitude. This different level of complexity in processing tactile information is what we referred to as *levels of perception* and are discussed in the following part, alongside describing the main dimensions relative to tactile perception.

2.3.1 Levels of Perception

Each dimension of touch can be categorised with different metrics relative to different levels of perception. These different levels of perception extend from the simple detection of a tactile sensation to the judgement one makes about the perceived sensation.

The first level of perception is detection. This is the simplest of all levels and distinguishes between a sensation being strong enough to be perceived, from one too weak to be perceived. Detection is often described as the absolute threshold. For instance, to perceive a vibrotactile stimulus, the vibration amplitude needs to be greater than a given value, referred to as the threshold of perception. If the vibration amplitude exceeds that threshold, the vibration will be perceived. If the vibration amplitude is lower than this threshold the vibration will not be perceived at all. As discussed previously, the perception threshold can depend on other factors. In our example, the vibration amplitude threshold depends on vibration frequency. Meanwhile the threshold of perception depends on the physical quantity perceived, and there are several methods to measure the absolute threshold (Macmillan and Creelman [2004]).

The second level of perception is discrimination, or in other words, one's ability to perceive changes in a physical stimulus. Discriminative abilities are often measured as Just-Noticeable-Difference (JND), which is the smallest amount of change one can perceive. Weber showed that JND increases with the stimulus amplitude Weber and Ross [1978].

$$\Delta A/A = C \tag{2.2}$$

Weber's findings are often represented using equation 2.2, where A represents the stimulus amplitude and ΔA the associated JND. C, expressed as a percentage, is referred to as the Weber fraction and represents the smallest changes in a physical stimulus that will yield to a perceptual change. The Weber fraction remains constant for a given physical quantity. For instance, for vibrotactile stimuli, at low frequency, one can perceive small changes in frequency, while at higher frequency, the changes in frequency needs to be greater to be perceivable.

Absolute threshold and JND for the dimension of touch can be found in Table 2.3 based on results extracted from Jones and Tan [2012].

The third level of perception is related to identification. Even though one can discriminate between various stimuli of the same nature but of different magnitudes, one's ability to recognise a specific stimulus among a given set is a more complex task. This ability is often measured as information transfer and is expressed in bits of information. While for audition, information transfer is around two or three bits of information according to the dimension considered, touch is often limited to two bits of information. This means that, for instance, one can recognise only up to four vibrotactile stimuli if the frequency alone is varied. Information transfer can increase using more dimension, but the exact increase depends on the dimension chosen and no clear relationship is defined.

Finally, the last level of perception is relative to judgement. In other words, it is the qualitative and subjective value one attributes to the dimension perceived. The main judgement considered is valence, which refers to one's ability to attribute a positive or a negative value to a given stimulus. Other judgements of a different nature can also be made (e.g. arousal).

2.3.2 Dimension of Touch

Tactile perception and the associated mechanoreceptors can perceive three main dimensions, namely, roughness, hardness and friction. Temperature, pain and other quanlities rely on different receptors to those current technology in mid-air haptic

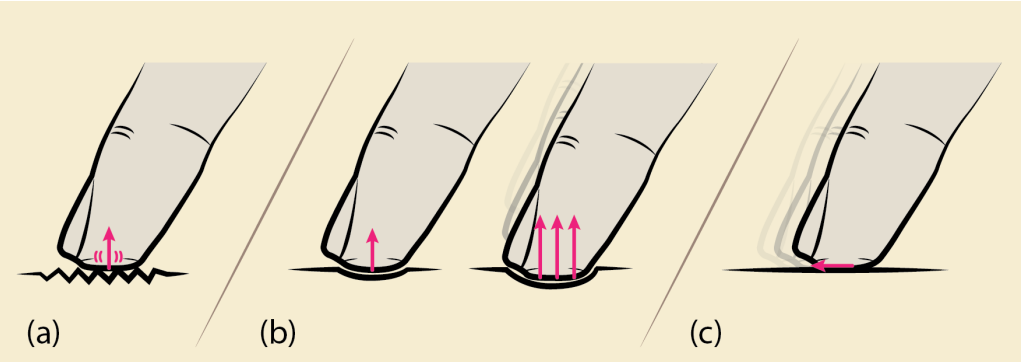

Figure 2.4: Touch encompass several dimensions: (a) Roughness, normal force and vibration induced. (b) Hardness, contact area and force amplitude increasing with the displacement. (c) Friction, tangential force opposite to the finger movement.

displays can stimulate (see chapter 3). Therefore, these dimensions of touch are out of the scope of this thesis.

Roughness

Texture roughness is the perception of the irregularities or asperities that composed a surface. In some engineering fields such as surface finish, texture roughness is usually described in terms of height profiles (e.g. ISO [1997]). When one's finger contacts a surface, the skin deforms across the contact area. However, due to the irregularities and asperities in the surface, the skin does not deform evenly.

Our somatosensory system developed mechanisms to decode these deformations and interpret it as texture roughness. It is currently admitted that the perception of texture roughness is dual (Weber et al. [2013]).

On one hand the somatosensory system uses spatial information to identify the coarse element of texture roughness (of the order of millimetres). On the other hand it uses temporal information to identify the vibration induced by finer elements of texture roughness (of the order of micrometres) (Klatzky and Lederman [2003], Bensmaia and Hollins [2003]). The coarse part of texture roughness, also referred to as macro-texture, is perceived through the spatial variation in skin deformation. However, this mechanism is limited as the space between consecutive asperities decreases. This limit is measured through two-point-discrimination tests and is around 1-2 mm on the fingertip, but is greater in other locations of the body (Lederman and Klatzky [2009]).

To perceive finer parts of texture roughness, also referred to as micro-texture, tactile perception relies on the temporal variation of skin deformation, across the whole skin surface. As shown in Manfredi et al. [2014], exploring a rough surface

with a finger induces vibration patterns that are correlated with the texture explored. Relying on this mechanism, one can perceived gratings whose amplitudes are as small as 10 nm (Skedung et al. [2013]).

Hardness

By pressing down on a surface with one's finger, one is able to determine whether an object is rigid or soft. This object property is referred to as texture hardness. In the case of moving parts (i.e. buttons), one might use the words "stiffness" and "compliance" instead. Hardness is often represented using the so-called Young modulus, in Newton per square meter.

The majority of the information on hardness is encoded through the force over displacement ratio. When one presses one's finger against a surface, the force will increase as the finger pushes on the surface. Many applications apply this phenomenon and implement different force over displacement curves to stimulate push-buttons with different levels of hardness (Kildal [2010], Kim and Lee [2013], Doerrer and Werthschuetzky [2002]). Recent studies have also pointed towards a relationship between the contact surface growth rate and texture hardness discrimination (Bicchi et al. [2000]). In this study, the authors used Hertzian equations to model the contact area between a finger with an elasticity of 0.25MPa and a different elastic surface whose Young modulus varied between 0.125MPa and 0.500MPa at increments of 0.075MPa. At 2 N the contact areas were as distinct as 1.2 mm^2 for the two extreme elasticity values and as close as 0.14 mm^2 for the two largest elasticity values. In terms of spatial resolution, this is the difference between square stimuli with side differences of 1.09 mm and 0.3 mm, respectively. Finally, Kildal showed that delivering a vibratory stimulus to the users' fingers when they are pressing against a rigid surface could create the illusion of hardness, instead of rigidity and that tuning the vibratory stimuli allow the perception of hardness to be adjusted (Kildal [2010, 2012]).

Friction

When moving one's finger across a surface, one experiences a resistance to its movement. This is referred to as texture friction. In solid mechanics, frictional forces are tangential to the surface and are defined as the product of the normal force against the surface and a so-called coefficient of friction, which depends on the two solid material properties. However, since the finger is viscoelastic, the relationship between normal and lateral load is more complex. Nonetheless, the friction coefficient between the skin and a range of different materials has been measured to be

on average 0.46 (Zhang and Mak [1999]).

Dimension	Threshold	JND
Roughness	0.06 µm	5-12%
Hardness		15-22%
Friction		10-27%

Table 2.3: Threshold and Just-Noticeable-Difference for the 3 tactile dimension (Jones and Tan [2012]

)

2.4 Tactile Feedback

As described in the previous two sections, tactile sensation and tactile perception are two aspects of the sense of touch, representing both ends of tactile information processing. In addition to investigating tactile sensation and tactile perception separately, the research community has been investigating the relationship between both. The aim behind such an approach is the ability to identify key physical quantities that will represent a given perception. For instance, when a person moves their finger over a rough surface to determine its properties, what are the main physical events at the skin level? Which events are perceived and encodeded by the mechanoreceptors? How do these events affects our perception of the surface roughness? To answer these questions, researchers have been investigating so-called parameter and perceptual spaces, as well as the relationship between these two spaces. The results of these studies have been used by the human-computer interaction (HCI) community to develop tactile feedback.

2.4.1 Parameter and Perceptual Spaces

As discussed previously, upon contact with a surface, the skin will deform. Skin displacement will then be encoded via mechanoreceptors, before the tactile information is decoded in the brain. The associated perception can then be characterised at different levels. However the precise encoding/decoding process is ill understood, and it can be overwhelming to understand what part of the tactile signal is interpreted as tactile information.

To address this, the research community has been investigating relationships between sensation and perception. More specifically, scientists have been developing abstract tactile stimuli to convey tactile information. Abstract tactile stimuli are

defined using a set of parameters (e.g. intensity or frequency) and the changes in parameters value are then scaled to changes in perception. The range of values for each parameter defines a so-called parameter space, and the corresponding range of perception defines a so-called perceptual space.

As one stimulus can be characterised with many parameters, and similarly tactile information can be characterised with many perceptual cues, both spaces are multidimensionnal. However the relation between the two spaces is not a one to one mapping. Changes in one parameter can affect the perception of two different dimensions and similarly, two different parameters can affect the perpcetion of the same perceptual dimensions. The relationships are also often not linear, making the transition from one type of information to the other non-trivial (Clark et al. [2017]).

For instance, in a vibrotactile device in which an actuator is driven by a specific signal, changing parameters such as frequency can have an impact on the perception of bumpiness or sharpness (Strohmeier and Hornbæk [2017]). Similarly, changing the waveform of the stimuli can have an impact on two dimensions of the perceptual space (MacLean and Enriquez [2003]). The results of these studies are often integrated into design tools, where user experience designer can rapidly design their desired perception (Clark et al. [2017], Schneider et al. [2015]).

2.4.2 Tactile Feedback

In HCI and design, the stimuli are used as feedback in various systems. Haptic feedback aims at reproducing realistic touch sensations and is therefore referred to as pseudo-haptic feedback (Pusch and Lécuyer [2011]).

There are two main categories of pseudo-haptic feedback, namely vibrations and texture. Vibrations are stimuli for which the output is time dependent. Vibrations, also referred to as vibrotactile feedback, are commonly used in all sort of systems such as phones, watches and game controllers to provide notification. Vibrotactile feedback is generally localised but can also be spatially distributed.

Textures, on the other hand, aim at being in synchronicity with the user's hand motion. Hence, the stimulus output will be position dependent rather that time dependent. Since the texture feedback is synchronised with the user motion, it is localised at the user fingertips, rather than localised at a given position on the system. While texture-like stimuli will feel more realistic, they require accurate tracking and are therefore less common.

These two categories of pseudo-haptic feedback can also be put in relation with the disctinction between active and passive touch, explained previously (see section 2.1.2).

In the rest of this thesis, we will focus on spatially distributed vibrotactile feedback.

Knowing how the sense of touch works and how tactile information processing occurs is crucial to any researcher aiming to reproduce tactile feedback using a tactile display. Indeed, this knowledge allows one to define the temporal and spatial requirements a given tactile display should have, as well as tailoring the tactile feedback to one's tactile sensibility. However, the results presented here comes from studies carried out with a mechanical apparatus which that required contact between the hand and the contact probe, while researchers have recently developed a new kind of tactile display that does not require contact between the hand and the display. This new way of conveying haptic feedback, relying on electromagnetic or ultrasound waves, presents contact properties, which are by nature, different from what the research community has studied until now. While it opens new possibilities, it is uncertain to what extent the results presented in this chapter apply. Finally, such devices present unique interaction cases for which the response of one's tactile sense of touch, has not yet been studied. The next chapter presents the working principles of this new generation of displays, simply referred to as mid-air haptic displays, as well as introducing possible haptic feedback rendering methods and their associated problematics.

Chapter 3

Mid-air Tactile Displays and Mid-air Tactile Patterns

Mid-air tactile displays are devices that have the ability to convey touch sensations, or tactile feedback, to the user without requiring the user to physically be in contact with any hardware. Developing such displays represents a technical challenge that has ocupied researchers' efforts for over a decade, resulting in a plethora of devices, each relying on distinct technologies and physical phenomena. The first section introduces these devices, alongside the technologies they rely on and the main advantages and disadvantages of each of these technologies. Among them, ultrasonic phase arrays have gained a growing popularity, thanks to their relatively high spatial and temporal resolution, as well as their large interactive space. In the second section, we detail further the working principles of ultrasonic phase arrays as well as their different driving methods. The third section covers how ultrasonic phase arrays have been used until now to convey distributed mid-air haptic patterns, from the aspects of both shape rendering and sensation rendering. To assert the rendering performance, one needs to evaluate the mid-air haptic patterns produced. To that end, the last section of this chapter discusses various metrics and evaluation approaches that could be employed to validate the rendering method explored later in this thesis.

3.1 Mid-air Haptic Display Technologies

With the development of volumetric displays (Konrad and Halle [2007], Holliman et al. [2011], Geng [2013]) as well as hand and gesture tracking technologies (e.g. Leap Motion, Kinect) the interaction zone of human computer applications is no longer constrained to surfaces but is free to occur everywhere in mid-air. Nonethe-

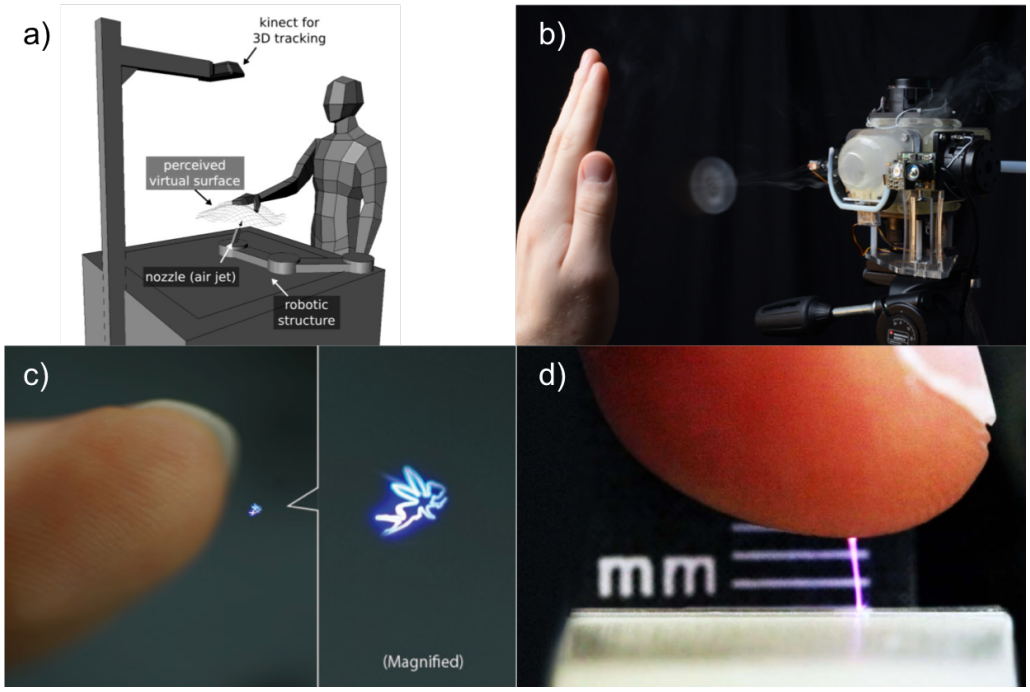

Figure 3.1: Mid-air Haptic displays rely on different technologies: a) air jet (Tsalamlal et al. [2014]), b) air-vortexes(Sodhi et al. [2013]), c) femtolaser (Ochiai et al. [2016]) and d) electric arcs (Spelmezan et al. [2016])

less, such applications still requires haptic feedback to make the interaction intuitive and seamless to the user. Previous work has involved the use of gloves and other wearable devices (Pacchierotti et al. [2017]), but ultimately, instrumenting the user can be seen as a drawback. Hence, researchers have investigated alternative ways to convey haptic feedback in mid-air, especially using contactless devices. From those various studies a wide variety of devices have been spawned, each relying on different physical phenomena. The common point of these devices is their ability to apply stress on a person's skin, and therefore, to induce skin displacement. As seen in the previous chapter, skin displacement is the first step in tactile perception. Due to its intrinsic nature, each technology comes with a different set of advantages and disadvantages. The current section introduces these technologies as well as their associated benefits and drawbacks.

3.1.1 Air-based

One approach to conveying tactile stimuli in mid-air is to use air flow. For instance, air jets with pressurised air can produce an air flow strong enough to deflect one's skin at a distance (Tsalamlal et al. [2014]). Such an air jet, once mounted on robotic arms or similar, allows dynamic targeting of the user's hand during the interaction. While applying forces up to 1 N on users' skin, air flow tends to spread with distance,

after leaving the device nozzle. Therefore, a stimulus as small as 35 mm in diameter at 150 mm from the device, can increase to 100 mm diameter at a distance of 450 mm.

To keep the stimulus size constant, researchers have proposed to produce air vortices instead (Sodhi et al. [2013]). Air vortices have a torus shape and keep their size as they travel. Air vortices' size is determined by the device aperture (25 mm diameter in Sodhi et al. [2013]), which is smaller compared to air flow, but still above tactile spatial acuity (around 1-2 mm, as seen in Chapter 2). Air vortices generate forces of up to 5 mN and accurately target users' hands as far as 1.25 m from the device. However, air vortices move at a relatively slow speed (7.2 $\mathrm{m\,s^{-1}}$ on average), which can induce latency in the feedback, especially when covering long distances.

It is worth mentioning here, that both approaches can only produce one stimulus at a time. Creating multi-points stimuli with such technology, would require increasing the number of apparatuses.

3.1.2 Laser-based

Jun et al. [2015] have shown that lasers, even though using low-power radiation, can evoke thermoelastic effect on users' skin. In other words, using a low energy laser pulse, Authors can locally heat the skin. The change in temperature then leads the skin to contract. In several user studies, the authors have shown that this effect yields to tactile sensation without any nociceptive sensation (i.e. pain). Leveraging those findings, Ochiai et al. [2016] developed a mid-air tactile display relying on a femtosecond laser. The authors show they could produce tactile pattern in 1 $\mathrm{cm^3}$ using a collection of 10 µm tactile points, produced one after the other. Laser based displays have the advantage of conveying mid-air visual stimuli simultaneously to the mid-air tactile stimuli. Even though the stimulus size is very small in such approaches, the interaction zone remains limited. Additionally, the underlying system is expensive and bulky.

3.1.3 Electric-arc based

Another approach is the use of electric-arcs to convey touch sensation (Spelmezan et al. [2016]). Using the principle of Tesla coils and high-voltage pins on the device surfaces, Authors can induce a tactile sensation through an electric arc to the user's finger. The electric arc heats the skin and evokes a thermoelastic effect like in laser-based devices. As for laser-based technology, electrical power is kept to a safety limit to avoid burns. Using custom hardware and an adapted modulation signal, the authors were able to tailor the sensation produced by the interaction. Additionally,

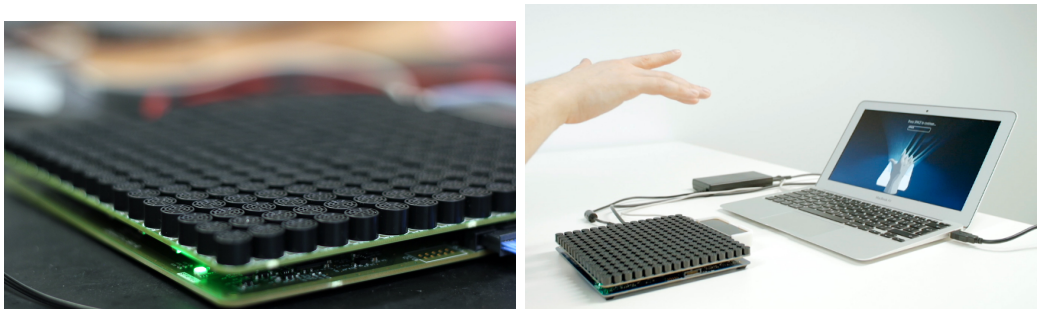

Figure 3.2: Left: One Ultrasonic phased array produce by Ultrahaptics Ltd. for mid-air haptics application. Right: A user perceiving a mid-air haptic force-field. (source: Ultrahaptics.com)

by nature, the size of the tactile sensation produced was very small. However, the interaction zone was limited to the near field, and could produce tactile sensation only up to 4 mm high. Furthermore, the scalability of the approach as not yet been demonstrated, and neither has its ability to produce a distributed pattern.

3.1.4 Ultrasound Based

Finally, researchers have explored the use of an array of ultrasound transducers, for which each pressure wave is controlled (Hoshi et al. [2010]). Indeed, by electronically shifting the transducers phase one could focus the acoustic pressure to a point in space and direct it to the user's hand. The force applied to the skin can reach 16 mN (Hoshi et al. [2010]), which is enough to deflect the skin and induce a tactile sensation. The stimulus size depends on the ultrasound wavelength and is 8.5 mm diameter with 40 kHz ultrasound speakers and 5 mm diameter with 70 kHz ultrasonic speakers (Ito et al. [2016]). It has also been shown how similar devices could be used to create multiple focus points with different tactile properties (Carter et al. [2013]). Unlike air-based technology, ultrasonic phase arrays generate tactile points at the speed of sound (343 mm/s in air) and therefore the latency is very low. Even though the force output is lower than in airflow devices, the small stimulus size and its wide interaction zone, make ultrasonic phase arrays a reliable and attractive technology for both researchers and industries interested in mid-air tactile applications.

The studies reported in this thesis aims at investigating rendering methods to produce spatially distributed mid-air haptic patterns. However, air and electrical based devices cannot produce spatially distributed mid-air haptic patterns. On the other hand, laser-based devices possess a limited interaction zone. Therefore, by process of elimination, ultrasonic phase arrays appear to be the most suitable tech-

Table 3.1: Mid-air Haptic Display performance according to different technologies

Technology	Diameter [mm]	Force [N]	Interaction Distance [m]
Air Jet	35-100	1	up to 0.45
Air Vortex	25	0.005	up to 1
Laser	0.02	n/a	n/a
Eletric-arc	n/a	n/a	up to 0.004
Ultrasound	5-8.5	0.016	up to 1

nology to investigate mid-air haptics patterns rendering. Hence, the work presented in this thesis will further investigate the capabilities of such technology to render mid-air haptic patterns. Specifically, we will make use of a ultrasonic phased array produced by Ultrahaptics Ltd. (see Figure 3.2). Before we explore pattern rendering with ultrasonic phase array, we further detail the technology's working principles in the next section.

3.2 Ultrasonic Phased Array

Ultrasonic phased arrays (UPAs) are composed of a collection of ultrasonic transducers. Even though they can come in differents sizes and layouts (Price and Long [2018]), UPAs all work on the same principle, using phase shift to shape the acoustic field above the device accordingly to the application. While the applications could involve levitating small polystyrene beads or creating parametric audio (Iodice et al. [2018], Shakeri et al. [2019]), UPAs are mostly used to convey tactile feedback in mid-air. This section will cover the creation of a single focal point whose ultrasonic pressure is great enough to deflect the skin and induce a tactile sensation. Finally, the different modulation techniques employed to convey specific tactile stimuli will be detailed.

3.2.1 Focal Point

We refer to a focal point as a point or region in the acoustic field where the acoustic pressure is maximised. To generate a focal point, there are different approaches.

The simplest approach is to consider the distance between the focal point's desired position and the transducers. As the speed of sound is constant ($343\,\mathrm{m\,s^{-1}}$ in the air at normal temperature and pressure), one can predict how long the ultrasound wave takes to go from the transducer position to the focal point position. This value can be referred to as the *time of flight*. After computing the time of

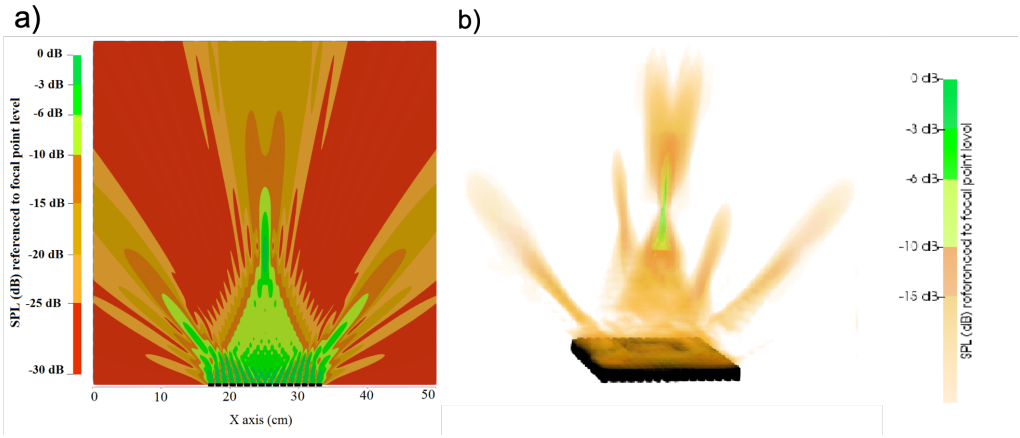

Figure 3.3: Mid-air haptic displays can focus acoustic pressure on a so-called focal point: a) 2D view, b) 3D view of the generated acoustic field. Acoustic pressure is represented as Sound pressure level (SPL). (Price and Long [2018])

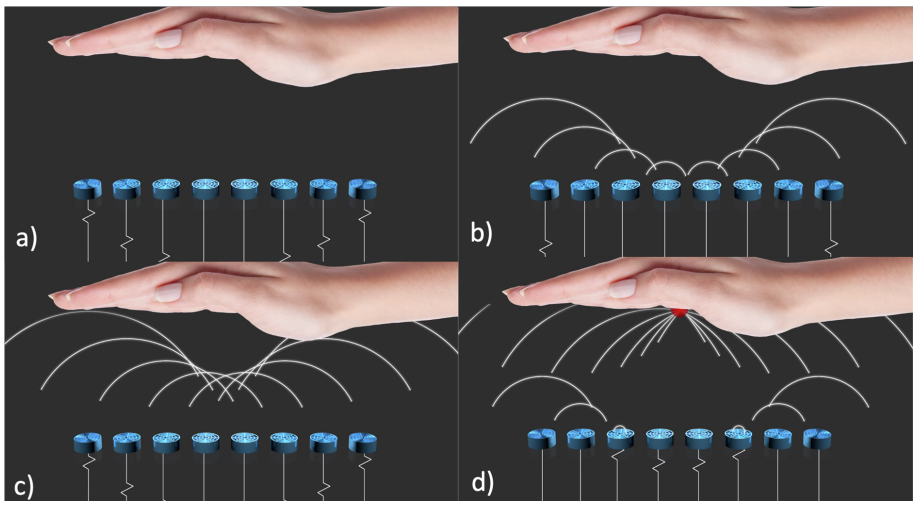

Figure 3.4: Signals are sent to the ultrasonic transducers with some delays (a). The transducers emit ultrasonic waves with corresponding delays (b). These waves propagate in air towards the user's hand (c). Finally the waves "focus" at the desired position (i.e. the user's palm) (d).

flight for each transducer, one can work backwards to determine the delays needed between each transducer, so that each corresponding ultrasonic wave arrives at the desired position at the same time. These delays can be considered as phase shifts between each ultrasonic wave. A simplified visualisation of this approach can be seen in Figure 3.4.

When applied to multipoint feedback, the above methods can provide different solutions. Some solutions are better than others as they maximise the constructive interference at the desired location, as well as maximising the destructive interference in the remaining acoustic field. Such solutions insures the saliency of the pattern. To find this optimal solution, Long et al. [2014] reformulated the problem as an Eigenvalue problem. The authors showed that solving the Eigenvalue problem is similar to maximising constructive interferences at the desired location, while minimising constructive interferences everywhere else.

The two approaches we just described both assume a free-field interaction. These approaches do not take into account ultrasound wave reflection on the user's hand. However, as soon as the user moves their hand in the interaction zone, perturbations occur due to ultrasonic wave reflections on the hand surface. These resulting reflections can alter the acoustic field unpredictably. To avoid this, Inoue et al. [2016] developed an adaptive method which includes the finger geometry as part of the problem (Inoue et al. [2016]). To solve this new problem, the authors leveraged the computational power of finite element modelling and found the solution providing the highest amplitude despite hand interferences.

Independently of the approach used, a focal point is generally described as a position and an amplitude, which can either remain constant or be varied through time according to the scenario (see sections 3.2.2-3.2.4). The amplitude of a focal point produced with a given UPA can be estimated as long as the position and the ultrasonic transducers properties are known.

For instance, in a free field, using the Huygens-Fresnel principle and the principle of superposition of waves, one can estimate the interference of N ultrasound waves, with the wavenumber k (i.e. $k = \frac{2\pi f}{c}$, with f the ultrasonic frequencies and c the speed of sound in air), and determine the total acoustic pressure produced P, to be equal to

$$P = \sum_{n=1}^{N} \frac{P_0}{r_n} H(\theta_n) e^{ikr_n} \tag{3.1}$$

where P_0 is the acoustic pressure produced by a transducer n positioned at a distance r_n and angle θ_n from the focal point and which possesses a directivity function $H(\theta)$. The above formula makes use of the complex notation, where the real part represents the pressure and the imaginary part the phase. The reader

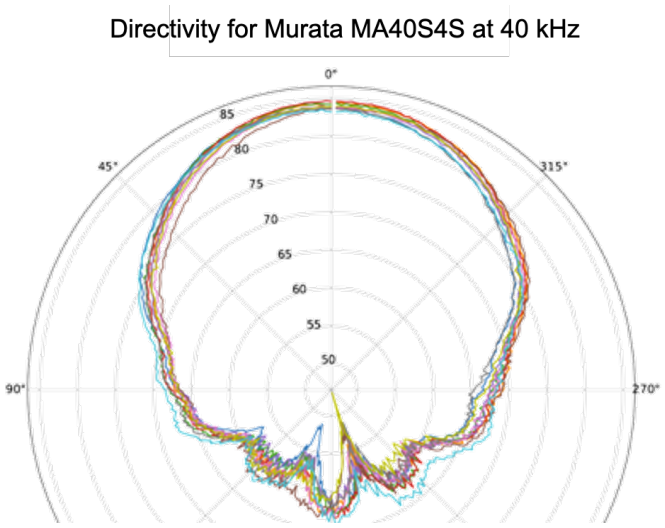

Figure 3.5: The directivity function of a 40kHz Murata Transducers in the polar coordinate. (Source Ultrahaptics - internal report)

will note here that the directivity function represents the relative acoustic pressure produced by the transducer in a given direction compared to the direction normal to the transducer surface. The notion of directivity here is similar to the notion of directivity of antennae in electromagnetics. An example of transducer directivity function is shown in Figure 3.5 for the 40 kHz Murata Transducers, the ones that are commonly used in ultrasonic phased arrays for mid-air haptics applications.

However, the focal point created is not punctual in the strict mathematical meaning and actually possesses a width, which can also be determined. It has been shown that the diameter w of the focal point is related to the ultrasound wavelength λ and estimated empirically as

$$w = 1.22\frac{\lambda}{sin\theta}, \quad sin\theta = \frac{D/2}{\sqrt{R^2 + (D/2)^2}} \tag{3.2}$$

where R and D represent the focal length and the aperture diameter respectively (Ito et al. [2016]). Using these equations, the focal point size is assumed to be 8.5 mm wide, with a traditional ultrasound phased array using 40kHz ultrasonic transducers, and 5 mm wide when using 70kHz ultrasonic transducers.

At this point, it is worth mentioning that for rectilinear arrays, the focal point has been shown to be rather elongated in the axis going away from the array surface (Price and Long [2018]). A representation of the acoustic field when a focal point is produced 20 cm above the ultrasonic phase array, can be seen in Figure 3.3 It is worth noting that the pressure applied to the skin is actually proportional to the square of the acoustic pressure at the focal point and is refered to as acoustic radiation pressure (ARP). In the case of a focal point produced with an array composed of

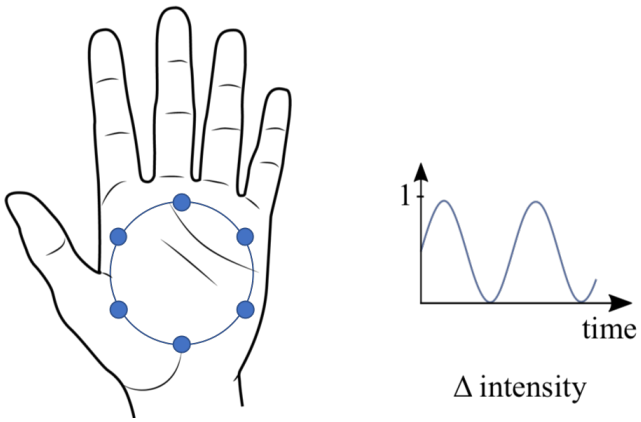

Figure 3.6: Amplitude modulation: To create a pattern (here a circle), one needs multiple points whose amplitudes vary across time

256 40 kHz transducers, ARP can reach 16 mN. Such pressure, once applied to the skin, is enough to slightly deform it, hence evoking a tactile sensation. Further details on how to derive ARP are described in section 3.4.1.

When the pressure amplitude is kept constant, our sense of touch is sensitive only to the onset and the offset of this pressure (see section 2.2.2). However, our sense is sensitive to dynamic pressure when the amplitude variation is within a rate of change of 0-500 Hz. Similarly, UPAs are digital system which output can be updated to rate greater than the kilohertz. Because the UPA's update rate is greater than the rate of the signal perceived by the sense of touch, it is possible to sample continuous function and use them as input signal for the focal point amplitude and position. Based on these facts, and because of the aim to produce long duration tactile feedback, researchers have developed various modulations techniques. The next section covers these techniques and their differences.

3.2.2 Amplitude Modulation

In most of the human computer interactions, feedback is aimed to last. In order to create a tactile feedback that is perceived over time, researchers have developed feedback with dynamic features. One way to create such dynamic features is to continuously vary the focal point amplitude over time between a minimum and maximum amplitude. This approach is referred to as amplitude modulation (AM) and mainly makes use of sinusoidal signals to modulate the focal point amplitude.

As stated previously, the sense of touch is sensitive to vibration in the range 0-500 Hz. However the sensitivity of the sense of touch through that range varies (Gescheider et al. [2002]). Various studies report the threshold of perception as being

lower at frequencies 200-250 Hz, independently of the location on which the study was conducted or the size of the contactor used. Hence, to produce the strongest perceived sensation, AM is commonly used around these frequencies. Nonetheless, it has been shown that in addition to affecting the strength of the sensation, frequency was responsible for the overall perception of the stimuli (Obrist et al. [2013]). Indeed, in the study, participants reported different qualitative properties whether the focal point amplitude was modulated at a low frequency (i.e. 16 Hz) or high frequency (i.e. 250 Hz). Monnai et al. [2014] have also reported using non-sinusoidal signals to convey different sensations.

It is worth highlighting here that such methods produce similar results to traditional vibrotactile devices. Indeed, when the focal amplitude increases and decreases, the skin deformation also increases and decreases. This is similar to a linear actuator indenting the skin. As the indenter goes into the skin, the skin deformation increases, and as then the indenter retracts, the skin deformation decreases. The analogy is important here, because it means that the results from the research community on the perception of vibrotactile signals can be adapted to mid-air haptics and AM. An argument towards this is the fact that results reported in Obrist et al. [2013] and Monnai et al. [2014] are coherent with results presented in MacLean and Enriquez [2003] where both frequency and signal waveform were found to affect the user perception of the tactile stimulus.

Amplitude modulation assumes the focal point position to remain constant throughout the stimulus. While this is effective for local stimulation, this approach reaches its limits when rendering distributed patterns. Indeed, to create spatially distributed patterns, one needs to produce several amplitude modulated points (Long et al. [2014]). Since a single UPA can only produce so much pressure, the absolute amplitude created at each point decrease drastically as the number of simultaneous points increase. While Long et al. [2014] have proposed a time multiplexing approach to limit this phenomenon, the number of focal points that can be simultaneously produced and perceived remains limited. In turn, this limits the distributed pattern complexity that can be created. This limit has lead researchers to explore new modulation techniques.

3.2.3 Lateral Modulation

The strength of a mid-air tactile stimulus is limited by the pressure it can produce. Even though one could increase the number of elements in an ultrasonic phase array to increase the pressure the array can produce, one can also make better use of the available pressure. In other words, one can modulate the pressure in such a way

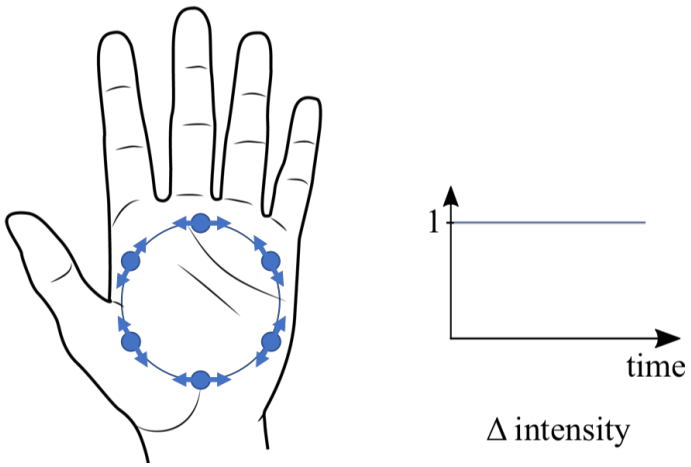

Figure 3.7: Lateral modulation: To create a pattern (here a circle), one needs multipoint whose positions oscillate across time, while the amplitude stays at its maximum

that LTMRs become more sensitive to it. For instance, we saw that LTMRs are more sensitive to vibration around 200 Hz and that therefore AM signals should be tuned to that same frequency. Similarly, Biggs and Srinivasan [2002] have shown that LTMRs were more sensitive to lateral forces than normal ones. Leveraging this fact, Takahashi et al. [2018] had the idea to modulate the focal point position rather than its amplitude (Takahashi et al. [2018]). The authors claimed that by doing so they were able to produce lateral force in the skin. However, since the focal point is made of air (i.e. a fluid), lateral forces should not occur in this interaction. Without appropriate physical measurements, the question remains open. Nonetheless, by moving the point position from side to side around a target position on the user's palm, the authors succeeded in producing focal points that are perceivably stronger than focal points created using AM. This approach of laterally moving a focal point is referred to as lateral modulation (LM). In their study, the authors investigated two parameters, namely the rate at which the oscillation occurred and the amplitude of those oscillations. They found that stimuli were perceived to be strongest for oscillations of between 50 and 200 Hz and amplitude of 5 mm. Lateral modulation produces stimuli noticeably stronger than those produced with AM. However, when it comes to spatially distributed patterns, the same issue exists, and the pattern complexity is limited by the number of tactile points that can be rendered at once. Additionally, one can easily imagine the impact of LM on the spatial resolution. Therefore, another method still needs to be found.

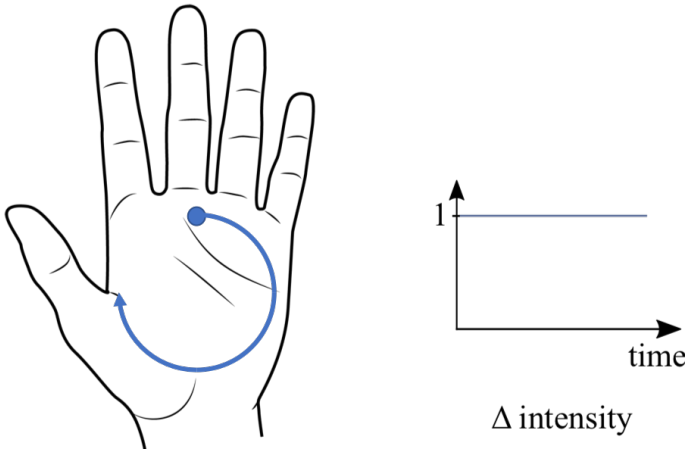

Figure 3.8: Spatiotemporal Modulation: To create a pattern (here a circle), one needs a single point moving repeatedly over the circle path, while the amplitude stays at its maximum

3.2.4 Spatiotemporal Modulation

When alternating between two pictures rapidly and repeatedly, one sees only one single and full picture. This phenomenon relies on the persistence of vision and inspired visual toys such as the thaumatrope. Recently Kappus and Long [2018] had the idea to adapt this phenomenon to mid-air haptics by rapidly and repeatedly moving a focal point on a given path. For instance, a focal point moving fast on a circular trajectory is perceived as a whole circle rather than a moving point. This effect is related to the temporal resolution capacity of one's sense of touch, which has been measured to be around 2 to 40 ms (Loomis [1981]). This approach is referred to as spatiotemporal modulation (STM) and is therefore mainly used to draw spatially distributed patterns on one's palm. The advantages of STM over the other two modulation techniques is that it uses only one focal point per pattern instead of many. Hence, all the pressure that can be generated by UPAs is concentrated on that single focal point. This results in perceivably stronger patterns, especially as the pattern size and complexity increase. Currently the approach of designers is to repeat the desired pattern at a rate equivalent to the other modulation type (i.e. around 200 Hz). Furthermore, a pattern repeated at 200 Hz, means that a single iteration takes 5 ms which agrees with the temporal resolution capacity of touch. However, the technique is not only recent to the field of mid-air haptics, but also to the haptic community in general. Therefore, it is unknown whether this approach is the best or if parameters different from the repetition rate should be optimised instead.

As this thesis is interested with rendering spatially distributed patterns, the use

of STM has been chosen. However, ultrasonic phase arrays being a recent technology, its parameter space and associated perceptual space still need to be investigated. In the next section, we will define what we call a mid-air tactile pattern and how we imagine its parameter space. Based on this definition, we will present existing studies that relate to mid-air tactile patterns.

3.3 Mid-air Tactile Pattern

Leveraging the advantages of STM, UPAs can be used to create spatially distributed tactile patterns. We will refer to these patterns as Mid-Air Tactile Patterns. In this section, we will discuss a more formal and detailed definition of spatiotemporal tactile patterns. This will be connected to a review of the related work on mid-air haptic rendering, hence highlighting the already known relations between mid-air haptic parameter space and perceptual space.

3.3.1 Definition

Before defining mid-air tactile patterns, it is interesting to examine the simplest form of tactile feedback: a mid-air tactile point. We consider a mid-air tactile point to be a localised vibration produced in mid-air using either Amplitude Modulation (AM) or Lateral Modulation (LM). As explained in the previous section, mid-air tactile points are similar to vibrotactile stimuli. The perception of mid-air tactile points varies as parameters such as modulation frequency or modulation waveform change.

Using a mid-air tactile point as a building block one can produce more complex feedback such as a mid-air distributed tactile pattern. Here, a mid-air distributed pattern refers to a collection of mid-air tactile points, with either the same or different modulation signals, where each of the points has a different position in the interaction space, as if distributed on a grid. In contact haptics, such distributed patterns are commonly produced using an array of vibrotactile actuators (Schneider et al. [2015]) or pin-arrays (Sripati et al. [2006], Wang and Hayward [2006]).

Drawing an analogy with vision, we can say that the approach is very similar to visual displays. In the same way that mid-air tactile points are building blocks for a mid-air distributed pattern, a pixel is like the building block for visual frames.

With this analogy in mind, mid-air tactile pattern can be defined as the haptic counterparts of visual frames. Pushing the analogy further, one can define the resolution of a mid-air tactile pattern as the number of mid-air tactile points per unit area. Additionally, within a mid-air tactile pattern, each mid-air tactile point

will have its parameters set according to the overall tactile information that one wants to convey via the pattern. But just as visual displays dynamically update the pixels colours, the mid-air tactile point parameters must be updated rapidly. To go through, each position, the mid-air air tactile point could make use of spacefilling curves such as raster scan (i.e. like visual display) or Hilbert curves (Frier et al. [2016]).

Pushing the analogy with visual displays one notch further, can help us to refine the definition of a mid-air tactile pattern. In graphics, visual elements of a given frame are usually handled as distinct objects. Each object is further defined into a mesh (i.e. the object geometry) and a texture (i.e. the object appearance). Similarly, with mid-air tactile patterns, we can define the pattern shape (i.e. the pattern geometry) and the pattern sensation (i.e. how the pattern feels). In graphics, the distinction between mesh and texture has numerous advantages. Using the same approach for mid-air tactile pattern, we could leverage the same advantages. Indeed, if mid-air haptic patterns are divided into two components, each component can be developed separately. It also means, that if one was to develop a new sensation, one could apply this sensation to all the existing shapes, rather than re-developing shapes oneself. Similarly, if one finds a better way to render a mid-air pattern shape, one does not need to re-develop all the sensation previously developed. One can just use the existing sensations with his new shape rendering algorithm. In terms of combinatory, separating shape and sensation has the advantage of increasing the set of mid-air haptic patterns available. Indeed, if one develops n shapes and m sensations, the set of available mid-air haptic patterns is $n \times m$ pattern, while only $n+m$ components have been developed. This would be particularly advantageous if each component developed were made available to mid-air haptic designers. Indeed, designers would then only need to pick up the shape and the sensation to customise the mid-air haptic patterns as they desire and would have access to a larger set of patterns. Finally, we would like to point out that such an approach is similar to that taken by haptic devices with force feedback. While user motions can be constrained through controllable torque and therefore convey the idea of shape, the feedback can be further refined with texture signals Culbertson et al. [2014].

Using an analogy with visual displays, we were able to define mid-air tactile patterns as the combination of two components, a shape and a sensation. We also determined that studying both components separately presents some advantages. Therefore, we propose to split the field of mid-air tactile pattern rendering into two areas of research, namely shape rendering and sensation rendering. The next two sections present the state of the art of mid-air tactile shape and mid-air tactile

sensation, respectively.

3.3.2 Mid-air tactile sensation

We defined in the previous section mid-air tactile sensation as the tactile feeling evoked by a given pattern. Unlike in chapter 2, we will use the colloquial sense of sensation as referring to both tactile sensation and tactile perception, independently of the stage of the information processing.

Even though the terminology may differ between studies, mid-air tactile sensation has been investigated prior to our work. Actually, an interesting property of mid-air haptics is the ability to convey a wide range of tactile sensations to the user. Firstly, Obrist et al. [2013] have shown that using sine function to modulate the tactile point pressure and varying the frequency of the sine function could greatly change the user perception according to different aspects. For instance, while a 16 Hz sine will be perceived as soft and pulsing, a 250 Hz sine will be perceived as dense and flowing. Interestingly, the study also report that 250 Hz sines were perceived to be stronger and bigger than 16 Hz sines. In a later study, Monnai et al. [2014] used percussion sounds with frequency components higher than 100 Hz to provide mid-air haptic feedback to the user during given interactions. Interestingly, the authors reported that depending on the percussion sounds chosen, users perceived the mid-air haptic stimulus in a completely different manner, from a stiff and light sensation to an air flow burst. While those studies focused on rather abstract sensations, Freeman et al. [2017] showed that mid-air haptic stimuli could also convey the feeling of realistic textures. Using a tessellation algorithm, the authors were able to render haptic surfaces with a given texture, such as gratings and grids of pyramids in mid-air. However, to our knowledge, other dimensions of tactile perception such as softness and friction have not been investigated in a mid-air context.

Nonetheless, research on mid-air tactile sensation, is not limited to discriminative touch. Obrist et al. [2015] have also demonstrated that mid-air haptic could be used to convey affective touch. In their study, the authors show that varying parameters such as motion speed, frequency content and location stimulation could affect the emotional content conveyed through ultrasonic mid-air haptics. Interestingly, the authors' use of ultrasonic mid-air haptics unveiled new insights into emotion perception that were not observed with traditional contact tactile displays. In otherwords, in addition to discriminative information such as texture or geometric feature like shape (see the following subsection), one could tune the emotion evoked to the user when they experienced the pattern. This last point highlights the potential of mid-air tactile displays for future research.

All the above studies show that the temporal and spatial components of mid-air haptic stimuli, as well as their frequency equivalents, can affect the sensation conveyed with ultrasonic mid-air haptics. However, given the plethora of parameters involved, further research is required to extend our knowledge of mid-air haptic perception and improve the efficiency of the rendering methods.

3.3.3 Mid-air tactile shape

We define mid-air tactile shape as the ability to convey geometric information relative to the pattern, independently of the overall pattern sensation. As shape is the component on which sensation is mapped, pattern shape can be seen as the primitive of mid-air tactile patterns. As for sensation, rendering a shape using a mid-air tactile display has been investigated prior to our work, and coming with numerous challenges that had to be overcome one after the other.

Initial investigations on mid-air tactile patterns focused on freeing the mid-air tactile point from its single position and moving it spatially. For instance Wilson et al. [2014] looked at the perception of mid-air tactile stimulus moving in a linear direction and across different distances (Wilson et al. [2014]). The authors highlighted the importance of temporal parameters according to the desired travel distances. These first mid-air tactile patterns were more similar to unistroke patterns rather than to the whole shape.

Later on, it was shown that ultrasonic mid-air displays could produce multi-points synchronously and therefore convey a tactile pattern with tactile points spatially distributed in the interaction zone (Carter et al. [2013]). Leveraging this new ability, Long et al. have demonstrated how multiple points feedback can be applied to render 3D volumetric shapes in mid-air (Long et al. [2014]). Here, the desired shapes were sampled using several tactile points and by modulating the amplitude of each point. Furthermore, as shape perception is based on contour following, as well as vertices and edges perception, the authors focussed on rendering the shape contour rather than its inside (Lederman and Klatzky [1987], Plaisier et al. [2009]). Using a similar approach Korres et al. investigated the effect of varying rendering parameters for circular tactile patterns (Korres et al. [2017]). Most previous works concerned with tactile patterns mainly focused on the stimulation duration and the stimulus onset asynchrony.

However, as discussed in the previous section, using a multi-point approach to render patterns' shapes presents an inherent probelem. Indeed, the available acoustic power is limited, and producing multiple points means that this acoustic power is spread across these points. To get around this issue, Kappus and Long introduced

a new approach dubbed spatial temporal modulation (Kappus and Long [2018]). The authors have shown that they can trace a shape's contour using solely one focal point that moves rapidly and repeatedly over the desired path.

While the literature informs us about the spatial (Skedung et al. [2013]) and temporal resolution (Loomis [1981]) of touch for two consecutive points separated in space and time, it is unsured how these values apply to a moving stimulus. Additionally, STM introduces many extra parameters such as draw speed, draw frequency, sampling rate and so on, for which the effects have not been studied. The work presented in these studies aims to tackle this wide parameter space and shine a light on the most relevant ones.

This section discussed how mid-air tactile patterns could be decomposed into sensation and shape, as well as the advantages of this approach. Interestingly related work found in the literature has already explored both sensation and shape rendering to some extent. However, since mid-air tactile patterns rely on a plethora of parameters which all influence perception in the end, there is still much work required to fully understand their effects. The end goal of such research is the establishment of a haptic pattern library from which designers would be able to choose the shape and sensation they desired and therefore customised their mid-air haptic patterns to the interaction they are designing. Such a library would be particularly relevant to human-computer interaction research, such as in media studies (Ablart et al. [2017]) or art studies (Azh et al. [2016]). However, before building such a library is built, the impact of mid-air tactile patterns parameters on the end perception needs to be further investigated and evaluated. The next section discusses what metrics could be used to evaluate and validate a given mid-air haptic pattern-rendering method.

3.4 Evaluation

As discussed previously, a mid-air tactile pattern can be decomposed into a shape and a sensation. The work presented in this thesis is concerned with the shape component, and moreover with how to improve shape rendering. Recall that shape information is extracted through vertices and edges perception (Plaisier et al. [2009]), making shape contour the most important part of the shape. Therefore, when rendering a shape in mid-air, only the contours are rendered. With the assumption that the more salient the contour, the better the shape recognition, one question remains: how to render a salient shape contour.

A straightforward approach would be to produce sharper contours. However, the width of a contour is related to the focal point width, we know that sharper contours cannot be produced (see section 3.2.1).

Another approach is to maximise the strength of the contour, since a stronger contour will be more obvious to the user. Hence, improving mid-air haptic shape rendering is equivalent to optimising a shape's perceived strength. As in any optimisation problem, the first task is to establish a metric to evaluate the performance of a given strategy over another.

One can identify four possible metrics, namely a) ARP, b) skin deformation, c) evoked potential and d) perceived strength. Each of these candidates represents the *intensity* of the pattern shape at a different stage of the interaction: a) when it leaves the device, b) when it hits the skin , c) when it is encoded by the mechanoreceptors and d) when it is perceived by the user.

However, measuring these quantities is not an easy task, and in addition, the relationship between one metric and another is not straightforward. The following part details these metrics along with their respective advantages and disadvantages.

3.4.1 Acoustic Radiation Pressure

Ultrasonic mid-air arrays focus ultrasonic waves to produce tactile stimuli. These focused ultrasonic waves apply pressure on the user skin, inducing a tactile sensation. The intensity of the produced stimulus is directly related to the force that the stimulus applies to the skin. In the case of ultrasonic mid-air haptics displays, this force is referred to as *ARP*.

By definition, Acoustic Radiation Pressure (ARP) is the resulting pressure applied to a surface according to the acoustic field pressure surrounding the surface. Acoustic Radiation Pressure arises from a non-linear effect on the acoustic field and can be calculated as follows (Settnes and Bruus [2012]).

$$\langle P_r \rangle = \frac{\langle p^2 \rangle}{2\rho_0 c_0^2} - \frac{\rho_0 \langle u^2 \rangle}{2} \tag{3.3}$$

where P_r is the ARP in Pascals, $\rho_0 = 1.225\text{kg/m}^3$ is the air density, $c_0 = 343\,\text{m}\,\text{s}^{-1}$ is the speed of sound, p is the acoustic pressure in Pascals, u is the air particle speed perturbation that can be obtained from the sound pressure gradient field, and the angled brackets represent a time average.

Integrating ARP over a surface yields the force applied. In the case of most ultrasonic display this force was measured to be 16 mN (Hoshi et al. [2010]). However, it has not been measured for dynamic stimulation (i.e. AM or STM).

An argument for optimising the applied force is that it is directly related to perception. Indeed, using Hooke's law, one can see that the greater the force, the greater the skin deformation (see section 2.2.1). The threshold of perception being measured relative to skin deformation, it is therefore safe to assume that the greater the skin deformation, the stronger the perception. Another argument for optimising applied force is that it is the only quantity that is related to the device itself. Other potential metrics such as skin deformation and perceived strength are relative to the user and will vary greatly across the population. Hence, ARP appears to be the only invariant in the interaction across user population and is a perfect candidate as a metric for a shape's perceived strength optimisation.

However, optimising ARP also presents some drawbacks. First, there are no systematic methods for measuring ARP directly. One could use a force balance to measure the force applied to the surface. However ultrasonic mid-air display outputs greatly vary over time due to the ultrasonic carrier and the modulation techniques. Current force balances do not possess the capabilities to measure ARP under such time constraints.

Estimating the theoretical ARP is a complex endeavour too. Indeed, one could measure acoustic pressure and then solve equation 3.3, but this equation has been developed for a single source transducer and there is no proof that it holds in the case of UPAs.

Finally, ARP does not exist in free space and only occurs due to the presence of a surface in the space. This means that the geometry and the mechanical properties of the surface may greatly affect the ARP value. Solving ARP while accounting for these surface properties will greatly increase the computational time and load.

Hence, measuring or estimating ARP for the case of ultrasound phased arrays applied to mid-air haptics is a challenge of its own and would require a tremendous amount of work to solve. Therefore, computing, estimating or measuring ARP is out of the scope of this thesis and other metrics are considered instead.

3.4.2 Skin deformation

Although ARP cannot be directly derived analytically or measured experimentally, this pressure will result in a force applied to the skin surface. This force, or load, is applied to the user's skin, and, the skin being viscoelastic, it will deform. As discussed in section 2.2, the skin deformation yield to tactile perception. Hence, characterising the skin deformation a given pattern produces is similar to knowing what information reaches the mechanoreceptors and therefore makes skin deformation a good predictor/metrics for the perceived strength of a given tactile pattern.

Recall that as the skin is similar to a viscoelastic medium, one can estimate skin deformation using Hooke's law:

$$\sigma = E\epsilon \tag{3.4}$$

where σ is the force, or stress, applied to the surface, E the medium's Young's modulus and ϵ the resulting deformation, or strain produced.

Liang and Boppart [2009] found a Young modulus of 25 kPa for the palm. Using this result and the above equation, one can estimate the deformation produced with an UPA to be around 0.64 µm. Furthermore, the limit of skin deformation estimation were highlighted in the section 2.2.1. It is worth mentioning that this estimate depends on ARP estimates, presented in the previous section, so one could argue for its validity. An alternative to estimation is to measure skin displacement experimentally. Shao et al. [2016] have shown that using an array of accelerometers one can measure vibration acceleration on the back of the hand. Integrating these data over time twice, will allow one to determine the skin displacement. Another approach would be to use laser Doppler vibrometry to measure vibration velocity (Manfredi et al. [2012]). This second approach has the advantages of being contactless.

An argument to optimise for skin deformation is the assumption that the greater the deformation, the greater the sensation strength. Additionally, results on psychophysics of touch are mostly reported as relative to 1 µm displacement. Therefore, knowing the skin deformation would allow a straight application of the literature.

The downside of measuring skin deformation is that measuring setup can be tedious. Indeed, in-vivo measurements require additional setups to immobilise participants for the duration of the experiment to prevent involuntary movements in participants. However, this drawback can be overcome by the use of skin mimicking material such as silicone. One could argue that absolute displacement on skin mimicking material may be different from the displacement, one would measure during in-vivo experiments. However, to get around this issue, one could study relative displacement between different rendering techniques.

In the light of these last statements, skin displacement might be considered as a metric in some part of the work reported in this thesis.

3.4.3 Microneurography

As mentioned in the previous chapter, LTMRs encode tactile information into electrical activity on the afferent nerves. This electrical activity is a succession of evoked potentials, often referred to as a spike train. Spike trains have been studied to determine how tactile information is encoded (Johansson and Flanagan [2009]). Spike

trains have been measured on animals (e.g. on cats Hayward et al. [2014]) and humans (McGlone et al. [2012]). The method used is referred to as microneurography (Vallbo et al. [2004]). Microneurography makes use of epoxy insulated tungsten microelectrodes, which are inserted into the subject's nerve. The microelectrodes have a diameter of 200 µm and a tip of diameter 5 µm. These microelectrodes are therefore small enough to target single nerve fibers with minimal discomfort. Recording of the nerve signal can then be carried out using signal amplifiers and a data acquisition system. However, being able to carry out microneurography correctly requires specific trainings and adequate equipments, as well as specific ethic's clearance. Even though the contribution of this technique could be beneficial for the work presented here, logistic, time and skills made the technique out of our reach. Nonethelss it would be considered in future collaborations.

3.4.4 Perceived Strength

Finally, perceived strength being the exact quantity that needs to be improved to deliver better and more salient mid-air haptic patterns, it is natural to consider it as a metric. Unlike the previous two metrics, perceived strength refers to a subjective judgement the user will make of a given mid-air tactile pattern. Therefore, there is no method to estimate it without querying the user itself.

Nonetheless, psychophysical techniques have been developed to measure such subjective judgments users make (Jones and Tan [2012]). While most of these techniques are focusing on whether a given stimulus will be detected, or whether two stimuli will be discriminated between, there are a few scaling techniques. Scaling techniques includes techniques such as the Likert scale, the visual analog scale and magnitude estimation. The common point in these scaling techniques lies in asking the user to rate a given stimulus according to a specific dimension. The rating is usually a number, and these methods vary according to how free the users are to choose this number. For instance, if someone was to rate the roughness of a given stimulus, they would be asked to give the stimulus a low rating if it was perceived to be smooth and a high rating if it was perceived to be rough. With the Likert scale, the rating scale is discrete (usually from 1 to 7), while with the visual analogue scale, the rating is continuous between a minimum and a maximum value (usually users will be presented with a slider). On the other hand, magnitude estimation is an open scale, and therefore users are free to rate the stimuli without being bound to a predefined scale. However, to account for participants using different scales, magnitude estimation requires results to be normalised within participants before being compared across participants.

Scaling techniques are easy to implement and if applied to perceived strength, they directly measure the quantity that mid-air haptic pattern rendering methods are aiming to optimise. Furthermore, magnitude estimation has already been applied for a similar task (Strohmeier and Hornbæk [2017]) and the literature has presented a systematic method for analysing the results (Han et al. [1999]). For these reasons, scaling techniques and especially magnitude estimation will be the preferred method for measuring perceived strength throughout the work reported in this thesis.

This section presented four metrics that could be used to assess mid-air haptic shape rendering method, and especially shape perceived strength. While ARP seems the natural candidate as it is the only metric that depends only on the hardware and algorithms, rather than on users' skin properties or users' perception capabilities, it has been shown that ARP is too complex to use efficiently. The second candidate considered was skin deformation. While skin deformation has also proved to be too complex to measure, some sensible simplification could be made to make the results usable for the purpose of comparing mid-air haptic pattern rendering methods. The third candidate considered was microneurography. However, microneurography will only provide limited information (i.e. only detection) and will not be able to answer questions such as "which patterns feel stronger?". Finally, perceived strength, measured via magnitude estimation, a scaling technique, was argued to be the easiest and the most sensible of all four metrics to use. Therefore, perceived strength will be the preferred metrics used in the work presented here.

This metrics will be used to measure - directly or indirectly - the perceived strength of a mid-air haptic shape. Recall that shape, is the building block of mid-air haptic patterns, onto which any tactile sensation, either discriminative or affective, can be mapped. It has been discussed that currently, UPAs are the most appropriate technology for rendering spatially distributed mid-air haptic patterns, because of its high spatial and temporal resolution, as well as its large interactive zone. However, the technology relies on a recent modulation technique referred as spatiotemporal modulation. Spatiotemporal modulation moves rapidly and repeatedly a tactile point into a predefined trajectory according to the shape one wants to convey. However, it is the first time, both for contact and contact-less, devices that such stimulus can be produced. Therefore, it is unknown what is the best approach to render mid-air haptic pattern with STM. For instance, should the pattern be repeated at a rate similar to that used for vibrotactile stimuli, or should it be rendered at a speed adapted to the temporal resolution time of touch? The next chapter will explore this research question.

Chapter 4

Rendering Speed

As discussed in the previous chapter, Spatiotemporal Modulation (STM) is an effective technique for conveying spatially distributed mid-air haptic patterns. However, being a relative new technique, little research on the perception of STM patterns has been carried out. In this chapter, we study what should be the main parameter to consider when producing a given pattern shape.

4.1 Theory

With the arrival of gesture tracking technologies (Kinect, Leap Motion), the interaction space is no longer constrained to tangible surfaces and can now move to mid-air. The previous chapter presented ultrasonic phased arrays (UPAs) as the leading technology for producing mid-air haptic stimuli (see section 3.1). Furthermore, we saw that STM was better suited to produce mid-air haptic patterns compared to amplitude modulation (AM) and lateral modulation (LM), which can only render a few points at a time. Recall that in STM the position of a single focal point is rapidly and repeatedly updated so as to describe a pattern by moving along a continuous trajectory, while the intensity remains at its maximum. Spatiotemporal modulation can still induce tactile sensation as mechanoreceptors are sensitive to motion (Johansson and Flanagan [2009]). Additionally, the temporal resolution of touch perception is only of a few milliseconds (the exact value may range from 2 ms to 40 ms according to Loomis [1981]). Therefore, if the focal point can complete the trajectory faster than the temporal resolution, the users will perceive the resulting stimulation as a single tactile pattern rather than a succession of tactile points or a moving sensation (see Figure 1.b). The effect is similar to the persistence of vision, whereby a source of light can be seen as a shape and not distinct points, when moved fast enough.

As far as we know, the perception of STM pattern has not been studied, and so it is unclear as how its parameters should be chosen to maximise the created sensation. One naïve approach would be to consider the rate at which patterns are drawn (we defined this rate as the spatial modulation frequency -F_{STM} for short-) and assign that rate to be the same as the amplitude modulation frequency (i.e. having $F_{\mathrm{STM}} = F_{\mathrm{AM}}$). The argument behind this approach is that if the pattern is periodic, each point forming the pattern will be repeated at a given frequency as in the case of amplitude modulation. For instance, if one observes the acoustic field in one position of the pattern, one will note an alternation of high and low acoustic power, which correspond to the focal point coming and going from this position, with a rate equal to F_{STM}. The observation that the displacement at a stationary point in the pattern looks a lot like amplitude modulation, and therefore one could optimise F_{STM} the same way one optimises F_{AM}, leads to fixing F_{STM} to 200 Hz or thereabouts. However, the average acoustic power present at that position will be far weaker than having an amplitude modulated focal point at this position, especially for large patterns.

Another approach is to consider the speed of the focal point during the stimulation (referred to as FP_{speed}). If L is the length of a given spatiotemporally modulated pattern, then we can define $FP_{\mathrm{speed}} = F_{\mathrm{STM}} \times L$. A useful analogy to spatiotemporal modulation can be made involving trains, where the carriages (analogously to focal points) move along the rails (here the pattern) and produce vibrations on the soil (similarly to the skin). To further continue the analogy, it has been both numerically predicted and experimentally demonstrated that in high speed rail networks, ground vibrations can be amplified when the speed of the travelling trains approaches or exceeds the speed at which the surface waves propagate in the ground (Krylov [1995], Krylov et al. [2000]). In the light of recent studies, which show that tactile stimuli produce surface waves that propagate on the skin and affect our perception (Delhaye et al. [2012], Manfredi et al. [2012], Shao et al. [2016]), the above train analogy becomes even more likely for the case of spatiotemporal modulation when surface waves are considered.

Therefore, we hypothesise that if the focal point moves at a correct speed, constructive interference will result and the deformation it induces could amplify the propagating surface wave it produces and *vice versa*. We then predict that there is an optimal speed for which the deformation induced with a focal point is amplified to a maximum, and moreover the required speed is equal to the propagation speed of surface wave across the skin. We further hypothesise that the speed of the focal point will have more impact on the resulting perception than F_{STM}, due to the

predicted surface wave effect.

Before discussing how we test this hypothesis it is worth remembering that the focal point motion is not continuous but discrete. Indeed, the focal point position is updated sequencially via the digital driving electronics that composed it. While the time interval between two updates is constant the distance between two subsequent positions can differ. This distance is function of the device sampling rate, the pattern spatial modulation frequency and the pattern total length. However, for all the patterns studied here, this distance is much smaller than the focal point diametre, and therefore the motion can be considered as continuous. The implications of a discrete motion are discussed in the Chapter 5.

To test our hypotheses and investigate whether the surface wave phenomenon in our analogy also holds true for spatiotemporally modulated patterns, we ran a series of vibrometry measurements where we recorded spatiotemporally modulated circles of different radii that were drawn at different speeds. A complementary user study was also performed to assess whether there was any effect of the spatiotemporal modulation speed of circular patterns on the perceived intensity of tactile sensations.

4.2 Vibrometry Study

In this study, we wanted to test for the existence of an optimal speed to drive spatiotemporally modulated patterns, which would ideally induce maximal displacement on a surface. We believe that the optimal focal point speed should be equal to the surface wave propagation speed. Additionally, we hypothesise that speed related effects on displacement are greater than frequency related effects. In other words, there should be an optimal speed that maximise the surface displacement, independently of the pattern size. To measure the displacement induced with spatiotemporally modulated patterns, as well as their interference with resulting surface waves, we ran a series of vibrometry measurements.

4.2.1 Measurement Set-Up

Our measurement set-up was composed of three main elements: An ultrasonic phased array to produce spatiotemporally modulated patterns, a silicone slab on which the patterns were projected and a Laser Doppler Vibrometer to measure the displacement induced by the spatiotemporally modulated patterns (as shown on Figure 4.1).

The ultrasonic phased array we used was a Ultrahaptics Evaluation Kit from

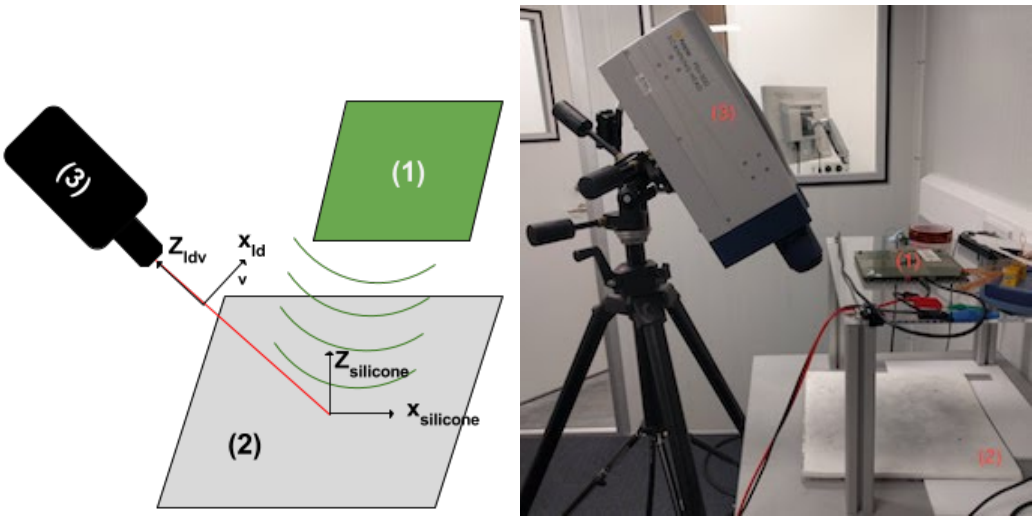

Figure 4.1: The Experimental Set-up was composed of 3 main elements 1)An ultrasonic phased array, 2) A silicone slab and 3) A Laser Doppler Vibrometer

Ultrahaptics Ltd.[1] and was composed of 16×16 (i.e 256) ultrasound transducers. The ultrasonic phased array is producing focal points 8.6 mm in diameters at a given position and with a given acoustic power. The produced output can be updated with a 16 kHz sampling rate.

The spatiotemporally modulated patterns were projected on a 35 cm×35 cm wide and 1 cm thick slab, cured with commercially available silicone, Ecoflex 0010[2], which was used as a mechanical analogue for human skin. The use of silicone rather than human subjects, provided control over the measurement condition. Ecoflex 0010, was selected as an analogue for human skin due to it having a similar density ($1100\,\mathrm{kg\,m^{-3}}$ for human skin, where the silicone is $1030\,\mathrm{kg\,m^{-3}}$) and similar viscoelastic material properties in both surface effects and in bulk (Kearney et al. [2015], Royston et al. [2011]). We acknowledge that the mechanical behaviour of Ecoflex will not be the identical to real skin, due to human skin being a much more complex structure (e.g., multiple layers and anisotropy) (Gerhardt et al. [2008]), however, it is thought that the vibrometry of silicone will provide insight into the general behaviour of viscoelastic materials when excited by focused ultrasound.

Due to the small amplitude of the vibrations, we used a laser Doppler vibrometer (abbreviated to LDV) to measure them. The LDV is a common tool to carry out non-contact vibration measurement (Manfredi et al. [2012]). Vibrometry data is obtained by firing a laser beam from the LDV towards the surface to be measured and capturing reflected incident photons using a photodetector diode also inside the

[1]https://www.ultrahaptics.com/products/evaluation-kit/
[2]Ecoflex 0010: https://www.smooth-on.com/products/ecoflex-00-10/

LDV head. Differences between the original and reflected laser signal are analysed to find the vibration modes of the reflecting surface based on the Doppler effect. For this study, we used a PSV-500-Scanning-Vibrometer from Polytec[3].

The silicone was placed on an experimental bench, on top of which, the ultrasonic phased-array was maintained up-side down with a stand, parallel to the silicone and at a distance of 28.5 cm. The LDV was placed at a 60° angle and pointed towards the silicone, which was 36.4 cm away from the LDV head. For each measurement scan, the LDV was measuring surfaces with a resolution of 1 mm. In other words, the distance between two consecutive measurement points was fixed to 1 1 mm. Each measurement point lasted 256 ms, was recorded with a sampling rate of 128 kHz and was repeated 6 times before being averaged. Each measurement was synchronised between the LDV and the Ultrasonic phased array using a trigger signal. Furthermore, a 50 ms null output was preceding and following each measurement. Two types of measurement were conducted: line measurements (see Section 4.2.2) and square measurements (see Section 4.2.3). The line measurements involved a 17.5 cm long section of the silicone and lasted 30 minutes, while the area measurements covered an area of 10 cm×10 cm and lasted 105 minutes. Micro-reflective beads were spread on the surface of the silicone to improve laser reflection and hence measurement quality.

The raw data obtained from the LDV is composed of the velocity over time for each coordinate position on the measured surface. Firstly, due to the 60° between the LDV and the silicone, the measurements from the LDV were in a different coordinate space relative to the silicone (see Figure 4.1). Using a Python script with the `scipy` package, we pre-processed the data, transforming each point into the correct basis using projective geometry. Further, measurements were carried in an anechoic room and band-pass filtered to remove the ultrasonic 40 kHz carrier frequency and remaining noise, where the low cut-off was at 50 Hz and the high cut-off frequency at 1 kHz. Finally, to be able to work with displacement data, we applied a time integral on the velocity data, hence obtaining the variation of displacement over time rather than the variation of velocity over time. We describe how we used the displacement data, according to the information we wanted to extract, in sections 4.2.2 and 4.2.3.

[3]https://www.polytec.com/uk/vibrometry/products/full-field-vibrometers/psv-500-scanning-vibrometer/

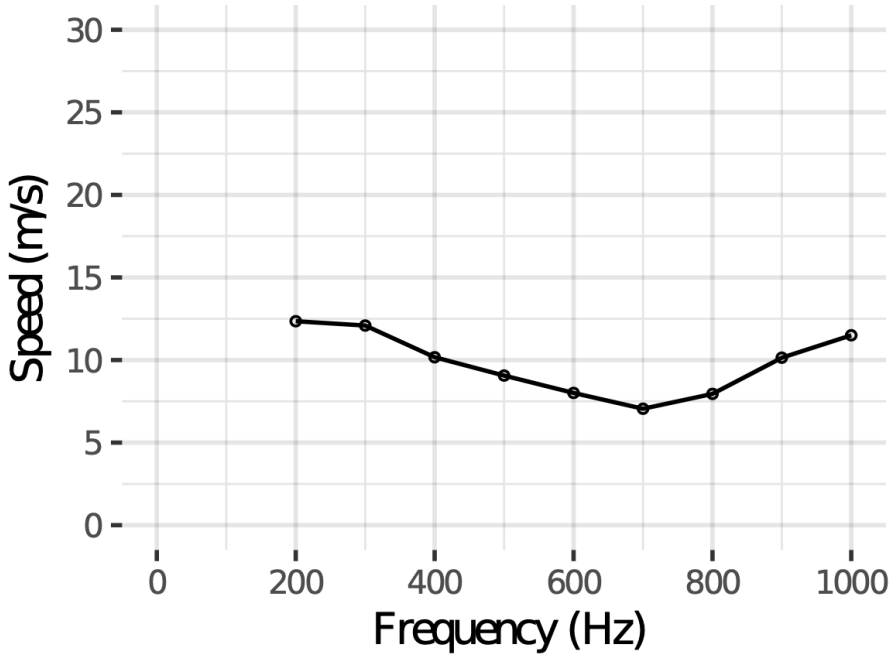

Figure 4.2: Measured surface wave propagation speed in the silicone slab. Speed averaged around $10\,\mathrm{m\,s^{-1}}$

4.2.2 Preliminary Measurement

Our study focuses on the displacement induced by the spatiotemporally modulated patterns and their associated surface waves. However surface waves propagate differently on different media, hence our first step was to characterise the surface wave propagation on the silicone we were using. To that end, we generated a focal point at the centre of the silicone slab and measured how induced surface waves propagated away from the position stimulated. As the silicone is a dispersive medium, surface waves with different frequencies travel at different speeds. To measure this we modulated the focal point at known frequencies ranging from 200 Hz to 1 kHz with 100 Hz steps. We assumed the silicone to be an homogeneous and isotropic medium, and therefore focus our measurements on a single line going from the silicone slab centre towards the edge (17.5 cm long in total). From the measurements data, we extracted the surface wave propagation speed and the frequency response of the silicone.

Surface wave propagation speed

To extract the surface wave propagation speed across the silicone, we calculated the speed at which wavefronts of surface waves propagated along the measured direction and took the average of repeated measurements of the speed. As predicted,

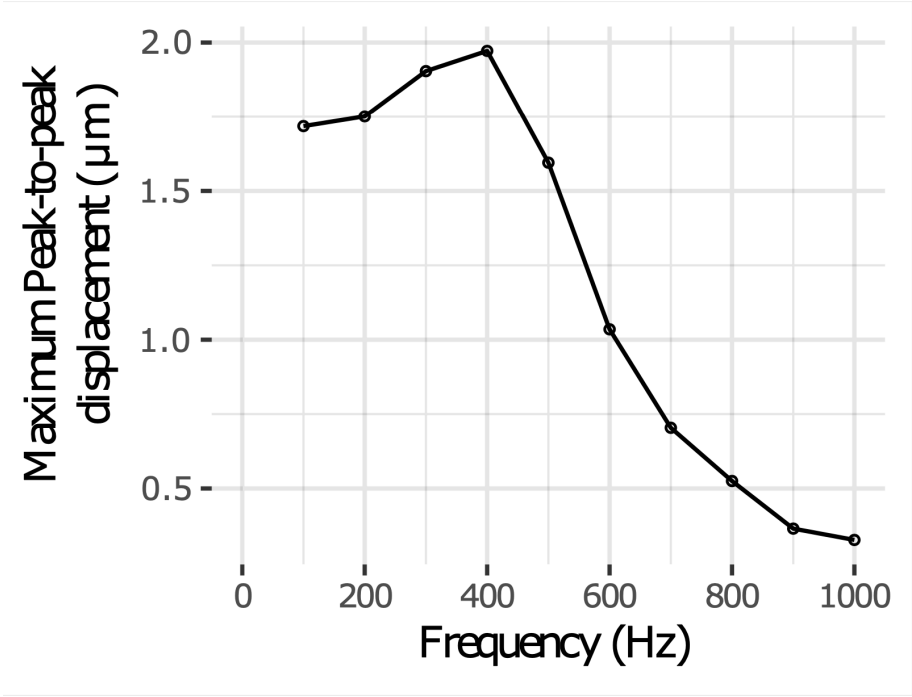

Figure 4.3: Measured frequency response in the silicone slab. One can see the silicone resonance behaviour around 400 Hz.

the surface wave propagation speed varied with the frequency (see Figure 4.2) but remains in the interval of $7\,\mathrm{m\,s^{-1}}$ to $13\,\mathrm{m\,s^{-1}}$, and has for average $10\,\mathrm{m\,s^{-1}}$. The average propagation speed is slightly greater than the one measured by Manfredi et al. on the fingertip, but the general trend is similar (Manfredi et al. [2012]). Therefore, we assume the difference in mechanical behaviour between the two media to be responsible for the differences observed.

Frequency response

To extract the frequency response of the silicone, we analysed the maximum peak-to-peak displacement at the focal point position and repeated over the frequency range. We found that the peak-to-peak displacement was also varying with frequency (see Figure 4.3) and was maximum at 400 Hz. This result suggests that the silicone slab has a resonant frequency at 400 Hz. It is sometimes suggested that human skin also possess a resonant frequency around 200 Hz (Manfredi et al. [2012]). Once again, we assume the differences in material properties to be responsible for the difference in the measured resonant frequency.

Overall, we can see that the silicone measurement shows similar behaviour to the skin even though the exact values differ.

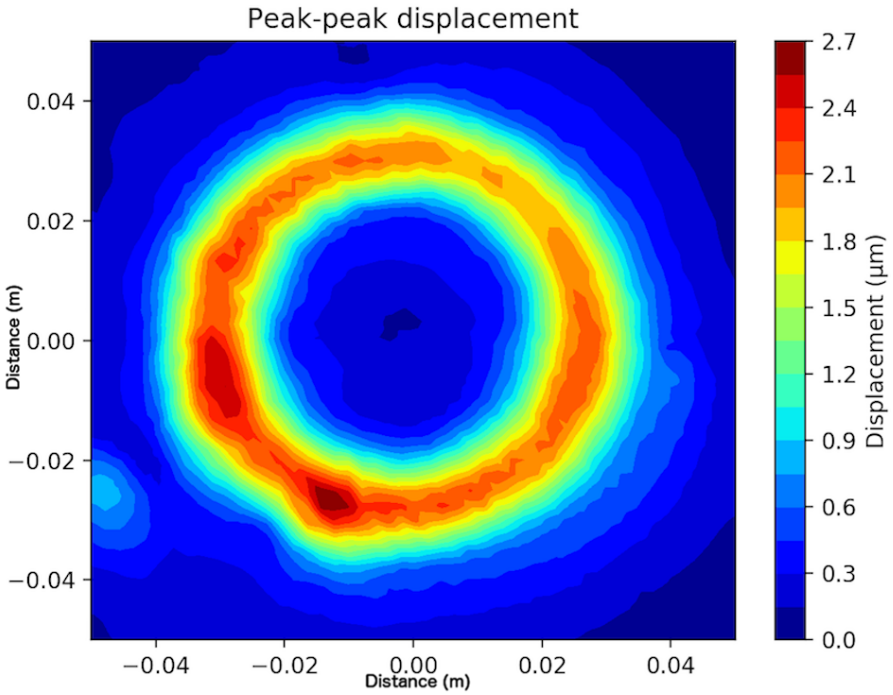

Figure 4.4: Example of the measurement obtained for the root-mean-squared of peak-to-peak displacement produced by a circular pattern.

4.2.3 Spatiotemporally Modulated Patterns

After characterising the surface wave propagation speed on the silicone and the silicone frequency response, we undertook to investigate the effect of surface waves on the displacement that spatiotemporal patterns induced. To that end, we generated a spatiotemporally modulated circular pattern, with its centre matching the silicone centre (equivalent to Figure 4.4). We chose a circular pattern for its numerous properties (continuous, periodic, without self-crossing points), which limits possible pattern-specific artefacts. We then used the LDV to measure a square area of the surface encompassing the pattern (see Figure 4.4). As defined in the introduction, knowing the pattern length (here the circle perimeters), one can go from the focal point speed to the spatiotemporal modulation frequency as follow: $FP_{\text{speed}} = F_{\text{STM}} \times$ perimeter. To compare the different effects of FP_{speed} and F_{STM} individually, we repeated the measurement while varying the perimeter and FP_{speed} each in turn. In our data set, we had 3 different circle perimeters of 5 cm, 10 cm, and 20 cm of perimeter. We chose these circle sizes as they could fit the user's palm that is 7.5 cm-9.5 cm wide on average (Komandur et al. [2009]). We picked 8 speeds around the measured average surface wave propagation speed and 4 additional speeds that match to 4 frequencies around the measured resonant frequency. Yet, for certain perimeter lengths, some speed values overlapped, making for somewhere between 9

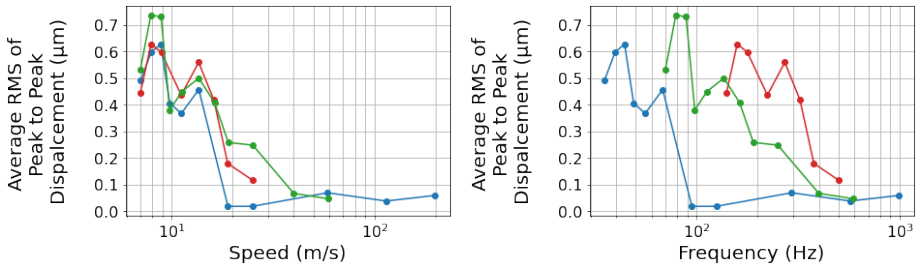

Figure 4.5: Left: Average root-mean-square of peak-to-peak displacement as function of speed for circular patterns with different perimeters. Right: Average root-mean-square of peak-to-peak displacement as function of draw frequency for circular patterns with different perimeters. Red: 5cm circumference circle, Green: 10cm circumference circle and Blue: 20cm circumference circle

and 12 distinct speeds measured per perimeter. In total 32 area measurements were taken. For each measurement, we computed the root-mean-square value of peak-to-peak displacement and extracted the average value along the measured circular path (see Figure 4.4).

4.2.4 Results

In Figure 4.5-left, we plotted the measured average root-mean-square values of peak-to-peak displacement induced by focused ultrasound on circular patterns with different perimeters, for which spatiotemporal modulation is run at different speeds. The root-mean-square of peak-to-peak displacement was computed by taking the peak-to-peak displacement for each pattern iteration and taking the root-mean-square of each peak-to-peak displacement henced obtained. These results show that the quantity of displacement varies with the focal point speed but remains similar across circle perimeters. However, when ploting the same results as a function of draw frequency, the trends across circle perimeters disapears (Figure 4.5-right). Moreover, the displacement is maximum for speed between 8 and 10 $\mathrm{m\,s^{-1}}$, which corresponds to the average of the surface wave propagation speed measured previously. Therefore, the results seem to support our hypothesis about a constructive interference between spatiotemporally modulated patterns and the wave surfaces they produced, when the focal point speed matches the speed of the surface waves propagation. Additionally, the results show a second maximum appearing at a focal point speed of 20 $\mathrm{m\,s^{-1}}$, which corresponds to twice the propagation speed of the surface waves. This behaviour that could be anticipated from the periodic property of the studied pattern is reminiscent of the kind of behaviour governed by "harmonics" often found in acoustics. Finally, the data does not show any evidence of a

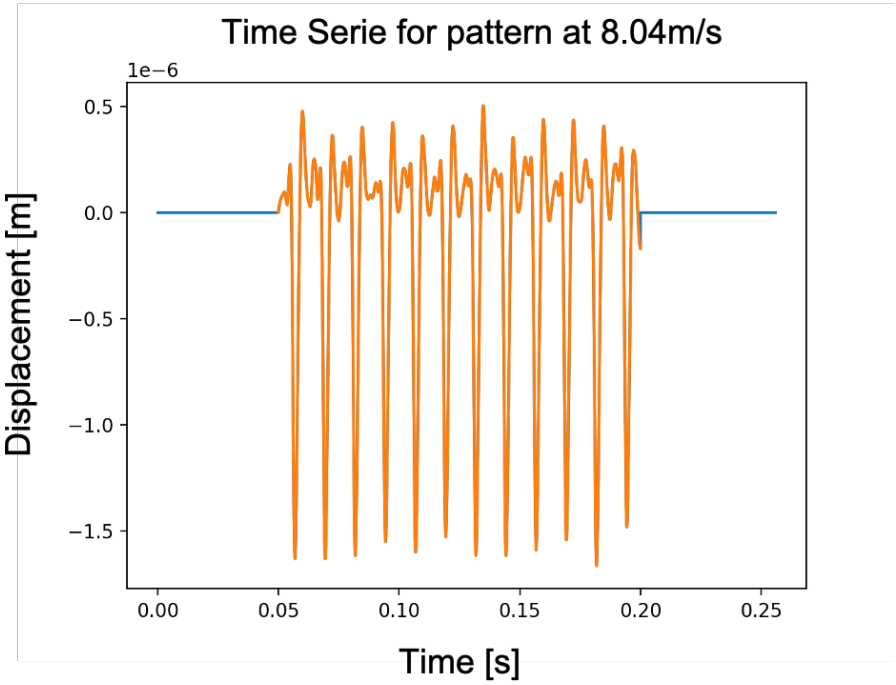

Figure 4.6: Time Series of Silicone Displacement for a point on the circular pattern (here 10cm circumference circle). In blue are the break period before and after the stimulation, and in orange is the stimulation itself. One can note that the displacement peaks at a frequency equalt to the pattern draw frequency (here 80Hz).

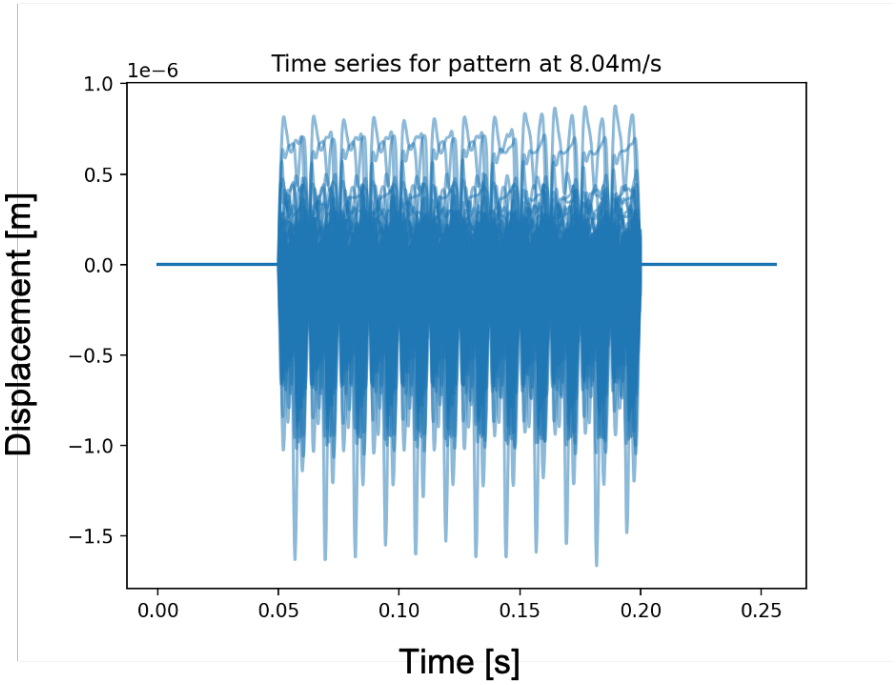

Figure 4.7: Time Series of Silicone Displacement for all points on the circular pattern (here 10cm circumference circle). One can note that the displacement increases and decreases at a frequency equal to the pattern draw frequency (here 80Hz).

resonating mode, which should appear at 20, 40 and 80 $\mathrm{m\,s^{-1}}$ for the perimeters 5, 10 and 20 cm, respectively.

As additionnal analyses we look at the time series of the silicone deformation. For instance, figure 4.6 shows the time series of displacement for a point on the circle 10cm drawn by a focal point moving at 8m/s (i.e. draw frequency 80hz). Note that this specific pattern, is the pattern that yields the greatest RMS of peak to peak displacement (see Figure 4.5). In this figure we can see that the displacement peaks at a rate equivalent to the draw frequency. This shows that the pressure applied on the silicone by the focal point is the main cause of the displacement. However, our hypothesis is that wave propogation and focal point yields to constructive interference and by extension greater peak to peak displacement. Yet, the peak displacement seems to be maximum from the first iteration, which could mean that the contructive interferences occur in the first iteration.

To highlight this effect, we decided to plot on one graph the times series of all the points on the circle. If our hypothesis is correct, we should see an increase in peak displacement over time and then a plateau after the first iteration. However, as we can see from figure 4.7, we cannot see a plateau occuring, on the contrary, peak displacement seems to increase and decrease over the iteration of one pattern. An explanation for this, is the irregular RMS peak to peak displacement over the circle as highlighted in figure 4.4. As already explained, these variations in the RMS peak to peak displacement are due to the angled LDV in our setup. Therefore, we concluded our measurements were too noisy to provide such a level of analysis. Nonetheless, we deemed our results presented in Figure 4.5 to be convincing enough.

The conclusion of the current vibrometry study was finally that varying the spatiotemporal modulation speed has a large effect on the indentation of the silicone along circular patterns. Because silicone Ecoflex-0010 possesses numerous similarities with human skin, it is likely that an equivalent amplification phenomenon could be observed on human skin, but it is difficult to predict to what extent. However, repeating the above measurement on human skin will not inform us about the consequences on the haptics of such spatiotemporally modulated patterns as they will be influenced by perceptual effects beyond simple displacement. To investigate the perceptual implications and especially the patterns perceived strength, we decided to run a user study with similar spatiotemporally modulated patterns. We hypothesise that there will be an effect of speed on the haptic stimulus perceived strength, although the nature of the interaction with haptics and whether it is detectable is not immediately clear.

4.3 User Study

In this user study, we assessed the perceived strength of haptic circles of different sizes and speeds, using a scaling technique (see Section 3.4.4). To this end, users rated the intensity of 39 different circles: 3 sizes (i.e. perimeter of 5 cm, 10 cm, and 15 cm) and 13 speeds (i.e. from $2\,\mathrm{m\,s^{-1}}$ to $20\,\mathrm{m\,s^{-1}}$ with gaps of $1.5\,\mathrm{m\,s^{-1}}$). The different conditions (i.e. sizes and velocities) were fixed after pilot testing involving 15 people. Users rated each condition 3 times, giving a total of 117 trials (i.e. 39×3).

4.3.1 Study set-up and procedure

First, users were given an oral introduction to the study and the software used, before signing a consent form. They were invited to sit comfortably on a chair in front of a computer screen and asked to place their left-hand on a custom-made armrest that was built as a box integrating the mid-air haptic device. Users would then put their left palm above an opening, so that they can perceive the haptic stimulus from below. They were then invited to wear headphones playing white-noise to remove auditory cues and were given two trials to familiarize themselves with the haptic set-up and the software. Users were asked not to move the left hand during the experiment and used the mouse with their right hand to answer the questions displayed on the screen between stimuli.

The study itself involved a succession of 117 trials. In order to avoid any order effects, trials were pseudo-randomized. To move to the next trial, users were instructed to click on a next button on the screen in front of them. Then, a four-second countdown was displayed and the haptic stimulus was then played for five seconds. After each stimulus, the users were asked on screen if they perceived it. If so, they were invited to rate the intensity of the haptic pattern using a ratio scaling method of magnitude estimation, which can be used to find the optimal parameters of a device (Jones and Tan [2012]). This approach is composed of 2 steps: (1) ask participants to rate the intensity of the stimulus on an arbitrary scale chosen by the participant and (2) normalize the values of each participant. No discrimination nor other qualitative information were asked during the experiment.

A combination of two software parts was used in the study: `c++` for programming the mid-air haptic device, and `c#` for presenting questions.

We recruited 16 users (mean age 30.0 ± 4.5, 3 female). Users had no touch, or auditory impairments. The experiment lasted on average 35 minutes. An ethics approval was obtained in advance.

		Perimeter		
		10	15	
Perim.	10	0	.901	
	15	0	.856	0.960

Table 4.1: Correlation matrix of the intensities ratings for the 5,10 and 15cm perimeter.

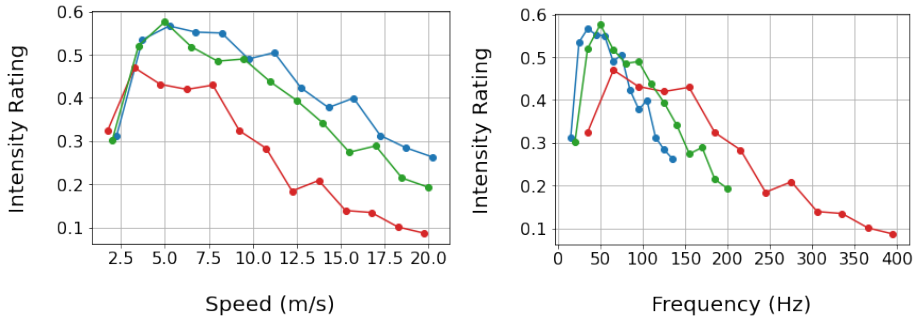

Figure 4.8: A plot of the intensity ratings of the haptic feedback by perimeter size as function of speed (left) and frequency (right). Red: 5cm perimeter, Green: 10cm perimeter, Blue: 15cm perimeter

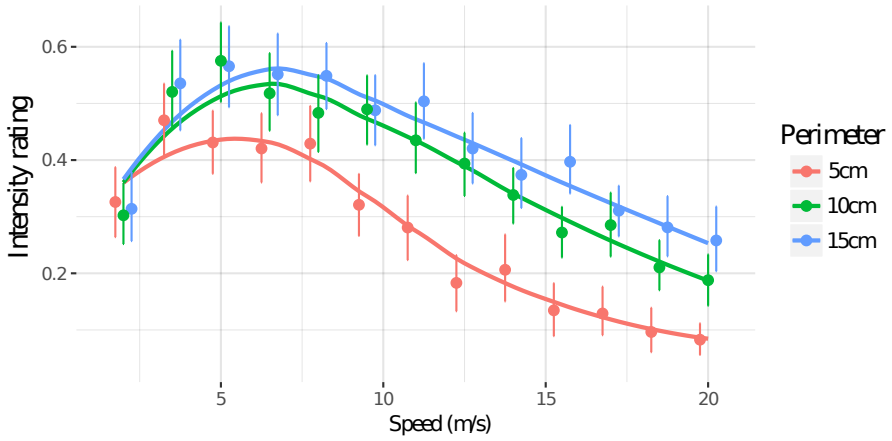

Figure 4.9: A plot of the intensity ratings of the haptic feedback by perimeter size.

4.3.2 Results

The data collected was normalized between 0 and 1 for each participant. Non-felt stimuli were set at 0. In order to assess if the speed of the point was driving the intensity felt by participants, we separated the data into 3 groups, depending on the perimeter of the circle used for the feedback. These results are plotted as a fucntion

of speed (Figure 4.8-left) and frequency (Figures 4.8-right). One can see that as in the vibrometry study, the different size circles seems to follow the same trend when we plot them as a function of speed. A detailed plot of the intensity ratings as a function of speed can be observed in Figure 4.9.

To check if our observation was correct, we then averaged the data for each speed and computed the Pearson correlation coefficients between the different pairs of perimeter sizes. The Pearson correlation was used here to test whether the curves were following the same trend. It is accepted that a pearson correlation coefficient greater than 0.8 indicates strong positive correlations between the two sets. The results are summarized in Table 4.1. The coefficient of correlation of intensity between the three perimeters show that the haptic feedback strength is correlated with the pattern speed.

However, it is worth noting here that the correlation coefficient is not equal to 1, which means that the correlation of the results according to speed is not perfect and that some other parameters comes into play. From the Figure 4.9 one can see that size could be another factor, especially since ratings for the smaller size seem constantly lower than for the two other sizes. We will discuss this observation in the next section.

4.4 Discussion

The vibrometry study showed that the variation in silicone displacement, caused by spatiotemporally modulated patterns, is a function of the spatiotemporal modulation speed. Moreover, the displacement seems independent of the circle perimeter and is maximised when the focal point speed equals the surface wave propagation speed. These results suggest that there is constructive interference occurring between spatiotemporal modulated patterns and the surface waves they induce, which leads to an amplification of the silicone displacement. However the results show no relation between silicone resonant frequency and displacement, even though the patterns studied were periodic. One could argue that variations in medium mechanical properties will lead to different results (see Section 2.2.1). Hence, future work will investigate the effect of spatiotemporal modulation on silicone slabs of different mechanical properties. Ultimately, measurement on human skin would more conclusively prove the amplification phenomenon existence we describe. Yet, such measurements on human skin could be proven challenging, as we will discuss later in this thesis.

The user study showed that the tactile pattern perceived strength is also a func-

tion of the spatiotemporal modulation speed. Moreover, the results showed that user's perceived strength was greater for the circles drawn around 5 and 8 $\mathrm{m\,s^{-1}}$, which is close to the surface wave propagation speed of 7 $\mathrm{m\,s^{-1}}$ measured on human fingertips (Manfredi et al. [2012]). The similarities between the vibrometry results and the user study results suggest that the increase in displacement measured in the vibrometry study is responsible for the increase in perceived strength in the user study. Therefore one could conclude that matching spatiotemporal modulation speed with surface waves propagation speed ensures the maximum perceived strength for human participants experiencing the tactile patterns.

One could argue that an individual mechanoreceptor, along the stimulation path, perceives a periodic signal with a given frequency. Therefore, to optimise the perceived strength, the stimulation frequency should match the mechanoreceptor frequency response (see section 2.2.2). Yet, no relation between pattern frequency and pattern perceived strength was found. Therefore, in the current study, the effect related to spatiotemporal modulation speed prevails over any effect related to the mechanoreceptors' frequency response.

Additionally, the user study shows, to a lesser extent, that perceived strength is a function of the circles' perimeters. The 5 cm perimeters were perceived to be weaker than those with 10 and 15 cm perimeters. We believe this effect might result from the fact that the 5 cm circle covers less surface area than the other two circles sizes, and therefore involves spatial summation (Gescheider et al. [2002]). However, with the current data set, no significant differences were observed after performing a one way anova test. Nonetheless the lack of significance might also be due to the dataset not being design to test this hypothesis. We suggest that further investigations are required to test for the relationship between pattern size and pattern perceived strength.

Our results have implications for the design of mid-air tactile stimuli, highlighting the importance of focal point speed as a parameter in the tactile patterns perception. When scaling up or down a given tactile pattern, the spatiotemporal modulation frequency must be scaled accordingly to maintain a constant STM speed, and hence insure a similar perceived strength of the tactile pattern. For instance, let's consider a circular pattern of perimeter P_1, our study show that the pattern should be driven at a rate $F_{\mathrm{STM}_1} = FP_{\mathrm{speed}} \div P_1$, where FP_{speed} produces the desired perceived strength. To scale that circle such as $P_2 = 2 \times P_1$ then, the spatiotemporal modulation frequency will need to be updated such that $F_{\mathrm{STM}_2} = 2 * F_{\mathrm{STM}_1}$. Being able to scale up and down a given pattern is particularly useful when rendering 3D-volumetric shapes (Long et al. [2014]). Adapting our results to more complex

and abstract patterns could prove challenging and would certainly require further investigations.

The present chapter introduces the first study investigating the parameter space of Spatiotemporal Modulation. Through both vibrometry and user study, we show that draw speed has a bigger impact on perceived strength than draw frequency. However, while designing the user study we noticed that draw frequencies below 10 Hz could not be perceived, independently of the associated draw speed, and therefore these were not tested in the present work. Nonetheless, we know from vibrotactile perceptual space, that frequencies below 10 Hz can be perceived. Hence, we hypothesise that another element of the STM parameter space was limitating the range of the perceptual space. The next chapter investigates a potential candidate responsible for this phenomenon, namely, the pattern sampling rate.

Chapter 5

Rendering Update Rate

The previous chapter presented the predominance of draw speed over draw frequency when seeking to optimise the perceived strength of mid-air haptic shapes. While this was the first study that attempted to extablish a relationship between spatiotemporal modulation (STM) parameter space and spatiotemporal perceptual space, a limitation of that space could already be observed. Indeed, draw frequencies lower than 10 Hz could not be perceived. This fact is all the more surprising as localised haptic perceptual space includes a stimulus at frequencies lower than 10 Hz. In the current chapter, we therefore investigate the effect of another parameter from spatiotemporal parameter space, namely the number of points per mid-air haptic pattern. While the number of points per pattern has been proved to affect haptic feedback quality (Campion and Hayward [2005], Choi and Tan [2007]), we will show in this chapter how the number of points per pattern can affect overall pattern perception.

5.1 Sampling Strategy

With STM, a tactile pattern is produced using a single mid-air tactile point. Therefore, producing the pattern shape as well as its associated sensation requires rapid and repeated updates of the point properties. However this motion is not continuous. Being created with a digital system, any mid-air STM pattern are actually discrete and each pattern constitutes a succession of samples that are updated at a given rate. In this part, we discuss the update rate requirements and its relation to the number of points per pattern. Then, we present the current sampling strategy applied in the literature. Finally, we evaluate the current strategies in an effort to find a new, more optimal sampling strategy.

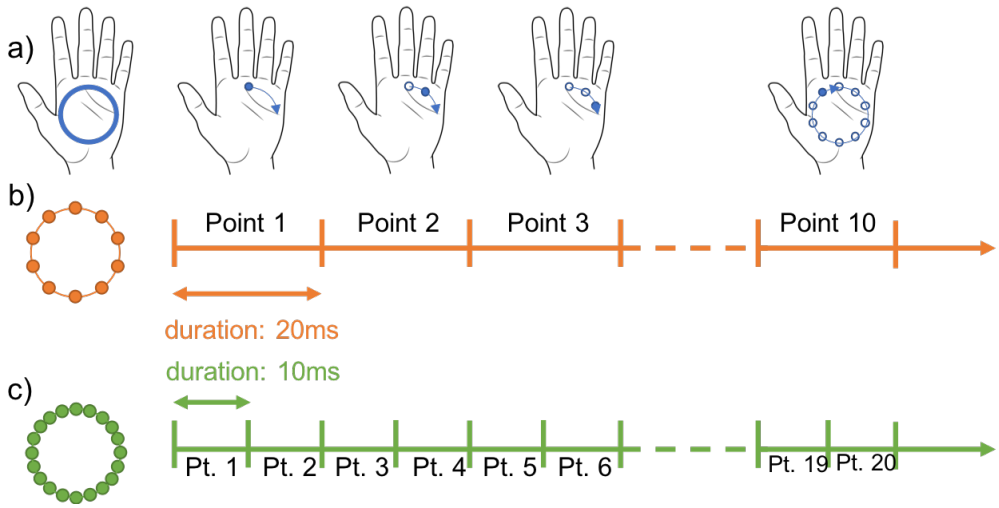

Figure 5.1: (a) A mid-air tactile pattern such as a circle is sampled into a set of successive positions, here 10. (b) Each sample point is presented during a given interval of time proportional to the total number of sample points. (c) Increasing the number of sample points will increase the rendering fidelity but will also decrease the stimulation duration of each sample point.

5.1.1 Number of points per Pattern

We saw in section 3.3 that a tactile pattern was composed of a shape and a sensation. However, tracing a pattern shape requires sampling the shape into a set of intermediate discrete positions, referred to as sample points (see Figure 5.1.a). When rendering the pattern shape, the tactile point position will thus be updated successively to each of those sample point positions. Hence no STM pattern is ever continuous but is instead discountinuous and the number of sample points per pattern may vary. However, the greater the number of sample points per pattern, the smoother the pattern representation. For instance a circle traced with 20 points will appear smoother than a circle traced with 10 points (see Figure 5.1-b&c).

With Amplitude Modulation, adjusting the tactile sensation is equivalent to tuning its modulation frequency (Obrist et al. [2013]). The modulation frequency being the rate at which a specific skin patch is repeatedly stimulated, in the case of STM the modulation frequency is similar to the rate at which the pattern is drawn, referred to as *draw frequency*. Indeed, drawing a circle at 5 Hz, means tracing out the circle path 5 times per second and therefore stimulating each position along the circle 5 times per second. Therefore, adjusting the tactile sensation is equivalent to tuning its draw frequency.

Furthermore, if there are 10 points per circle, it means that the point will move through each 10 positions 5 times a second. In other words, the point position

will be updated 50 times per second (5 Hz × 10 points). Thus, a mid-air tactile display, updating a given pattern, needs an *update rate* equivalent to the product of the number of points per pattern times the pattern modulation frequency (see equation 5.1).

$$\text{update rate} = \#\text{ of points per pattern} \times \text{draw frequency} \tag{5.1}$$

We would like to highlight that the update rate thus defined is not necessarily the maximum update rate that a mid-air tactile display can achieve. Therefore, for update rates lower than that achievable by the hardware, it is possible to increase either the number of points per pattern or draw frequency without decreasing the other. However, at update rates close to hardware maximum capabilities, a trade-off between number of points per pattern and draw frequency exists.

5.1.2 Current Sampling Strategies

We define as sampling strategy the tuning of number of points per pattern according to specific criteria. We found that all previous work use the same strategy that is to determine the number of points per pattern as the maximum update rate the hardware can achieve, divided by the draw frequency. For instance, Kappus and Long [2018] are producing a circle at 200 Hz using the full 20 kHz update rate achievable by the hardware used in their experiments. We believe the reason is that the researchers assume that the greater the update rate the better. This assumption seems pertinent as it is a strategy already being used for different modalities. For instance, in vision and audio a higher number of points per pattern will reduce artefacts such as motion blur and flickering, for vision, and aliasing, for audio. We referred to this strategy as the *high number of points per pattern strategy*.

5.1.3 Pros and Cons for High Number of Points Per Pattern Strategy

A high number of points per pattern strategy can support high draw frequencies without distorting the tactile pattern shape. For example, a simple pattern shape such as a 150 mm circumference circle can be rendered at 500 Hz (the upper limit of vibrotactile frequency relevant to touch) using 40 sample points spaced out every 3.75 mm. The spacing between two consecutive points being less than the tactile point radius (≈ 4.3 mm), one would expect that the pattern will still be perceived as smooth and continuous.

However, the problem is that a high number of points per pattern strategy results in shorter stimulation durations. Indeed, increasing the pattern resolution decreases the relative stimulation duration of each point. For example a device running at an update rate of 20 kHz, this means that the stimulation duration of one sample is 50 µs. This duration is 2 to 3 orders of magnitude lower than the perceptible sense of touch temporal resolution found by Loomis [1981] that was estimated to be between 2 ms and 40 ms. Moreover, this draw frequency is 2 orders of magnitude higher than the vibrotactile frequency range relevant to our mechanoreceptors. It is therefore unlikely that our skin can perceived such rapid tactile stimuli.

Another challenge of using a higher number of points per pattern strategy is the possible inconsistency in number of points per pattern between tactile patterns being traced with different draw frequency.

The discussion thus far has therefore revealed that pattern variability demands customised number of points per pattern, otherwise inherent variations will manifest themselves in an uncontrolled and misunderstood tactile perception. This chapter is addressing the above mentioned challenges and proposes mitigation strategies.

5.2 User Study 1

There are various modulation methods and sampling strategies that can produce a mid-air tactile pattern using focused ultrasound. These methods and strategies predominantly depend on the available hardware being used. There has not been however any discussion on how sampling strategy affects the overall pattern perception. This section describes how we undertook to investigate the relation between sampling strategy and pattern perception. In particular, we focus on the perceived pattern strength relative to the number of points per pattern.

5.2.1 Method

Our hypothesis was that the number of points per pattern will have an effect on the perceived strength. To test this, we ran a magnitude estimation task (Jones and Tan [2012]). In this task, participants had to estimate the perceived strength for patterns rendered with different number of points per pattern.

In total 26 participants took part in the user study (6 females, average age±SD: 29.3 ±5.2). Participants were sitting comfortably on an office chair, which they were free to adjust to their liking. On the left of the participant, there was an acrylic box, roughly at their hip level. The box was 200 mm high and a mid-air tactile display UHEV1 from Ultrahaptics Ltd. was lying at the bottom of the box. An aperture was

Figure 5.2: The set-up for the user studies. Participants were perceiving the mid-air tactile pattern on their left palm while rating each pattern on a designated laptop.

cut on the top box, so participants can rest their left hand over it while experiencing the different mid-air tactile patterns. Before starting the study, an initial focal point was presented to the user hand, so they can align their palm with the array output. To avoid participants' responses to be biased by surrounding noises, participants were wearing noise cancelling headphones which were playing pink noise. On the desk, in front of the participants, a laptop was running the experimental protocol. Participants could read instructions from the laptop screen and input their strength estimates via a computer mouse. Figure 5.2 shows the overall set-up.

To test our hypothesis we used a set of patterns with various number of points per pattern. To avoid shape related effects, all of these were variations on a circular pattern. All patterns were a 150 mm circumference circle (i.e. $\approx$ 24 mm centimetre radius), as it covers most of the palm of the participant (human palm width mostly varies between 75 mm and 95 mm (Komandur et al. [2009])). Circles have also a clear periodic property and their sample points can be easily made equally spaced, all of these limiting possible artefacts due to shape geometry. In this study, we also wanted to test whether the number of points per pattern will affect the sensations of different patterns equally. Therefore we picked 6 different draw frequencies for the presentation of the pattern, as to cover different octaves and the sensitivity ranges of different mechanoreceptors (Johansson and Flanagan [2009]). An illustration of such circular patterns is depicted in Figure 5.1-a, while Figure 5.1-b&c show how

the number of points per pattern affect the pattern spatiotemporal properties. The range of possible samples rates varied with the draw frequency. Due to this, we picked a total of 6 to 11 number of points per pattern, depending on the draw frequency, which accounted for a total of 51 distinct patterns. Each pattern was repeated 3 times, making for a total of 153 stimuli in the study.

Each mid-air tactile pattern was presented to the participants left palm for 3 seconds. At the end of the stimulus, a numeric pad was displayed on the screen as well as an instruction inviting participants to enter their perceived strength estimates. Prior to the user study, participants were instructed to estimate the pattern perceived strength using their own scale. Additionally, participant were asked to rate the perceived strength from 0 as the minimum (i.e. did not feel the pattern), to infinite, using whole numbers (i.e. no decimal) and to be as consistent as possible in their estimation throughout the study. Finally, participants were reminded to focus only on the pattern perceived strength and to omit any other qualitative evaluation from their rating (e.g., smoothness or simultaneousness). After participants validated their response, the next pattern was presented after a two seconds break until participants rated all stimuli. The patterns order were presented in a randomised order. The whole study lasted about 20 minutes.

5.2.2 Results

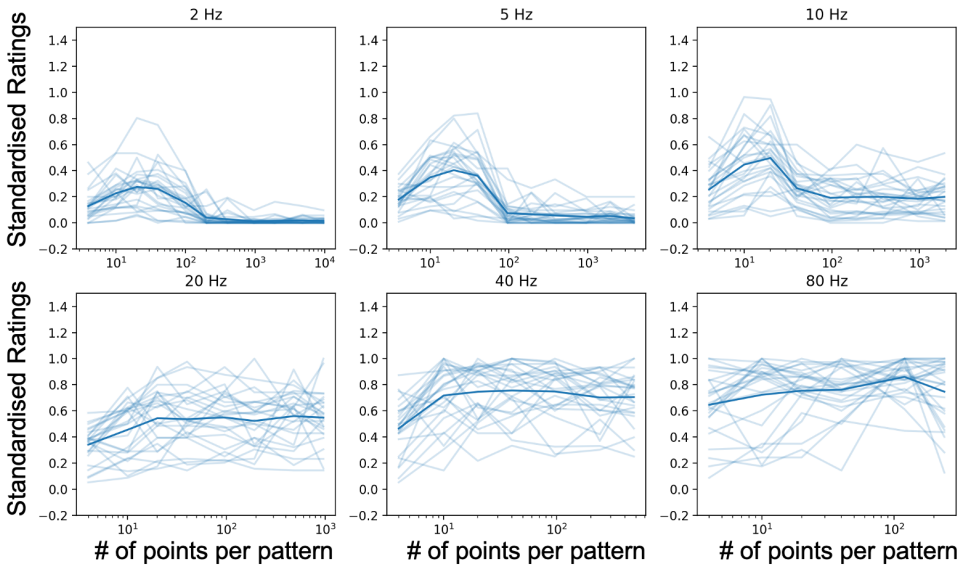

Figure 5.3: The standardised perceived strength as a function of the number of sampling points, for a 150 mm *circumference circle rendered at different frequencies. Light and bold curves represent participants' responses and responses average, respectively.*

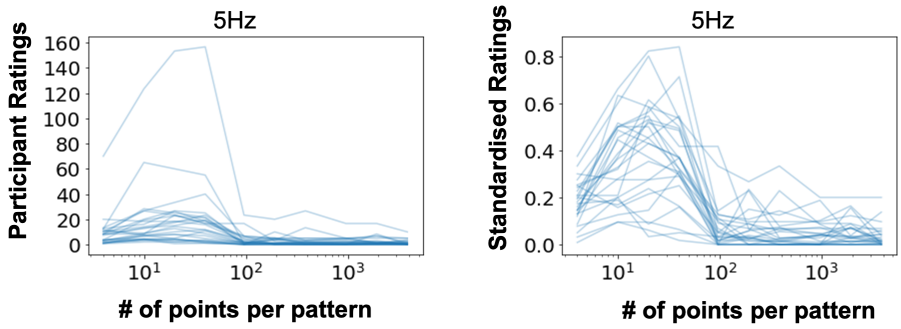

Figure 5.4: Participants strength ratings were pre-process before analysis. The raw data (left) were standardised by the maximum rating (right)

As we were interested in studying each pattern sensation separately, we separated the data into 6 subsets, one for each pattern draw frequency. However participants were using different scale to estimate the pattern perceived strength. To be able to compare participants' responses, we had to bring all the ratings to the same scale. To do so, we had to startadise each participants' responses and therefore divided each participants' estimates by their highest response (Jones and Tan [2012], Strohmeier and Hornbæk [2017]). In other words, if R_n is the set of ratings from one participant for the pattern n, then we standardise the answer from this participants into Rs_n as follow

$$Rs_n = \frac{R_n}{max(R_n)}$$

This standardisation approach is shown in Figure 5.4 using the subset with draw frequency 5Hz. The results of standardisation for each draw frequency subset is shown in Figure 5.3 as a function of the number of points per pattern. We invite the reader to note that the x-axis of the figure is logarithmically scaled as the number of points per pattern spread across 4 orders of magnitude.

Each data subset was found to be unlikely to follow a normal distribution (Shapiro-Wilk, $p < .05$). Therefore we ran a Friedman test on each data subset to test whether the perceived strength ratings were significantly different across the number of points per pattern. The Friedman test indicated significant differences between the number of points per pattern groups for each draw frequency: $2\,\text{Hz}(\chi^2(10) = 199.1, p < .001)$, $5\,\text{Hz}(\chi^2(9) = 179.4, p < .001)$, $10\,\text{Hz}(\chi^2(8) = 109.9, p < .001)$, $20\,\text{Hz}(\chi^2(7) = 43.4, p < .001)$, $40\,\text{Hz}(\chi^2(6) = 45.6, p < .001)$ and $80\,\text{Hz}(\chi^2(5) = 15.26, p = .009)$.

To further determine whether the differences were significant across the whole range of sampling patterns, we ran a pairwise Wilcoxon signed-rank test, with Bonferroni correction to avoid obtaining false-positive for significant difference between

	Quadratic Mixed Model		
Rate	R^2	*N. opt.*	*N. lim.*
2 Hz	0.28	22.4	236.6
5 Hz	0.37	17.5	119.2
10 Hz	0.23	15.8	149.4

Table 5.1: Quadratic mixed model results for frequency 2 Hz*,* 5 Hz *and* 10 Hz*. Results include* R^2*, optimal number of points per pattern and number of points per pattern limit.*

pair of data (i.e. error of type 1). For draw frequencies 20 Hz, 40 Hz and 80 Hz, the Wilcoxon test indicated significant differences only between 1 or 2 pairs of number of points per pattern. We therefore discarded these draw frequencies for the end of the data analysis. However, for draw frequencies of 2 Hz, 5 Hz and 10 Hz, the Wilcoxon test indicated significant differences for all pairs of number of points per pattern, as long as the number of points per pattern was lower than 200, 96 and 48 points, respectively.

The fact that the upper number of points per pattern interval leads to no significant differences, suggests that no specific behaviour could be extracted from that part of the data. Furthermore, the fact that the corresponding perceived strength plateaus around 0, suggests that the participants did not perceive these patterns. Those two points, motivated us to discard the data for the next step of the analysis and focus on the lower number of points per pattern interval.

On the remaining data, which correspond to the left part of the curves in Figure 5.3, the reader can see that, the pattern perceived strength seems to follow a quadratic behaviour. This apparent quadratic behaviour motivated us to use a quadratic model, to fit our data. The model we used for regression can be seen in equation 5.2

$$\text{strength} = a \log_{10}^2(\text{sampling}) + b \log_{10}(\text{sampling}) + c \tag{5.2}$$

We remind the reader, that the model uses logarithmic values as the plots on Figure 5.3, where the quadratic behaviour can be observed, are using logarithmic x-axes. The model gave R^2 values of 0.28, 0.37 and 0.23 for the pattern draw frequency 2 Hz, 5 Hz and 10 Hz respectively.

Using the coefficient from the model, we estimated the number of points per pattern that was giving the highest perceived strength. We found that the optimal number of points per pattern was 22.4, 17.5 and 15.8 points for draw frequency 2 Hz, 5 Hz and 10 Hz, respectively. Finally we estimated the number of points per

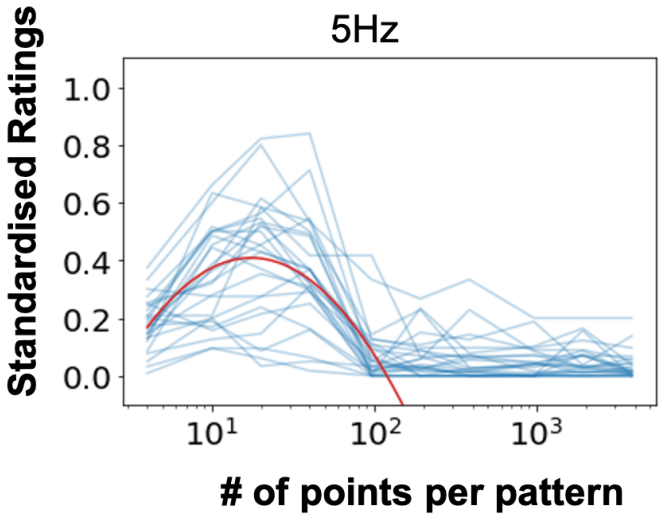

Figure 5.5: Standardised participants strength rating can be fitted to a quadratic model.

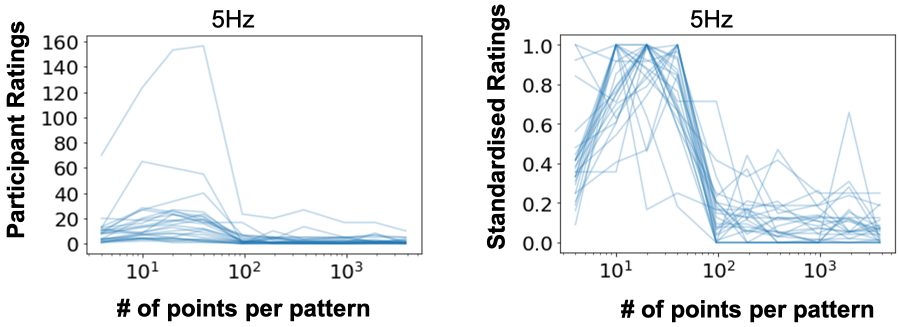

Figure 5.6: Participants strength ratings were pre-process before analysis. The raw data (left) were standardised by the maximum rating of the frequency of interest (right).

pattern threshold that was leading to the pattern to be perceived or not. We found a threshold of 236.6, 119.2 and 149.4 points for pattern draw frequency 2 Hz, 5 Hz and 10 Hz, respectively. An example of data fitting for draw frequency 5Hz is shown in Figure 5.5 and the results of the data fitting are summarized in Table 5.1.

An R^2 value around 0.3 is considered low. In order to obtain a better regression model, we investigated an alternative method to standardise participant responses. Since, we seperated the participants responses in 6 subset according to the pattern draw frequency, we decided to standardise each participants reponses by their highest answer for the frequency of interest. In otherwords, if Rf_n is the set of ratings from one participants for the pattern n and of draw frequency f, then we standardise the answer from this participant into Rfs_n as follow:

$$Rfs_n = \frac{Rf_n}{max(Rf_n)}$$

Note here, that $max(Rf_n)$ will yield different value for each draw frequency f. An

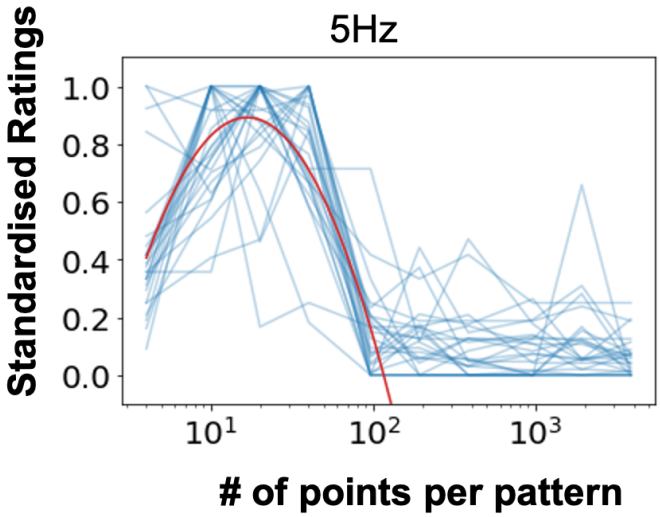

Figure 5.7: Standardised participants strength rating can be fitted to a quadratic model.

	Quadratic Mixed Model		
Rate	R^2	*N. opt.*	*N. lim.*
2 Hz	0.55	22.6	230.0
5 Hz	0.62	16.7	116.5
10 Hz	0.40	16.1	146.6

Table 5.2: Quadratic mixed model results for frequency 2 Hz, 5 Hz *and* 10 Hz *after second standardisation approach. Results include* R^2*, optimal number of points per pattern and number of points per pattern limit.*

example of this new approach to standardise participants responses is shown in Figure 5.6 using the subset with draw frequency 5Hz.. using these new standardised responses, we updated our quadratic model.

This time, the model gave R^2 values of 0.55, 0.63 and 0.4 for the pattern draw frequency 2 Hz, 5 Hz and 10 Hz respectively. Using the coefficient from this new model, we estimated the number of points per pattern that was giving the highest perceived strength. We found that the optimal number of points per pattern was 22.6, 16.7 and 16.1 points for draw frequency 2 Hz, 5 Hz and 10 Hz, respectively. Finally we estimated the number of points per pattern threshold that was leading to the pattern to be perceived or not. We found a threshold of 230.0, 116.5 and 146.61 points for pattern draw frequency 2 Hz, 5 Hz and 10 Hz, respectively. An example of data fitting for draw frequency 5Hz is shown in Figure 5.7 and the results of the data fitting are summarized in Table 5.2.

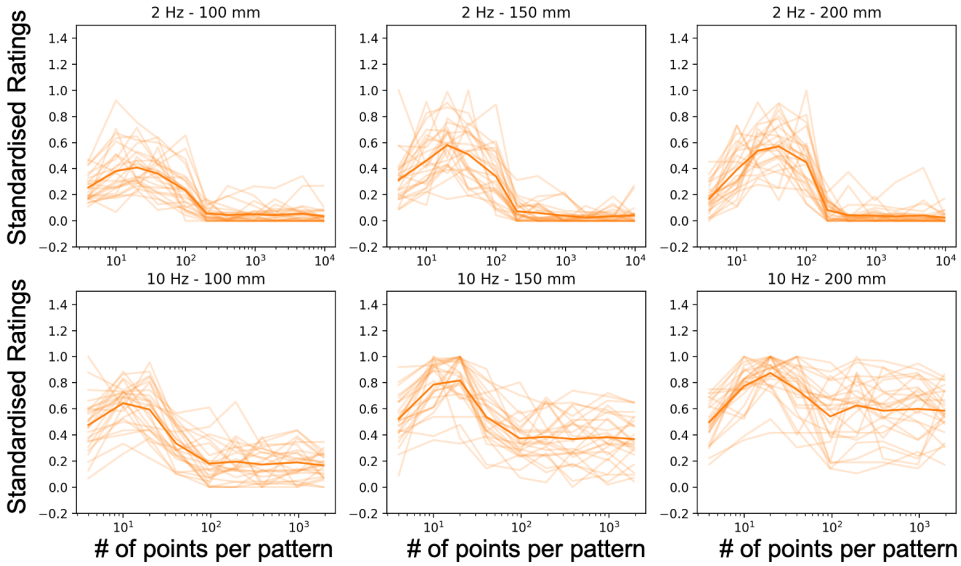

Figure 5.8: The standardised perceived strength as a function of the number of sampling points, for different frequencies and circle circumferences. Light curves represent participant responses and bold curves represent responses average.

An R^2 value around 0.5 is still considered low and could probably be improved further if we looked into eliminating outliners or into additionnal standardisation approaches. However one can see that the information obtained with the two models are very similar. Therefore, leveraging the principle of parsimony, we decided to keep the analysis simple and stick to the results from the first standardisation method we used.

5.3 User Study 2

In the first user study, we were able to determine a relation between perceived pattern strength and number of points per pattern. However these relation parameters are varying with the pattern draw frequency. In this second user study, we aim to determine whether these relation parameters vary as well when the pattern size changes.

5.3.1 Method

We use the same protocol and set-up as in the first study. The new stimuli set was composed of 2 draw frequencies. We chose 2 Hz and 10 Hz, as they are the two boundary frequencies for which the effect of sampling strategy was observed in the first user study. There were 11 and 9 number of points per pattern for the two

		Quadratic Mixed Model		
Rate	*Circum.*	R^2	*N. optimal*	*N. limit*
2 Hz	0.10m	0.69	18.72	240.55
2 Hz	0.15m	0.60	20.95	241.76
2 Hz	0.20m	0.61	27.95	260.29
10 Hz	0.10m	0.67	10.77	92.09
10 Hz	0.15m	0.60	15.01	90.54
10 Hz	0.20m	0.60	20.30	84.52

Table 5.3: Quadratic mixed model results for frequency 2 Hz *and* 10 Hz *across the different pattern sizes. Results include* R^2*, optimal number of points per pattern and number of points per pattern limit*

draw frequencies, 2 Hz and 10 Hz, respectively. We used 3 different pattern sizes, which were 100, 150 and 200 mm circumference. There was a total of 60 distinct patterns. Each pattern was repeated 3 times, making a total of 180 stimuli. The user study lasted about 25 minutes. In total 26 participants (4 females, average age±SD: 30±5.9) took part in the study.

5.3.2 Results

The data collected were standardised as in the first user study. We also separated the standardised responses into 6 subsets according to pattern draw frequency and pattern size. Figure 5.8 shows the resulting rating after standardisation for each data subset.

Each data subset was likely not normally distributed (Shapiro-Wilk, $p < .05$).

Therefore, we ran a Friedman test on each data set to test whether the perceived strength rating were significantly different across the corresponding number of points per pattern. For patterns at 2 Hz, a Friedman test indicated significant differences as $\chi^2(10) = 200.5, p < .001$, $\chi^2(10) = 212.3, p < .001$ and $\chi^2(10) = 208.9, p < .001$, for circumferences 100 mm, 150 mm and 200 mm, respectively. For patterns at 10 Hz, a Friedman test indicated significant differences as $\chi^2(8) = 138.1, p < .001$, $\chi^2(8) = 111.0, p < .001$ and $\chi^2(10) = 84.0, p < .001$, for circumferences 100 mm, 150 mm and 200 mm, respectively. To further determine whether the differences were significant across the whole range of sampling patterns, we ran a pairwise Wilcoxon signed-rank test, with Bonferroni correction to avoid type 1 error, on each data subset, and thus determine which pair of points per pattern were significantly different.

As in the first study, we found that the pairs of number of points per pattern were significantly different only for number of points per pattern below 200 and 96 points, for modulation 2 Hz and 10 Hz, respectively. Hence, for the same motivations as the first user study, we discarded the non-significant part of the data and ran a quadratic mixed model on the significant part of the data. The model indicated R^2 values of 0.70, 0.60 and 0.61 for the pattern draw frequency 2 Hz and circumference 100 mm, 150 mm and 200 mm, respectively. For pattern draw frequency of 10 Hz the model gave R^2 of 0.67, 0.60 and 0.60 for the patterns with circumference 100 mm, 150 mm and 200 mm, respectively.

An R^2 value greater than 0.6 is considered high. We can therefore conclude that the quadratic model is a good fit to model our data. Then we use the coefficients from the model to estimate the number of points per pattern that was giving the highest perceived strength. We found that for 2 Hz draw frequency, the optimal number of points per pattern was 18.72, 20.95 and 27.95 points for circumference 100 mm, 150 mm and 200 mm respectively. We also found a number of points per pattern threshold of 240.55, 241.76 and 260.29 points for circumference 100, 150 and 200 mm respectively. For a draw frequency of 10 Hz, we found an optimal number of points per pattern rate of 10.77, 15.01 and 20.30 points for circumference 100 mm, 150 mm and 200 mm respectively. As for 2 Hz modulation, the perceived strength of pattern at 10 Hz plateau when the number of points per pattern is greater than a given number. Using the model parameters and the plateau values, we found that the number of points per pattern threshold was 92.09, 90.54 and 84.52 for circumference 100 mm, 150 mm and 200 mm respectively. The results of the data fitting are summarized in Table 5.3.

5.4 Discussion

In the current paper, we investigated a sampling strategy that maximised the pattern perceived strength. Using circular patterns rendered with different amounts of sampling points, we established a relationship between number of points per pattern and pattern perceived strength. After discussing the user studies results, we will try to explain those same results using the psychophysical literature on the perception of touch. Finally, we will cover the implications of our work for tactile feedback designers.

5.4.1 User studies Results

In the two user studies, we demonstrated that number of points per pattern has an effect on perceived pattern strength. However, significant effects were limited to patterns with draw frequencies ranging from 2 Hz to 10 Hz. Although variability can be observed in the magnitude of users' results, which could be accounted for users' subjective judgement, the overall trends are common across participants and can be modelled. Using a regression model, we successfully fitted the perceived pattern strength to a quadratic function of the logarithm of the number of points per pattern (see equation 5.2).

From these regression functions, we identified an optimal number of points per pattern for patterns rendered at 10 Hz, of 10.77, 15.01 and 20.30 points for circumferences 100 mm, 150 mm and 200 mm respectively. By taking the ratio of the pattern circumference over the optimal number of points per pattern, we obtained an optimal distance between sample points of $9.7\,\text{mm} \pm 0.3$ The low variation between optimal distances between sample points, designate this distance as an invariant for maximising perceived pattern strength across pattern sizes. We found similar results with draw frequency of 2 Hz, for which the optimal distance between samples points was on average equal to $6.5\,\text{mm} \pm 0.8$. However, the optimal distances obtained are different across pattern draw frequencies and despite our effort, we could not establish a clear relationship between optimal distance and draw frequency.

Using the user study results, we also found that perceived strength plateaus when the number of points per pattern is greater than a given threshold. This threshold is on average 245 ± 6.2 points and 89 ± 3.3 points for patterns at 2 Hz and 10 Hz, respectively. The low variation between threshold averages suggests the number of points per pattern threshold to be invariant across pattern sizes, although we could not establish the relationship between threshold and pattern draw frequency.

Even though our study showed no effect of number of points per pattern on perceived strength for patterns at high frequency, we would like to point out that, when observed, the effect occurs only for sampling rate under 200 points. However, high frequency patterns can not currently be rendered with number of points per pattern up to 200 points. For instance, the mid-air tactile display we used could render a pattern at 80 Hz with only 24 points at most. It is likely that technology will improves and allow to render high frequency patterns with number of points per pattern of 200 points or more. Until then, we cannot completely ruled out the effect of number of points per pattern on perceived strength in the case of high frequency patterns.

Finally, on Figure 5.8, one may note that the maximum perceived strength varies

with the pattern draw frequencies and sizes. However, this can be explained with the work presented in chapter 4, which shows that perceived strength varies with the tactile point speed (i.e. draw frequency times pattern circumference).

5.4.2 Haptic Implications

Higher number of points per pattern does not always improve tactile perception and quite often, the old cliche is true: less is more. Such design insights can be hugely beneficial to haptic engineers, developers and designers. Using the general trend found in the user-study results, we therefore propose ways and relationships for such parameters and variations to be hidden behind easy-to-use software packages.

First, we encourage tactile feedback designers working with mid-air tactile displays to decrease the number of points per pattern whenever rendering tactile pattern with low frequency. Decreasing the number of points per pattern for a pattern that initially cannot be perceived, might suddenly unlock the said pattern. For instance, circular patterns as studied here, could not be perceived below 20 Hz with a high number of points per pattern. However, when the number of points per pattern was lowered, the same circular pattern could be perceived as low as 2 Hz. We would like to emphasise that since tactile perception of frequency follows a Weber-law, the range 2-10 Hz is half as wide as the range 10-200 Hz. Hence increasing by 50% the range of discriminable frequency one could now apply to mid-air tactile patterns. We also would like to remind our readers, that in our study, we consider low frequency any frequency less than or equal to 10 Hz. However our study focusing only on circular patterns, the 10 Hz frequency threshold might vary for other pattern shapes, and hence ask the reader to interpret the values of this study carefully when applied to different pattern shapes.

Then, we would like to invite feedback designers to adjust the number of points per pattern of a given mid-air tactile pattern, whenever it is possible, in order to maximise its perceived strength. We also remind designers that this optimal number of points per pattern is proportional to the pattern size. Hence, when scaling a given pattern, the number of points per pattern should be scaled accordingly.

As no previous work exploring adjusting sampling strategy has been undertaken, we expect the possibility to render low frequency patterns to be unveiled for most designers working with mid-air tactile displays. Moreover, low frequency patterns, operating at much lower speed than usual patterns rendered with STM, are now expected to be perceived as moving points rather than complete shapes. Moving points, providing richer information (such as start & end locations, direction of motion and rate of movement, all of which are masked at higher speeds), are

better recognised than multi-point patterns. This has already been demonstrated for contact devices, which used unistroke patterns (Ion et al. [2015]). We believe the distinction to hold between low and high frequency mid-air tactile pattern too. Hence, thanks to the sampling strategy we presented, a new horizon of possibilities has been made available to the designers. We encourage designers to experiment with and investigate those new possibilities.

Finally, we are conscious all the results presented here could be overwhelming for tactile feedback designers. However, the invariants identified in the second user study should ease the implementation of our results into design tools as hidden parameters. Thus improved design tools will allow current tactile feedback designers to stay oblivious to sampling strategies.

5.4.3 Psychophysical Explanation

In an attempt to further understand the results reported in this study, we discuss here some hypotheses related to the psychophysics of the sense of touch.

Firstly recall that, for AM, different modulation frequencies are perceived with different strength, even though the amplitude of the stimulation remains the same, 200 Hz being the frequency perceived the strongest (Gescheider et al. [2004]).

However, STM stimulation can no longer be described as a sinusoid like for AM and LM, but more like a pulse train with alternation between intervals of stimulation and non-stimulation. Using a Fourier expansion, this pulse train can be decomposed as a sum of sinusoidal signals, thus unveiling the presence of harmonics that are higher in frequency, with an amplitude depending on the pulse width. Decreasing the number of points per pattern may inadvertently increase the harmonic's amplitude close to 200 Hz, and thereby increase the associated perceived strength.

Another hypothesis is related to the skin viscoelastic properties (see section 2.2.1). A high number of sampling points leads to stimulation durations being too short for the skin deformation to reach the required mechanoreceptors' depth. At first, this hypothesis might seem unlikely since higher frequency patterns yield to tactile perception nonetheless. However by definition the rate at which the stimulation is repeated at a single location is much faster for high draw frequencies than for low draw frequencies. Therefore, it is plausible that at high frequencies the skin indentation builds up as the pattern is repeated over and over again whereas at low frequencies the elastic skin relaxes entirely between stimulation intervals.

Until now, mid-air haptics was relying on stimulating RA and PC mechanoreceptors that are sensitive to vibrations higher in frequency than the one involved in this study (Johansson and Flanagan [2009]). However, one could note that as the

tactile points moves across the skin surface, different groups of SA1 mechanoreceptors might be stimulated. Indeed, SA1 mechanoreceptors are mostly sensitive to the stimulus onset and offset (i.e. transient stimulus). Therefore, as the mid-air stimulus moves from one position to another, the stimulus is offset at the old position and onset at the new position. However, when a number of sampling points is too high the sample position difference is lower than SA1 receptive field (Vallbo et al. [1984]), and do not lead to this transient behaviour and therefore to tactile perception.

Ultimately, using a mechanotransduction model as the one presented by Saal et al. [2017], one could test some of these hypotheses. Although, such models only predict stimulus detection, but will not determine optimal stimulation.

While these hypotheses cannot be tested within the scope of the present study, the next chapter tries to overcome this issue. We discuss in Chapter 6 how a new research paradigm is required to answer the implications of varing the number of points per pattern on the psychophysics of touch. The next chapter therefore introduces a new research framework as well as initial investigations taking place within this new research framework.

Chapter 6

Outlook and Future Work

The previous chapter demonstrated that the perception of spatiotemporal mid-air haptic patterns was not only dependent of the pattern draw frequency, but also of the number of points per pattern used. While the study was able to show evidence of perceptual differences, it could not establish the causes behind these differences.

Nonetheless, several suggestions, potentially explaining these differences, have been formulated. The results of this study are pointing towards an optimal distance between consecutive samples, the first suggestion is that mechanoreceptors' receptive field size plays a role. This suggestion assumes that at low draw frequency (and therefore low draw speed), perception relies on a class of mechanoreceptors only sensitive to the onset and offset of stimuli. Indeed, the higher the number of points per pattern, the smaller the distance between two consecutive sample positions, and therefore the smoother the onset and offset of the mechanoreceptors' stimulation. The second suggestion states that the frequency components of the haptic signal vary with the number of points per pattern. These changes in frequency content could also potentially be responsible for the change in perception.

However, these suggestions could not be tested within the frame of the previous study. The main reason is that the frame of reference of the study is the focal point. When considering only the focal point, this frame of reference moves accordingly and assumes that the focal point intensity is constant. Since we saw that focal point intensity and force applied to the skin were directly related, one could think that the force applied to the skin is therefore constant too. However, if one changes frame of reference and now considers a fixed point on the skin surface (e.g. one mechanoreceptor centre), the force applied at this location is no longer constant. Indeed, the force applied to this location is increasing and decreasing, as the focal point comes and goes over it. These variations in the force applied to a location on the skin have implications for the perception. Yet, with the current research

framework (i.e. frame of reference of the focal point), these variations were not captured and therefore their implications could not be tested. To be able to capture and study the effect of the variations of force applied to the skin, we propose to shift our research framework from a frame of reference centered around the focal point position, to a frame of reference centered around the mechanoreceptor position.

In this chapter, we first define this new framework of research, and then using this new framework, formulate some suggestions to explain the suggestions made in the previous paragraph. These suggestions are tested theoreticaly and will need to be tested experimentally as part of future studies.

6.1 Theory

6.1.1 From constant pressure to pulse train

When investigating spatiotemporal mid-air haptic patterns, there are two possible frames of reference than can be used to determine the evolution of the applied force over time. The first one, the one that has been used through this thesis, is to consider the frame of reference of the focal point. In other words, it considers the force applied to the skin at the center of the focal point. In this frame of reference, since the intensity of the focal point is fixed to a constant value, one could say that the force applied to the skin is constant too. The second frame of reference is centered to a fixed position on the skin. In other words, it considers the force applied to this position on the skin. In this frame of reference, as the focal point comes and goes, the force applied to the skin is no longer constant. It is either *high* if the focal point is at the position of interest, or *low* if the focal point is at another position. The difference between the two frames of reference have implications on how we approach the perception of mid-air haptic patterns.

To understand better these implications, it is relevant to take a step back and look at Amplitude Modulation (AM). In AM, the focal point is assumed to be directly over the mechanoreceptor's receptive field. Therefore, the pressure applied to the skin is equal to the pressure applied to the mechanoreceptor's receptive field, and hence in both frames of reference (i.e. focal point and mechanoreceptor) applied pressure over time is the same. In this case, choosing one frame of reference or another has little implication on the observations made. Now, if we move the focal point away from the mechanoreceptor's receptive field, the pressure applied to the skin and the pressure appplied to the mechanoreceptor's receptive field will be different. In both cases the pressure is constant but its magnitude is different.

Moreover, if we move the focal point back and forth over the mechanoreceptor's receptive field while keeping the pressure at the focal point constant, one can see that the pressure applied to the mechanoreceptor's receptive field varies over time. This observation remains unchanged wether we include parameters such as wave propagation (see Chapter 4) or focal point size (see Chapter 3).

Now, let's try to express the pressure applied to the mechanoreceptor's receptive field for a simple STM pattern. For this, let's take the example of a mid-air haptic pattern describing a circle of 10 cm circumference and rendered with a focal point moving at $8\,\mathrm{m\,s^{-1}}$ (i.e. 80 rotations per second). In this example, the pattern is rendered in 12.5 ms and one can therefore propose that the mechanoreceptor's receptive field is actually stimulated 80 times per second (i.e. 80Hz).

Using the frame of reference of the focal point, we know that the pattern is drawn in 12.5 ms and therefore that the mechanoreceptor's receptive field is at most stimulated for 12.5 ms. Using the analysis from the previous chapter (see chapter 5), one could say that the lower bound for this stimulation time is the duration of 1 sample. If we used 10 points per pattern, that lower bound stimulation time decreases to 1.25 ms and if we used 100 points per pattern, that lower bound stimulation would decrease to 0.125 ms. In the previous chapter we saw that for pattern at 80Hz, using 10 or 100 samples had little impact on the perception, and both patterns were perceived as strong. Moreover, we know from Loomis [1981] that mechanoreceptors cannot feel stimuli shorter than a few milliseconds, hence the real stimulation time has to be higher than this lower bound we just defined.

The advantage of using the frame of reference of the mechanoreceptor is that one can leverage information like size of the focal point, the size of the mechanoreceptor receptive field, and the distance between the mechanoreceptor centre and the focal point position. Recall that a focal point created with a 40 kHz array would have a diameter of 8.5 mm and therefore an area of $56.7\,\mathrm{mm^2}$ (see chapter 3). Similarly, we saw that mechanoreceptors could have receptive field varying between 11 and $101\,\mathrm{mm^2}$ (i.e. diameter 3.7 to 11.3 mm) (see chapter 2). Using this information, it becomes easier to determine for how long the mechanoreceptor is stimulated. Furthermore the hand being dense with receptors it is likely that there is always a mechanoreceptor under the focal point position. Additionnally, the focal point describes a constant (i.e. neither acceleration nor deceleration) and periodic motion. Hence, the signal hence obtained for one position is similar to the signal that would have been obtained at another positon, minus a small time delay. This time delay corresponds to the time it took for the focal point to travel between the two positions of interest.

Coming back to our example, we can now apply this new approach and one could easily agree that a focal point is actually overlapping the mechanoreceptor receptive field for a distance equal to the sum of both diameters.

In the case of a an array at 40 kHz and Pacinian Corpuscle, these diameters are equal to 8.5 mm and 11.3 mm, respectively. Hence a total distance of almost 20 mm, which will take about 2.5 ms to travel for a focal point moving at $8\,\mathrm{m\,s^{-1}}$. Using this approach, it becomes easier to determine the stimulation time of a mechanoreceptor for various patterns of different sizes and rendered at different speeds. Furthermore, one could start to assume the stimulation, no longer as a perfect sine stimulation of the mechanoreceptor, but more like a pulse train approach. In general, the pulse duration τ of such a pulse train can be expressed as follow

$$\tau = \frac{\oslash_f + \oslash_m}{L \times f_{draw}} \tag{6.1}$$

Where $\oslash_f$ and $\oslash_m$ are the diameter of the focal point and the diameter of the mechanoreceptor receptive field, respectively, L the length of the pattern and f_{draw} the draw frequency of the pattern (i.e. the number of pattern repetion per second).

or:

$$\tau = \frac{\oslash_f + \oslash_m}{v_{draw}} \tag{6.2}$$

Where v_{draw} is the focal point motion speed.

Refining the pulse train envelope

This change of frame of reference highlights one important difference between Amplitude Modulation and Spatiotemporal Modulation. The mechanoreceptors are no longer stimulated with sinusoidal stimuli but with pulse trains.

In the literrature, it has been shown that periodic stimuli that do not possess a sinusoidale waveform are percived differently (MacLean and Enriquez [2003]). While most studies on the topic were concerned in defining a perceptual space for a familly of waveforms, or a continuous perceptual dimension to go from one waveform to another, few studies have looked at explaining why various waveforms lead to various perceptions.

In the research community, it is admitted that there are different kinds of mechanoreceptors that are each sensitive to various stimulus properties. Moreover, each kind of mechanoreceptors tends to have different frequency sensitivity. We already highlighted mechanoreceptors' frequency sensitivity in the Chapter 2 (see fig. 2.3). Leveraging this aspect, Vardar et al. [2017] propose to filter the frequency

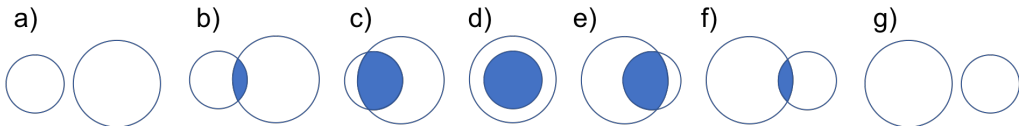

Figure 6.1: As the focal point (small circle) moves towards the mechanoreceptor receptive field (big circle), the overlap of the two (blue area) grows (a-d) and then decreases (d-g).

content of the pressure input at the mechanoreceptors with the frequency sensitivity. The authors argue that if after filtering, there is still a component remaining in the range of frequencies related to touch, then perception should occur. In other words, the authors suggest the perceived strength associated to a stimulus could be understood in terms of an expansion of the signal in terms of sinusoids, and the sum of the the perceived strength of each of these sinusoids taken individually. However, another work from Bensmaia and Hollins [2000] showed that people could discriminate between signals mixing various frequencies according to the phase delay between the pure tone signals (i.e. pure sines). Hence this last study suggests a potentail limitation of this approach.

Our short thought exercise in the previous section tells us what the pulse duration is, but does not say anything about what the pulse envelope is. Since this envelope determines the amplitude of the associated frequency components, we started investigating what is the envelope of a pulse train signal produced by a mid-air haptic pattern.

The simplest case is to assume that the pressure applied to the mechanoreceptor to be equivalent to a perfect pulse train, g(t), one could see from its Fourier expansion (see equation 6.3) that every odd harmonics will be non-null.

$$g(t) = w + \sum_{n=1}^{\infty} \frac{2}{n\pi} sin(\pi n w) sin(2\pi\ n\ f_d\ t + \frac{\pi}{2}) \tag{6.3}$$

Where ω is the stimulus angular frequency (i.e. equal to $2\pi f$) and f_d is the draw frequency of the mid-air haptic pattern. Using this case, one could hypothesise that in some cases a fundamental at 80 Hz might not be perceived since mechanoreceptors' threshold is high around this frequency, while its non-null third harmonic at 240 Hz might be perceived since mechanoreceptors's threshold is low around this frequency. Recall, that with AM stimulation, the pressure applied to the mechanoreceptor were perfect sinusoidal signals, and therefore harmonics were absent.

However microphone recordings from a spatiotemporal pattern, show that the acoustic pressure at the location of the mechanoreceptor's receptive field is neither a perfect pulse train nor a perfect sine (see Figure 6.2).

Indeed, if we consider in Figure 6.2 the microphone B to represent the mechanore-

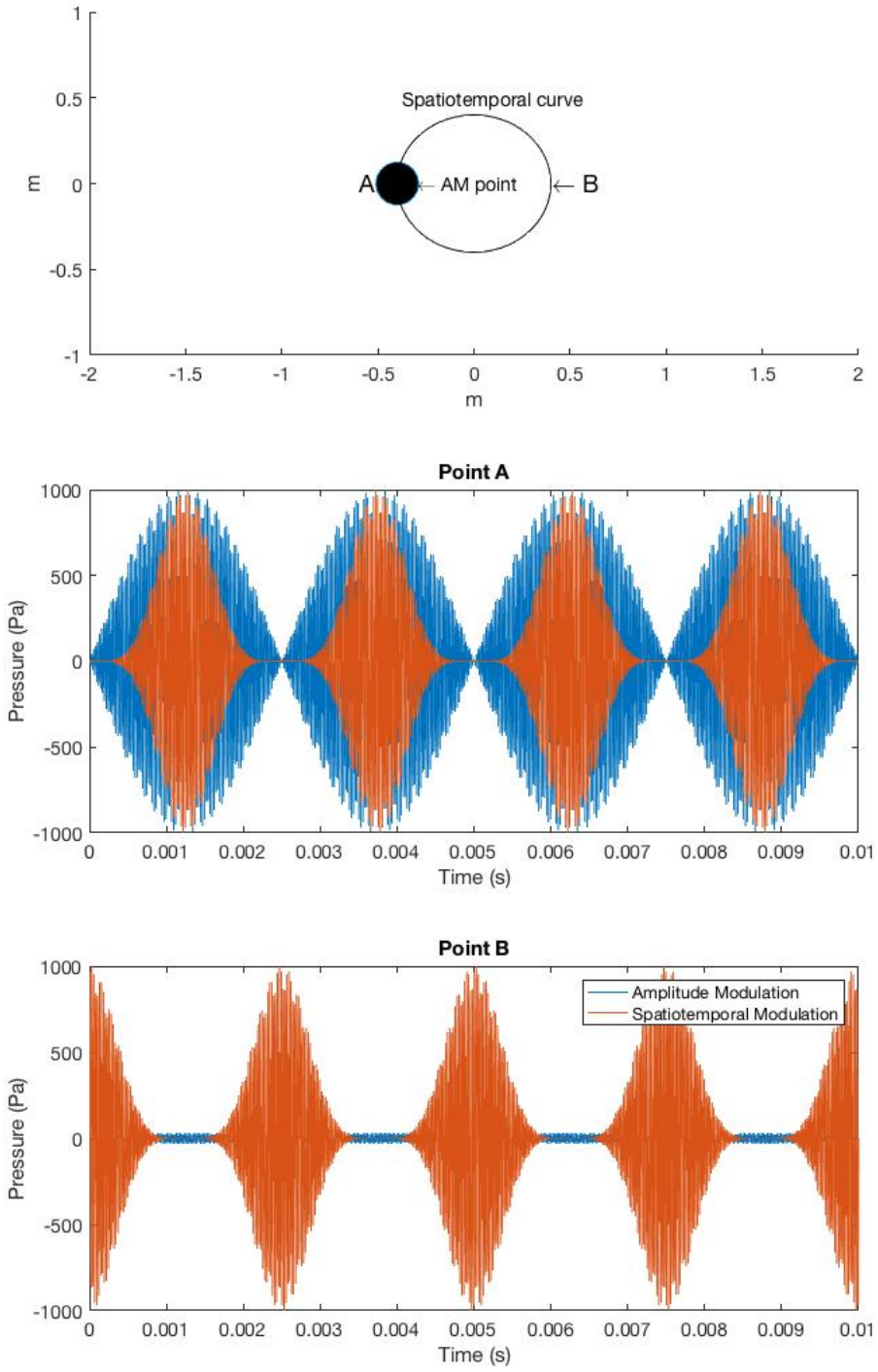

Figure 6.2: Recordings of an AM points at point A, and of an STM point traveling on the circle of diametre AB. Recordings are taken at the position A (middle) and the position B (bottom). Kappus and Long [2018]

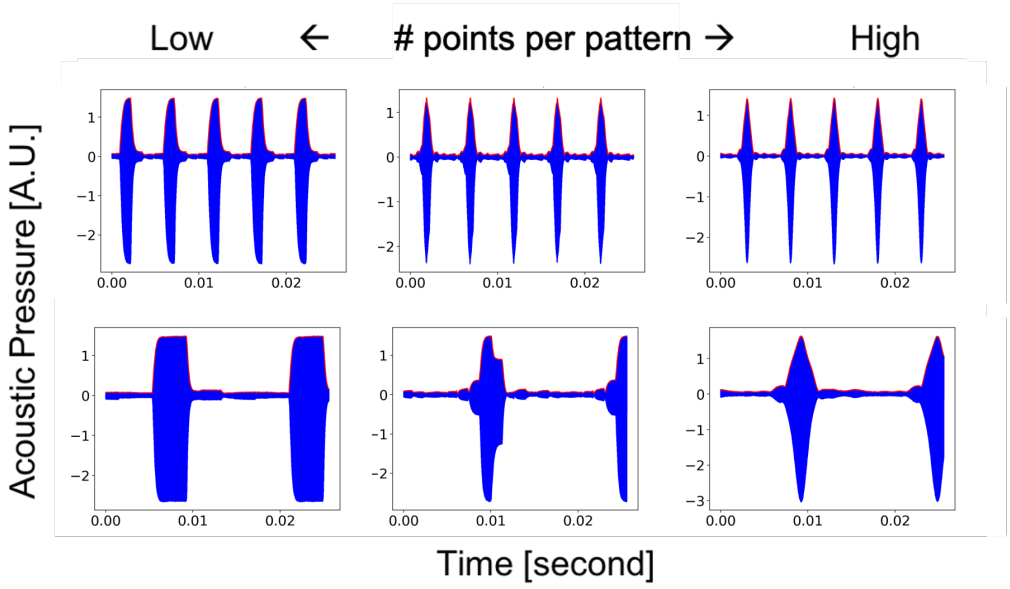

Figure 6.3: Microphone recording of the acoustic pressure produced by a mid-air haptic circle rendered at 200 Hz *(top) and* 64 Hz *(bottom) with number of points per pattern ranging from low (left) to high (right)*

ceptor, we can see that the acoustic pressure is not a pulse train. Moreover, we can see from microphone A and comparison with the pressure produced by an AM point, that the acoustic pressure is not a sinusoidal signal either. We remind the reader that the pressure applied to the skin, the acoustic radiation pressure (see Chapter 3), is roughly proportionnal to the acoustic pressure. Therefore, the envelope of the pulse representing the pressure applied to the mechanoreceptors should be similar to the envelope of the pulse observed in figure 6.2. That envelope being different from a square pulse train signal and a sinusoidal signal, the frequency components will be different too. Therefore, it becomes relevant to try to predict and determine the exact envelope that a mid-air haptic pattern produces.

In order to investigate further the shape of this envelope, we decided to replicate the setup introduced by Kappus and Long [2018]. We use a 1/8"microphone from B&k (ref 4138) and digitally acquired audio recordings using an oscilloscope from Pico. As in Kappus and Long [2018], the microphone was placed on the path of a 3cm radius circular mid-air haptic pattern. We took several audio recordings for patterns with draw frequency of 200Hz and 64Hz. Additionnally we varied the number of samples per pattern from 4 to 300 samples per pattern. Results can be observed in fig. 6.3.

As in Kappus and Long [2018], we found a pulse train for which the envelope was neither a square nor a sinusoidale signal. Additionnally we can see that the envelope varies with the number of samples per pattern. One could start to draw parallel

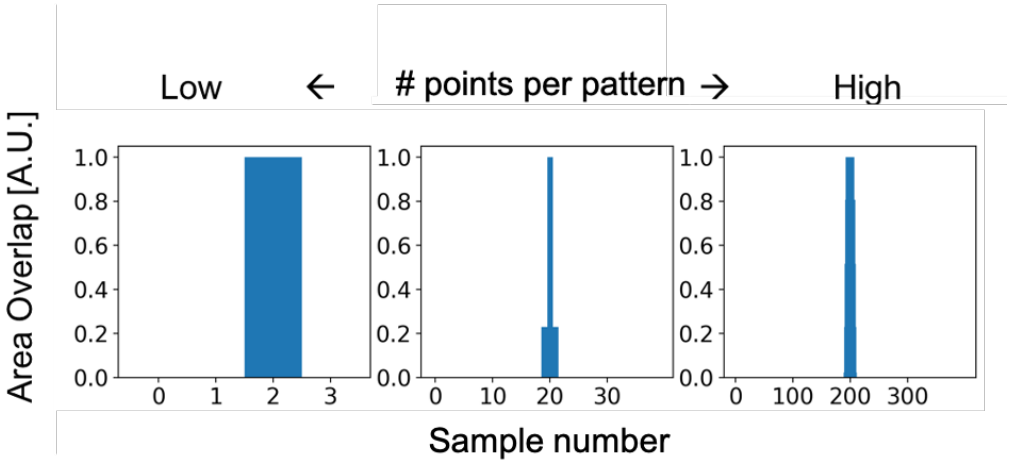

Figure 6.4: Overlap as a function of sample number. Overlap were computed for a a mid-air haptic circle rendered with 4, 40 and 400 points.

between these recordings and the results obtained in chapter 5. However, the current setup provides some limitations that need to be taken into account first. Indeed the microphone membrane is 3.2 mm in diameter while the sizes of mechanoreceptors' receptive field vary from 3.7 to 11.3 mm.

To acount for the differences in size between microphone membrane and mechanoreceptor receptive field, we undertook to write a small script that will predict the envelope observed in the audio recording. More specifically we computed the overlap area between the focal point and the mechanoreceptor field for each sample composing the pattern. In this script we represented the focal point as a circle of diameter 8.5mm and the mechanoreceptor as a cirle of diamter 3.6mm. The focal point was moving on a circular trajectory of 3cm radius (i.e. as in the microphone recordings) and the mechanoreceptor centre was placed on the circle. As for the audio recording we used a various numbers of sample per pattern from 4 to 400 samples. The results of these simulations can be observed in Figure 6.4.

We use trigonometry to compute the overlap between the two circles. The area of interest in the area in purple as seen in figure 6.5 To do this, we define two intermediate areas "Pie" and "Triangle" for each circle, in green and orange, respectively. Let's consider P1 and P2 as the area of the "Pie" for the first circle and the second circle, respectively. Similarly, let's consider T1 and T2, the "Triangle" area for both circles. Then the overlap area A, is the results of $A = (P1 - T1) + (P2 - T2)$.

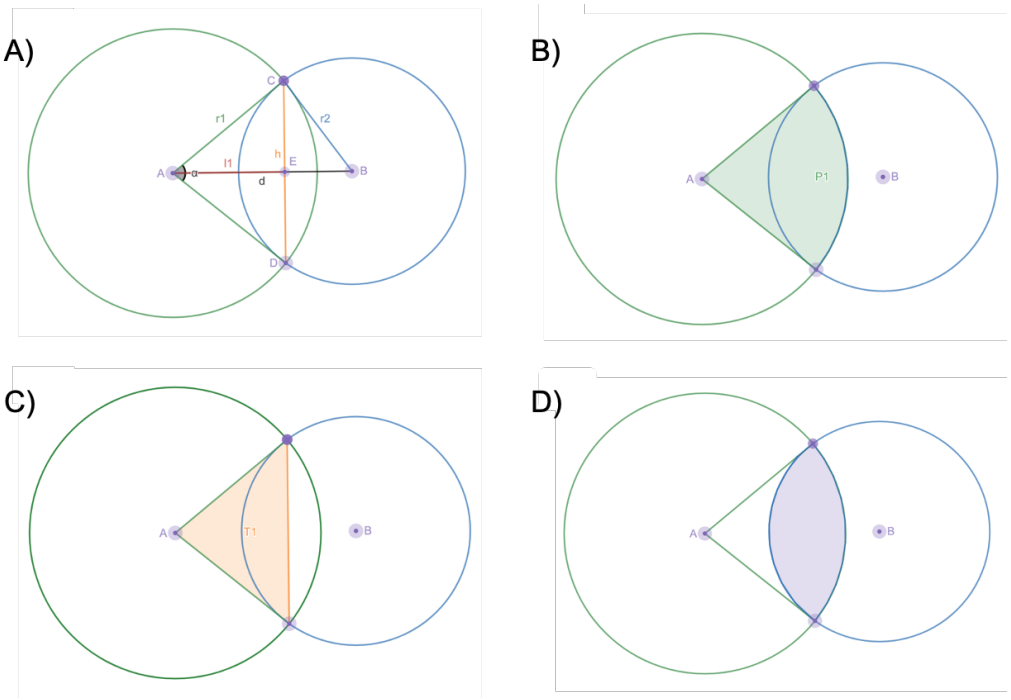

Figure 6.5: The area of two overlapping circles (d), can be computed the difference of the "pie" area in (b) and the "triangle" area in (c) for both circles of centres A and B (a).

The area P1 can be obtain as follow:

$$P1 = \int_0^{\alpha} \int_0^{r_1} r d\theta dr \tag{6.4}$$

Where r_1 is the radius of the circle of centre A, and alpha the angle between the two lines that pass through A and are tangent of the circle of centre B. (see Figure 6.5-a)

The area T1 can be obtained as follow:

$$T1 = \frac{H}{2} r_1 \tag{6.5}$$

Where H represent the distance between the point C and D and r_1 still represent the radius of the circle of centre A. Area P2 and T2, can be obtained similarly.

In the above area computation, there are two unknowns, namely the angle α and the distance H. Using the ACB and the segment H passing through C and perpendicular to AB, we can use the law of sinus to define

$$r_2^2 = r_1^2 + d^2 - 2dl1 \tag{6.6}$$

Where r_2, r_1 are the circles radius, d the distance between the two centre and l_1 the shortest distance between the point A the line CD.

With some reorganising we obtain the following relation:

$$l1 = \frac{r_1^2 + d^2 - r_2^2}{2d} \tag{6.7}$$

l_2, which is the shortest distance between the point B and the line CD, can be obtain similarly, or more directly using the fact that:

$$d = l1 + l2$$

Using this result, one can then define α as:

$$\alpha = arccos(\frac{l_1}{r_1})$$

and

$$H = 2\sqrt{r_1^2 - l_1^2}$$

Using the results of the last two equations, one can therefore obtain the overlap area of two superimposed circles. One would also define two specific cases. First, the case where the circle centres are perfectly overlapping (i.e. A = B). In this case, the overlap area is equal to the area of the smallest circle (see Figure 6.1-d) The second case, is where the circle are not overlapping, and occurs when $r_1 + r_2 > d$ and in which case the area is null(see Figure 6.1-a and g)

By applying this methodology to all the sample position of the focal point, and fixing the mechanoreceptor position, one can simulate the pressure applied to the mechanoreceptor's receptive field. For instance Figure 6.4 presents how the number of points per pattern affects the overlapp between focal point area and mechanoreceptor receptive field for a circular mid-air haptic pattern. The simulation assumed a focal point of radius 4.3 mm, moving around a circle of radius 3 cm and crossing a PC mechanoreceptor receptive field with radius 50.5 mm.

It is worth noting that the simulation presented in figure 6.4 seems to agree that the pulse period is independent of the number of points per pattern. Additionally, such simulations have the advantages to be simple as they only involve simple geometry and trigonometry functions. However, it assumes that the pressure distribution is constant over the surface. Hoshi et al. [2010] showed that in the case of a focal point produced with an ultrasonic phased array driven by 40 kHz transducers, the focal point acoustic radiation pressure distribution could be assimilated to a Gaussian. Although, Price and Long [2018] suggest that this distribution is dependent of the transducer alignment within the ultrasonic phased array, as well as the focal point position in space. Similalry, Vallbo et al. [1995] observed that the perception over the mechanoreceptors' receptive field was not constant. In their research, Authors noticed that the mechanoreceptors' receptive fields were composed of small and packed high sensitivity spots with diffuse borders. Furthermore, mechanoerceptors' receptive fields are elogated, rather than perfect circles (Gibson and Craig [2005]).

Therefore, rather than taking the overlapp area as a measure of the pulse train envelope, it will be better to work with probability functions. One probability function would represent the focal point pressure distribution (i.e. a Gaussian), and a second one would represent the mechanoreceptor sensitivity. By then looking at these two functions, one would be able to determine how much pressure actually reaches the mechanoreceptors and determine the envelope of the pulse train with finer granularity. Future work will look at improving the current script with these probability functions. This investigation will be part of a bigger framework of research that we will present in the next section.

6.2 Future work

6.2.1 A new framework of research

In the previous sections and chapters we saw that the spatiotemporal modulation method discussed in this thesis cannot be investigated systematically by considering only the pressure at the focal point like it was the case with the Amplitude Modualtion method. Therefore, we suggested to rather concentrate on what information reaches the mechanoreceptors, and further deepen the analysis by considering the mechanoreceptor sensitivity. Figure 6.6 shows the steps one could consider for such an approach. This new framework can be divided between two blocks, sensation and perception.

First, the sensation block determines the pressure a focal point applies to a given mechanoreceptor's receptive field as it moves along a spatiotemporal pattern. The resulting information is function of pressure applied to a single mechanoreceptor's receptive field, centred on a single position on the palm. One could argue that the process needs to be repeated at each location across the spatiotemporal pattern, to record accurately the pressure variations over the spatiotemporal pattern. However, Spatiotemporal patterns are periodic signals, for which sample position are resulting from their path being linearly sampled according to a given number of points per pattern (see chapter 5). Hence, a reasonable assumption is that for steps smaller than the haptic point width, the computed pressure signal will be equivalent in all positions across the pattern path, even if the considered position is not a sample position. Steps greater than the focal point width are unlikely to be produced, as it will mean that some parts of the pattern path are not stimulated, and therefore it is likely that the rendered pattern feels discontinuous, which is undesired. The previous section shows preliminary work and investigations into determining the

pressure applied to the mechanoreceptors for a range of mid-air haptic pattern.

Then, the perception block compares the deformation resulting from the pressure function, and in particular its frequency content, to the mechanoreceptor frequency sensitivity. To do so, one can apply Fast Fourier Transform to the deformation signal and hence obtain the frequency content produced by the mid-air haptic pattern. The advantage to analyse the frequency spectrum of the deformation signal rather than the pressure signal, is that mechanoreceptor frequency sensitivity is defined in relation to skind displacement, making the comparison between the two straightforward. Hence, if the magnitude of one of the deformation harmonics is greater than the magnitude of the mechanoreceptor sensitivity at the same frequency, one could predict that the spatiotemporal pattern will be perceived. To account for variation in skin properties and perception thresholds across users, the difference between magnitudes, might need to be greater that a certain level. This level could potentially be refined through a user study. Additionally, one could hypothesise that the greater the difference magnitudes, the stronger the pattern will be perceived.

While the sensation block defines a pressure function, the perception blocks processes deformation information. Therefore, a third block is required between the two. This third block will translate pressure information into deformation information, using the knowledge on skin viscoelastic properties. This step can either be analytical using the various rheological models presented in section 2.2.1. Alternatively, a Finite Element Model capturing skin deformation under the pressure stimuli of ultrasonic phased arrays could be developed and implemented. Even though this step is unlikely to affect where the harmonics stands on the frequency spectrum, it is known that the skin response is frequency dependent and therefore, some frequencies might be attenuated compare to others.

Once this new framework implemented (Figure 6.6), one could use it to determine whether spatiotemporal patterns can be perceived. First, we will need to validate this new framework with simple stimuli, for which detection is already known. Once validated, this new framework could be employed to explore more complex mid-air haptic patterns. Additionally, a given pattern could be optimised by varying some of its parameters and looking at the combinations of parameters that maximise the perceived strength.

It is worth mentioning that this approach is not the first of its kind. For instance, a similar framework has been successfully implemented for studying electrostatic display (Vardar et al. [2017]). However, beyond this new framework of research, there are still various research activities that could be carried out around the topic of mid-air haptic patterns. The next section will suggest such potential research

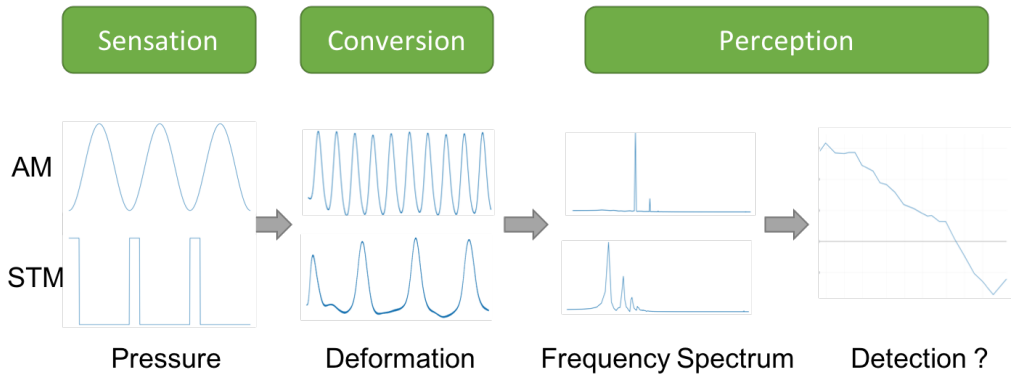

Figure 6.6: Proposed Research Framework. Characterising the pressure applied at the mechanoreceptor's receptive field could help to predict whether a given mid-air haptic stimulus will be perceived.

activities.

6.2.2 Beyond the framework

In section 3.3 we defined mid-air tactile patterns as made of two components, namely pattern shape and pattern sensation. However, the work reported here, as well as the short term future work is only focusing on rendering the verteces and edges of a mid-air tactile shape.

In the previous section we discussed the lack of systematic studies about mid-air tactile pattern shape recognition. Even though we expect increased performance compared to previous studies, it has recently been shown that mid-air haptic shape identification performance can vary significantly according to the shape itself (Rutten et al. [2019]). In their work Authors introduced a distinction between static and dynamic shape, however, we plan to run systematic studies to probe further which categories of shapes can or cannot be conveyed efficiently to the user. Once more, the results would be pertinent to mid-air haptic experience designers, and provide insight into which pattern shape they should use to convey compelling experiences.

This future work still assumes to render only the outline of a pattern shape. However, to render the second component of a mid-air tactile pattern, namely the pattern sensation, it will be more appropriate if the whole surface of the shape was rendered. Indeed, most of the tactile sensation that can be produced (e.g. roughness, hardness, stickiness) rely on variations of the shape surface (see section 2.3.2). To that end, we will define two long term works, namely rendering mid-air tactile surfaces and rendering mid-air tactile sensations.

Mid-air tactile surfaces is something we touched on briefly in section 3.3, when discussing space-filling curves. The same way a cathode-ray tube scans through the

screen to update the visual information, one could define a scanning function for the mid-air tactile point to scan a defined space and update the haptic information. However, the length of this path will increase drastically the surface area one wants to display tactile information onto. Therefore, systematic studies on how to render mid-air tactile surfaces are required. Rendering surface with spatiotemporal modulation will include many explorations on the impact of parameters such as the maximum surface one can render, the density of mid-air tactile points within a surface, the scanning function used and so on. Furthermore, according to the scanning function chosen, the overlap between sampling positions is likely to occur both for consecutive sampling positions in time and for sampling position close in space. This extra complexity can lead to a refined or expanded framework introduced in chapter 6.

Then, we would like to investigate the second component of mid-air tactile patterns, namely the sensation. Until now, our effort has been focused on rendering spatial information such as verteces and edges, but also discussing potential rendering methods for mid-air tactile surfaces. However, all these methods leverage the spatial properties of the mid-air tactile point, while keeping the pressure at the mid-air haptic point constant. Indeed, ultrasonic phased arrays allow control over the mid-air tactile point pressure. Using a dynamic pressure over space and time has the potential to further control the pressure applied to the mechanoreceptor receptive field. One could hypothesise that tuning this pressure, would have effect on the perceptual space beyond the perceived intensity. Therefore, using dynamic pressure, we will be able to start exploring other dimensions of mid-air tactile pattern perceptual space. Or in other words, we will be able to start exploring the sensation associated with a given mid-air tactile pattern. As touch is divided into different dimensions (see section 2.3), mid-air tactile pattern sensations have the potential to cover the same dimensions. Therefore, future work will investigate rendering methods to improve roughness, hardness and friction information transfer. These studies could leverage hypotheses from contact devices, as well as introducing novel methods. However, the work reported here showed that varying position over time leads to a wide parameter space where each variable could have an impact more or less important on the perceptual space. Therefore, it is expected that varying pressure magnitude over time will increase drastically the parameter space, and by extension the number of studies required to fully understand the full extent of spatiotemporal modulation perceptual space. Additionally, one could hypothesise, that in some instances pattern shape perception and pattern sensation perception are affected by the same parameter. Therefore, future work will also focus on rendering methods

accommodating both pattern shape and sensation requirements.

6.2.3 Complimentary Work

The work reported in this thesis, as well as the future work presented in the previous sections investigate the limit of conveying tactile information in mid-air using technology such as ultrasonic phased arrays. However, such displays are only able to stimulate the cutaneous part of the somatosensory system. Therefore, it is likely that ultrasonic phased arrays fail to convey all the aspects of touch information.

Nonetheless, it is worth to mention that mid-air haptic displays are unlikely to be used on their own. As stated in the introduction, mid-air haptic displays are born from the necessity to enhance 3D-Display interaction with touch information. Therefore, it is sensible to assume that mid-air tactile stimuli will be used in synergy with stimuli from other modalities. Additionally, it is well-known in the literature, that perception is a joint effort between the different modalities. On a daily basis, one's brain uses information from the different senses to draw conclusions from one's surroundings.

For instance, it has been shown that the use of visuals in virtual environments could influence one sensation of compliance (Di Luca et al. [2011]). Similarly, it has been demonstrated that audio stimuli could affect one's perception of roughness (Jousmäki and Hari [1998]).

Therefore, it is likely that results from multisensory interaction could be applied to mid-air tactile patterns. Hence, future work could also explore how to re-enforce mid-air tactile pattern sensation through the design of multisensory stimuli using both visuals and auditory signals, and vice versa.

Ultimately, this Thesis only presents initial work on getting stronger mid-air tactile patterns. The future work should be pursuing investigations on how to render stronger mid-air tactile patterns, but also how to render richer patterns. Strength is only one aspect and the technology will only become widely adopted if one manages to produce richer stimuli. As presented in this Thesis, the research in mid-air haptic patterns needs to be cross-disciplinary. Only collaboration between experts in different key-fields will allow further progress. Therefore, I not only hope to be able to carry out working on the ideas and work presented here, but also have the chance to collaborate with many experts on those fascinating research questions.

This chapter presented initial investigations on a new research framework to predict the perception of spatiotemporal patterns according to various parameters such as pattern length, repetition rate and device update rate. Even though further

investigations are necessary to validate the approach, the current results provides interesting cues. Indeed, using simple equations, we derived the width of the local pulse signal and determined this width was independent from the number of points per pattern. This observation leads us to refute the suggestion that the number of points per pattern was affecting the signal pulse width and therefore the pattern perception. It is encouraging for the future work, which has the potential to address the remaining suggestions we formulated at the end of chapter 5. This progress has been made possible by considering the haptic signal produced at a specific location on the skin, rather than the haptic signal produced at the focal point centre. We believe that this approach should lead to further breakthroughs in understanding the perception of mid-air haptic patterns in the near future. However, we could not fully explore our suggestions in this thesis. The next and final chapet will summarise our work's contribution but also highlight its limitations.

Chapter 7

Conclusion

Mid-air haptics is a growing field, which has a great potential to enhance a wide range of interactions such as AR, VR and 3D-displays. As we discussed in chapter 3, the field relies on various technologies, among which ultrasonic phased arrays have a growing popularity amid academia and industry. The work presented in this thesis is essentially focusing on investigating the use of such technology to convey continuous and distributed spatiotemporal tactile feedback. While, in section 3.3, we presented an approach to render spatiotemporal mid-air tactile patterns where patterns are divided into shape and sensation, we focused our work mainly on the former. In other words, our work focused on rendering strong mid-air tactile pattern shapes. In particular, in the work reported here, we looked at exploring and strengthening the relationship between spatiotemporal parameter space and perceptual space, with a focus on perceived pattern strength.

While our work includes a significant contribution to the field, we acknowledge that the results reported in the chapters also have some limitations. This final section first summarizes the contributions and limitations of our work and then identifies future opportunities. We acknowledge that the work presented in this thesis is only a stepping stone towards better spatiotemporal mid-air tactile feedback and does not solve all the problems we have identified at the beginning of this thesis.

7.1 Contributions

The main goal of the work presented in this thesis was to investigate how to convey stronger spatially distributed mid-air tactile patterns. To do so, we leveraged the rendering capabilities of a recent modulation technique, namely Spatiotemporal Modulation. While most researchers focused their effort on engineering and algorithmic challenges, which lead to the development of spatiotemporal modulation,

little attention has been paid to the relationship between spatiotemporal parameters space and its associated perceptual space. In that sense our research is the first step towards a better understanding of the relationship between STM parameter space and STM perceptual space. Our research results are mainly valuable to the mid-air haptic experience designers, who can reuse our contributions within their work. However, our results also provide insights into the perception of spatiotemporal tactile pattern, which are beneficial to the broader haptic community. The current section summarise our contributions to both communities.

7.1.1 Mid-air Haptic Applications

Until now, mid-air haptic experience designers were targeting temporal information at a given location, to convey tactile information to the users. Additionally, designers could further tune the temporal information to change the corresponding sensation to their desire. However, to convey the perception of shape, designers were constrained to align multiple tactile points along the desired shape. This approach is consequently limited by the number of tactile point that can be produced simultaneously without decreasing their relative strength below the threshold of perception. Hence, only simple and small mid-air tactile patterns could be produced.

With spatiotemporal modulation, this constraint is no longer present, and mid-air haptic experience designers can start producing bigger and more complex shapes. Although, the drawback of this method, is that since the modulation technique is recent, guidelines relative to STM usage are absent from the literature. Designers, therefore, have to tweak the various variables from spatiotemporal parameter space without knowing their impact on the perceptual space. Through successive studies, we attempted to overcome this issue and provide designers with insightful guidelines to render spatiotemporal patterns.

Recall that rendering spatiotemporal patterns involves moving a mid-air tactile point rapidly and repeatedly. Hence, one can define two parameters, namely the draw speed and the draw frequency, which represent the speed at which the haptic point moves, and the rate at which the pattern is repeated, respectively. Furthermore, the draw speed, S is proportional to the draw frequency F, with the pattern length L as coefficient of proportionality.

$$S = F \times L$$

§

Designers might have intuitively been tempted to tune the drawing frequency, as

it is usually done with Amplitude Modulation (see section 3.2.2). Hence, setting the drawing frequency around 200 Hz, which is the frequency perceived the strongest. However, we show in chapter 4, that on the contrary, the approach should be to tune the draw speed, for two reasons.

- Optimising draw speed maximises pattern perceived strength
- Fixing draw speed causes perceived strength to be invariant to scaling

These results were demonstrated through both a vibrometry study (see section 4.2) and a user study (see section 4.3).

Furthermore, we showed in chapter 5 that the number of points per pattern was another important variable from spatiotemporal parameter space. Recall, that the number of sampling point per pattern designates the number of positions the mid-air haptic point goes through to draw one pattern iteration. Until now, and especially for vibrotactile stimuli, the number of point per pattern was always related to pattern quality and therefore maximised whenever possible. However, our results highlight that for draw frequencies under 10 Hz, changing the number of point per pattern could have an important impact on perceived pattern strength. Yet, the number of points per pattern effect on the pattern is twofold. First, increasing or decreasing the number of points per pattern, decreases and increases the distance between two sample positions. Second, increasing or decreasing the number of points per pattern, decreases and increases the stimulation duration at each sample position. Before our study, it was unknown which of the two quantities was the most relevant. Our user studies revealed that optimising the distance between two sample positions could maximise perceived pattern strength for draw frequency lower than 10 Hz. However, the optimal distance was varying with the draw frequency. The contributions of these studies are therefore twofold.

- Optimising distance between two sample positions maximises perceived pattern strength, for a draw frequency lower than 10 Hz
- Fixing the distance between two sample positions causes perceived pattern strength to be invariant to scaling.

Additionally, our results extended the lower limit of the perceptual space from draw frequency at 10 Hz to draw frequency at 2 Hz. Thanks to Weber's Law, we know that the sense of touch, as every other senses, is logarithmic. Therefore, this new range represents an increase of 50% of the range of draw frequencies one could perceive until now.

All these discoveries on spatiotemporal modulation parameter space are beneficial to mid-air haptic experience designers. Indeed, thanks to our contributions, designers can use our guidelines to improve mid-air tactile perceived pattern strength, as well as ensuring constant perceived strength through scaling. One could easily imagine these guidelines bein implemented in mid-air haptic authoring tools, so designers can remain oblivious to the intricacies of mid-air haptic perception, and focus on designing compelling user experiences. Our results also provide insights into the perceptual mechanism related to spatiotemporal modulation. These contributions are of interest to the larger haptic perception community and are discussed in the next section.

7.1.2 Haptic Perception

While our main goal was to provide mid-air haptic experience designers with a set of guidelines in order to design better and stronger mid-air haptic patterns, our results also provide an interesting set of contributions for the haptic perception community, both in the biomechanics and psychophysics fields.

First, it is worth noting the unique nature of ultrasonic phased arrays compared to other contact and non-contact tactile displays. Usually, tactile displays stimulate the skin in specific and predetermined locations. State of the art tactile displays include either a dense amount of actuators but cover a small area (Sripati et al. [2006], Wang and Hayward [2006]) or cover a large area but include few actuators (Schneider et al. [2015]). Ultrasonic phased arrays, especially using spatiotemporal modulation, are the first occurrence where a display can stimulate a large area such as the palm with a high spatial resolution. This particularity makes ultrasonic phased arrays a unique opportunity to study the perception of rapid and repeated stimulation of the skin. This is confirmed with the results of our studies, which make new contribution the haptic perception community and are discussed in this section.

To the field of biomechanics, our work provides new insights on wave propagating on the skin surface. Propagating waves on the skin have already been observed in the literature (Manfredi et al. [2012]). The fact that propagating waves travels fast and far on the skin surface leads researchers to stress their importance in texture perception (Delhaye et al. [2012]) and whole hand interactions (Shao et al. [2016]). However, these studies focused on characterising the propagation of skin surface waves from a unique source. With our vibrometry study (see section 4.2), on the other hand, we are able to stimulate the skin on various locations and observe the interference between the corresponding propagating waves. In particular, our vi-

brometry study revealed that producing a spatiotemporal pattern with a rendering speed equivalent to the propagating waves speed is maximising the displacement produced on the medium. Hence, we showed that mid-air tactile patterns could be rendered in such a way that they are interacting with the same propagating wave they produced, in order to optimise the displacement they induced when projecting on a viscoelastic surface. We later showed in a user study, that in such a specific scenario, the strength users' perceived was increased. While previous research highlight the importance of propagating waves in haptic perception, our work is the first to suggest that propagating waves could be a central component of the haptic pattern design itself.

To the field of psychophysics, the work presented here includes valuable data that refine further the relationship between spatiotemporal modulation parameter space and its associated perceptual space. Through a set of three user studies, we determined the effect of 4 parameters (i.e. draw frequency, draw speed, pattern size and the number of points per pattern) on the perceived pattern strength. In all three studies, we systematically used a scaling task (i.e. Magnitude Estimation) to measure the effect of each parameter on the perceived pattern strength. The first user study (see section 4.3) showed how perceived strength varies with mid-air pattern size and draw speed. While the results showed that draw speed affects greatly the pattern perceived strength, they also show that smaller pattern (i.e. 5 cm long) are perceived weaker than bigger ones (i.e. above 10 cm long). In the second and third user study (see sections 5.2 and 5.3), results showed that perceived strength is further affected by the number of points per pattern, and especially the resulting distance between two consecutive sample positions. As in the first study, the perceived strength is significantly lower for smaller pattern than for bigger ones. Using the results of these studies, we can also conclude on the order of importance of each parameter. Hence, we show that the perceived strength depends mainly on pattern draw speed. However, at speed lower than $2\,\mathrm{m\,s^{-1}}$, the perceived strength depends mainly on the number of points per pattern. Finally, in both cases, studies show that pattern size plays a role in pattern perceived strength.

Overall, the work reported here opens new horizons on how haptic perception mechanisms process spatiotemporal patterns. Until now tactile perception was mostly related to vibrotactile perception, which rely on a small parameter space mainly dominated by the temporal signal components (e.g. frequency and waveform). Therefore, only mechanoreceptors' frequency sensitivity was considered. With spatiotemporal modulation, we show that this was a limitation and that now spatial signal components should be considered too, to take into account factors such

as mechanoreceptors' receptive field and tactile point width. We discussed in chapter 6 how the assumptions regarding the tactile point width and the mechanoreceptor receptive field area, could lead to misleading conclusions regarding the stimulation duration of a given mechanoreceptor during spatiotemporal modulation. Additionally, spatiotemporal modulation motivates researchers to consider more than the draw frequency of a mid-air haptic stimulus. Accounting for these new considerations, we undertook to define a new framework of research for the specific case of spatiotemporal patterns. This new research framework rejects the assumptions previously made for the study of vibrotactile stimuli. While it still needs refinement, we additionally contribute towards the development of the blocks composing this new framework of research. Especially, we propose a paradigm shift, where instead of observing the evolution of the tactile point in space over time, we observe the pressure applied to a given location over time. In other words, instead of observing the behaviour of the tactile point over time, we propose to observe the evolution of skin displacement at the skin surface over time.

While our work presents various contribution to both the mid-air haptic experience designers community and the haptic perception community, we acknowledge that our work presents a set of limitations. The next section will discuss these limitations.

7.2 Limitations

No study is perfect, and the ones reported here are no exceptions to the rule. We will in this section look back at our work and discuss the different limitations of our work. These limitations are of two different natures. On the one hand, limitations can be found in the methodology and the way we collected data. On the other hand, the limitations can be found in the results, and the way we analysed the collected data. In addition to acknowledging these limitations, we will compare with the standard within the research community and how we could improve in the future.

7.2.1 Methodology

First we acknowledge the methodology we used to collect our data presents some drawbacks.

For instance, the vibrometry study was taking place on skin-mimicking material (i.e. silicone) rather than in-vivo. While silicone has been repeatedly used to model skin behaviour (Royston et al. [2011], Kearney et al. [2015]), readers could argue that whether the phenomenon observed in our vibrometry study occurs on the skin

is undetermined. We agree that the averaged propagating wave velocity measured on the silicone (i.e. $10\,\mathrm{m\,s^{-1}}$) cannot be directly transfered to the skin, because propagating wave velocity depends on the medium's shape and viscoelastic properties. However, we would like to remind the reader that propagating waves have been observed on the skin surface on many occasions (Delhaye et al. [2012], Manfredi et al. [2012], Shao et al. [2016], Fradet et al. [2017]) and that their averaged speed has been measured to be $7\,\mathrm{m\,s^{-1}}$ on the finger. In our study we predicted that the peak perceived strength observed around 5-8 $\mathrm{m\,s^{-1}}$ means the averaged propagating wave velocity on the palm is around 5-8 $\mathrm{m\,s^{-1}}$ too. It is correct that without measuring this velocity first, we cannot fully conclude about the relationship between propagating waves and perceived strength. Nonetheless, our estimate is in agreement with the measured velocity from previous work. Furthermore, the similarities between silicone's vibrometry and user study results are uncanny. Therefore, it is unlikely that in-vivo measurement would yield results in disagreement with our assumptions. Nonetheless, we suggest that in-vivo measurement should be considered for subsequent investigations.

Another concern is the method we used to determine perceived strength. Perceived strength has consistently been measured through magnitude estimation tasks, which is a method that relies on user ratings. However one could object that users data is made of discrete subjective answers as opposed to continuous quantitative magnitudes. Furthermore, users' ratings are very much biased by external factors such as the context within which the rating was occurring as well as the properties with which the set of stimuli was designed (Jones and Tan [2012]). However, we would like to let the reader know that we carefully analysed participants' answers according to the recommendations of various references (Han et al. [1999], Jones and Tan [2012], Strohmeier and Hornbæk [2017]).

7.2.2 Results

We are also aware that the results and the conclusions we draw from them, are limited to the context in which we tested them for. Therefore, one could argue against the applicability of our results to other contexts.

First, it is worth noting that while we show evidence that surface wave propagation could positively interefers with a focal point trajectory to produce greater displacement in the surface, we did not directly observe this interaction. Reardon et al. [2019], whose work was published after mine, also suggest that such effects could occur. Our recordings only show indirect evidence of this effect via both a vibrometry study and a user study. To confirm this hypothesis, one would need to

carry another vibrometry study. In such a study, the focal point could move on a linear trajectory and only once (as opposed to repeatedly as in spatiotemporal modulation). By observing the displacement over this line, the vibrometry should highlight the presence of a wavefront moving ahead or behind the focal point. In a way, the observation should be similar to the one of a shock wave observed for planes moving faster/slower than the speed of sound in air.

One could also question the applicability of our results to other devices. Indeed, our work reports mainly trends which are all expressed in arbitrary units. The explanation for that is the fact that our stimulus output is unitless in the first place. Indeed, as explained in 3.4.1, the actual force (and associated distribution) ultrasonic phased arrays produce is too complex to compute accurately. Therefore, one could argue that not knowing what our device output is, limits the application of our results with other ultrasonic phased arrays than the one we used. Indeed, Verrillo [1971] show that force magnitude and force distribution can have major impacts on the perception. We agree, that we have not characterised force magnitude and force distribution in our studies. However, our work fits within a body of research about ultrasonic phased arrays for which the output has been characterised repeatedly and empirically. Estimates of both force magnitude and force distribution have been defined and reported in chapter 3. Therefore, one could apply these empirical estimates on one's own device and compare their relative difference with our estimates.

The applicability of our results to other shapes can also be questioned. Indeed, our studies only focus on circular shapes rather than a wide range of geometric shapes (Long et al. [2014]) or distributed patterns (Obrist et al. [2015]). Therefore, one could argue that our results only stand for circles and whether these results can be applied to other shapes such as squares or triangles cannot be answered without further investigations. Recall that our results express guidelines for the draw speed and the sampling rate of a device. These two parameters can be defined using the properties of two consecutive sampling points. Indeed, draw speed can be defined as the ratio of the distance between two consecutive samples and the duration between these samples. Additionally, changing the sampling rate will modify the distance between two consecutive samples and the duration between these samples, in equal proportions. Therefore, we will argue back that our results only consider the spatial and temporal properties between two consecutive points, and by extension are independent of the resulting pattern shape. To that end, it was easier to focus on a single shape and the choice of a circle is only here for the sake of simplicity. We would like to point out that this choice is common with other research group in

the field (Korres et al. [2017]).

Finally, our results are limited by the fact that our studies focus mainly on the perceived strength of a given mid-air haptic pattern. One could argue that it would have been more appropriate to focus on the users' ability to correctly discriminate between patterns or recognise a given pattern among a given set. We would like to remind the reader that Plaisier et al. [2009] demonstrated that edges and vertices are the most important cues in shape recognition. Therefore, making edges and vertices more salient through increasing their perceived strength is directly contributing to increasing shape recognition. As Long et al. [2014] and Korres et al. [2017] before us, our work focused on the shape rendering algorithm and making shape features more salient, rather than a systematic study on shape recognition. Furthermore, both works used Amplitude Modulation as opposed to Spatiotemporal Modulation. As pointed in chapter 3 Amplitude Modulation presented some inherent drawbacks when it comes to perceived strength. Indeed, as explained in the corresponding chapter, producing a distributed pattern with AM will yield an acoustic pressure per location significantly lower than with STM. This same chapter discussed how this reduced acoustic pressure leads to a weaker pattern strength, even though no direct proof were provided as far as we know. Our approach using spatiotemporal modulation, which leads to stronger pattern strength, we hypothesise that our method should build on, or at least equal, Long et al. [2014] results, where user could recognise a shape from a set of 7 volumetric shapes. We agree that to validate this hypothesis, one would need to measure to what extent the performances in shape recognition have increased between the studies and compare these performances to Long et al. [2014] and Korres et al. [2017]. However, this was beyond the scope of this work, and will be part be of future work as discussed later.

The limitations presented in this section are related to both the methodology used during our studies and the conclusions we made from these studies results. However, the impact of these limitations does not discard entirely the validity of the work presented in this thesis. Nonetheless, the doubt discussed in this section could be overcome with additional work. This future work has already been discussed in the previous chapter.

In summary, in this thesis, we have shown that spatiotemporal tactile patterns can be rendered in mid-air with the use of ultrasonic phase arrays. Moreover, the studies presented here show the importance of two main parameters, namely, the *speed* of the focal point, and the *update rate* of the device used to render the pattens. Based on the results of these studies, we suggested a set of guidelines for mid-air

tactile pattern designers. We believe this thesis contributes significantly to the field of mid-air haptics and will benefit any human-computer interaction systems making use of mid-air haptics.

Bibliography

D. Ablart, C. Velasco, and M. Obrist. Integrating mid-air haptics into movie experiences. In *Proceedings of the 2017 ACM International Conference on Interactive Experiences for TV and Online Video*, pages 77–84, 2017.

M. Azh, S. Zhao, and S. Subramanian. Investigating expressive tactile interaction design in artistic graphical representations. *ACM Transactions on Computer-Human Interaction (TOCHI)*, 23(5):1–47, 2016.

S. J. Bensmaıa and M. Hollins. Complex tactile waveform discrimination. *The Journal of the Acoustical Society of America*, 108(3):1236–1245, 2000.

S. J. Bensmaia and M. Hollins. The vibrations of texture. *Somatosensory & Motor Research*, 20(1):33–43, 2003.

A. Bicchi, E. P. Scilingo, and D. De Rossi. Haptic discrimination of softness in teleoperation: the role of the contact area spread rate. *IEEE Transactions on Robotics and Automation*, 16(5):496–504, 2000.

J. Biggs and M. A. Srinivasan. Tangential versus normal displacements of skin: Relative effectiveness for producing tactile sensations. In *Proceedings 10th Symposium on Haptic Interfaces for Virtual Environment and Teleoperator Systems. HAPTICS 2002*, pages 121–128. IEEE, 2002.

G. Campion and V. Hayward. Fundamental limits in the rendering of virtual haptic textures. In *First Joint Eurohaptics Conference and Symposium on Haptic Interfaces for Virtual Environment and Teleoperator Systems. World Haptics Conference*, pages 263–270. IEEE, 2005.

T. Carter, S. A. Seah, B. Long, B. Drinkwater, and S. Subramanian. Ultrahaptics: multi-point mid-air haptic feedback for touch surfaces. In *Proceedings of the 26th Annual ACM Symposium on User Interface Software and Technology*, pages 505–514, 2013.

S. Choi and H. Z. Tan. Perceived instability of virtual haptic texture: Iii. effect of update rate. *Presence: Teleoperators and Virtual Environments*, 16(3):263–278, 2007.

B. Clark, O. S. Schneider, K. E. MacLean, and H. Z. Tan. Predictable and distinguishable morphing of vibrotactile rhythm. In *2017 IEEE World Haptics Conference (WHC)*, pages 84–89. IEEE, 2017.

H. Culbertson, J. J. Lopez Delgado, and K. J. Kuchenbecker. The penn haptic texture toolkit for modeling, rendering, and evaluating haptic virtual textures. 2014.

K. Dandekar, B. I. Raju, and M. A. Srinivasan. 3-d finite-element models of human and monkey fingertips to investigate the mechanics of tactile sense. *Journal of Biomechanical Engineering*, 125(5):682–691, 2003.

B. Delhaye, V. Hayward, P. Lefèvre, and J.-L. Thonnard. Texture-induced vibrations in the forearm during tactile exploration. *Frontiers in Behavioral Neuroscience*, 6:37, 2012.

S. Derler and L.-C. Gerhardt. Tribology of skin: review and analysis of experimental results for the friction coefficient of human skin. *Tribology Letters*, 45(1):1–27, 2012.

M. Di Luca, B. Knörlein, M. O. Ernst, and M. Harders. Effects of visual–haptic asynchronies and loading–unloading movements on compliance perception. *Brain Research Bulletin*, 85(5):245–259, 2011.

C. Doerrer and R. Werthschuetzky. Simulating push-buttons using a haptic display: Requirements on force resolution and force-displacement curve. In *Proceedings of Eurohaptics: International Conference on Human Haptic Sensing and Touch Enabled Computer Applications*, pages 41–46, 2002.

Y. Dong, S. Mihalas, S. S. Kim, T. Yoshioka, S. Bensmaia, and E. Niebur. A simple model of mechanotransduction in primate glabrous skin. *Journal of Neurophysiology*, 109(5):1350–1359, 2013.

B. Dzidek, S. Bochereau, S. Johnson, V. Hayward, and M. Adams. Frictional dynamics of finger pads are governed by four length-scales and two time-scales. In *2016 IEEE Haptics Symposium (HAPTICS)*, pages 161–166. IEEE, 2016.

L. Fichera, C. Pacchierotti, E. Olivieri, D. Prattichizzo, and L. S. Mattos. Kinesthetic and vibrotactilehaptic feedback improves the performance of laser microsurgery. In *2016 IEEE haptics symposium (HAPTICS)*, pages 59–64. IEEE, 2016.

C. Fradet, L. R. Manfredi, S. Bensmaia, and V. Hayward. Fingertip skin as a linear medium for wave propagation. In *2017 IEEE World Haptics Conference (WHC)*, pages 507–510. IEEE, 2017.

A. W. Freeman and K. O. Johnson. Cutaneous mechanoreceptors in macaque monkey: temporal discharge patterns evoked by vibration, and a receptor model. *The Journal of Physiology*, 323(1):21–41, 1982.

E. Freeman, R. Anderson, J. Williamson, G. Wilson, and S. A. Brewster. Textured surfaces for ultrasound haptic displays. In *Proceedings of the 19th ACM International Conference on Multimodal Interaction*, pages 491–492, 2017.

W. Frier, K. Seo, and S. Subramanian. Hilbert curves: A tool for resolution independent haptic texture. In *Proceedings of the 29th Annual Symposium on User Interface Software and Technology*, pages 211–212, 2016.

J. Geng. Three-dimensional display technologies. *Advances in Optics and Photonics*, 5(4):456–535, 2013.

L.-C. Gerhardt, V. Strässle, A. Lenz, N. Spencer, and S. Derler. Influence of epidermal hydration on the friction of human skin against textiles. *Journal of the Royal Society Interface*, 5(28):1317–1328, 2008.

G. A. Gescheider, S. J. Bolanowski, J. V. Pope, and R. T. Verrillo. A four-channel analysis of the tactile sensitivity of the fingertip: frequency selectivity, spatial summation, and temporal summation. *Somatosensory & Motor Research*, 19(2): 114–124, 2002.

G. A. Gescheider, S. J. Bolanowski, and R. T. Verrillo. Some characteristics of tactile channels. *Behavioural Brain Research*, 148(1-2):35–40, 2004.

G. O. Gibson and J. C. Craig. Tactile spatial sensitivity and anisotropy. *Perception & Psychophysics*, 67(6):1061–1079, 2005.

S. H. Han, M. Song, and J. Kwahk. A systematic method for analyzing magnitude estimation data. *International Journal of Industrial Ergonomics*, 23(5-6):513–524, 1999.

V. Hayward, A. V. Terekhov, S.-C. Wong, P. Geborek, F. Bengtsson, and H. Jörntell. Spatio-temporal skin strain distributions evoke low variability spike responses in cuneate neurons. *Journal of The Royal Society Interface*, 11(93):20131015, 2014.

N. S. Holliman, N. A. Dodgson, G. E. Favalora, and L. Pockett. Three-dimensional displays: a review and applications analysis. *IEEE Transactions on Broadcasting*, 57(2):362–371, 2011.

T. Hoshi, M. Takahashi, T. Iwamoto, and H. Shinoda. Noncontact tactile display based on radiation pressure of airborne ultrasound. *IEEE Transactions on Haptics*, 3(3):155–165, 2010.

S. Inoue, Y. Makino, and H. Shinoda. Mid-air ultrasonic pressure control on skin by adaptive focusing. In *Proceedings of Eurohaptics: International Conference on Human Haptic Sensing and Touch Enabled Computer Applications*, pages 68–77. Springer, 2016.

M. Iodice, W. Frier, J. Wilcox, B. Long, and O. Georgiou. Pulsed schlieren imaging of ultrasonic haptics and levitation using phased arrays. *arXiv preprint arXiv:1810.00258*, 2018.

A. Ion, E. J. Wang, and P. Baudisch. Skin drag displays: Dragging a physical tactor across the user's skin produces a stronger tactile stimulus than vibrotactile. In *Proceedings of the 33rd Annual ACM Conference on Human Factors in Computing Systems*, pages 2501–2504, 2015.

ISO. *Geometrical Product Specifications (GPS) – Surface texture: Profile method – Terms, definitions and surface texture parameters.* 1997.

M. Ito, D. Wakuda, S. Inoue, Y. Makino, and H. Shinoda. High spatial resolution midair tactile display using 70 khz ultrasound. In *Proceedings of Eurohaptics: International Conference on Human Haptic Sensing and Touch Enabled Computer Applications*, pages 57–67. Springer, 2016.

R. S. Johansson. Tactile sensibility in the human hand: receptive field characteristics of mechanoreceptive units in the glabrous skin area. *The Journal of Physiology*, 281(1):101–125, 1978.

R. S. Johansson and J. R. Flanagan. Coding and use of tactile signals from the fingertips in object manipulation tasks. *Nature Reviews Neuroscience*, 10(5):345–359, 2009.

R. S. Johansson and A. Vallbo. Tactile sensibility in the human hand: relative and absolute densities of four types of mechanoreceptive units in glabrous skin. *The Journal of Physiology*, 286(1):283–300, 1979.

R. S. Johansson and Å. B. Vallbo. Tactile sensory coding in the glabrous skin of the human hand. *Trends in Neurosciences*, 6:27–32, 1983.

L. A. Jones and H. Z. Tan. Application of psychophysical techniques to haptic research. *IEEE Transactions on Haptics*, 6(3):268–284, 2012.

V. Jousmäki and R. Hari. Parchment-skin illusion: sound-biased touch. *Current Biology*, 8(6):R190–R191, 1998.

J.-H. Jun, J.-R. Park, S.-P. Kim, Y. M. Bae, J.-Y. Park, H.-S. Kim, S. Choi, S. J. Jung, S. H. Park, D.-I. Yeom, et al. Laser-induced thermoelastic effects can evoke tactile sensations. *Scientific Reports*, 5:11016, 2015.

B. Kappus and B. Long. Spatiotemporal modulation for mid-air haptic feedback from an ultrasonic phased array. *The Journal of the Acoustical Society of America*, 143(3):1836–1836, 2018.

S. P. Kearney, A. Khan, Z. Dai, and T. J. Royston. Dynamic viscoelastic models of human skin using optical elastography. *Physics in Medicine & Biology*, 60(17): 6975, 2015.

J. Kildal. 3d-press: haptic illusion of compliance when pressing on a rigid surface. In *International Conference on Multimodal Interfaces and the Workshop on Machine Learning for Multimodal Interaction*, pages 1–8, 2010.

J. Kildal. Kooboh: variable tangible properties in a handheld haptic-illusion box. In *Proceedings of Eurohaptics: International Conference on Human Haptic Sensing and Touch Enabled Computer Applications*, pages 191–194. Springer, 2012.

S. Kim and G. Lee. Haptic feedback design for a virtual button along force-displacement curves. In *Proceedings of the 26th annual ACM symposium on User interface software and technology*, pages 91–96, 2013.

R. L. Klatzky and S. J. Lederman. Touch. *Handbook of Psychology*, pages 147–176, 2003.

S. Komandur, P. W. Johnson, R. L. Storch, and M. G. Yost. Relation between index finger width and hand width anthropometric measures. In *2009 Annual In-*

ternational Conference of the IEEE Engineering in Medicine and Biology Society, pages 823–826. IEEE, 2009.

J. Konrad and M. Halle. 3-d displays and signal processing. *IEEE Signal Processing Magazine*, 24(6):97–111, 2007.

G. Korres, T. Aujeszky, and M. Eid. Characterizing tactile rendering parameters for ultrasound based stimulation. In *2017 IEEE World Haptics Conference (WHC)*, pages 293–298. IEEE, 2017.

V. V. Krylov. Generation of ground vibrations by superfast trains. *Applied Acoustics*, 44(2):149–164, 1995.

V. V. Krylov, A. Dawson, M. Heelis, and A. Collop. Rail movement and ground waves caused by high-speed trains approaching track-soil critical velocities. *Proceedings of the Institution of Mechanical Engineers, Part F: Journal of Rail and Rapid Transit*, 214(2):107–116, 2000.

S. J. Lederman. The perception of surface roughness by active and passive touch. *Bulletin of the Psychonomic Society*, 18(5):253–255, 1981.

S. J. Lederman and R. L. Klatzky. Hand movements: A window into haptic object recognition. *Cognitive Psychology*, 19(3):342–368, 1987.

S. J. Lederman and R. L. Klatzky. Haptic perception: A tutorial. *Attention, Perception, & Psychophysics*, 71(7):1439–1459, 2009.

S. Lee and S. Zhai. The performance of touch screen soft buttons. In *Proceedings of the SIGCHI conference on Human Factors in Computing Systems*, pages 309–318, 2009.

X. Liang and S. A. Boppart. Biomechanical properties of in vivo human skin from dynamic optical coherence elastography. *IEEE Transactions on Biomedical Engineering*, 57(4):953–959, 2009.

B. Long, S. A. Seah, T. Carter, and S. Subramanian. Rendering volumetric haptic shapes in mid-air using ultrasound. *ACM Transactions on Graphics (TOG)*, 33 (6):1–10, 2014.

J. M. Loomis. Tactile pattern perception. *Perception*, 10(1):5–27, 1981.

Z. Ma, D. Edge, L. Findlater, and H. Z. Tan. Haptic keyclick feedback improves typing speed and reduces typing errors on a flat keyboard. In *2015 IEEE World Haptics Conference (WHC)*, pages 220–227. IEEE, 2015.

K. MacLean and M. Enriquez. Perceptual design of haptic icons. In *Proceedings of Eurohaptics: International Conference on Human Haptic Sensing and Touch Enabled Computer Applications*, pages 351–363, 2003.

N. A. Macmillan and C. D. Creelman. *Detection theory: A user's guide*. Psychology Press, 2004.

L. R. Manfredi, A. T. Baker, D. O. Elias, J. F. Dammann III, M. C. Zielinski, V. S. Polashock, and S. J. Bensmaia. The effect of surface wave propagation on neural responses to vibration in primate glabrous skin. *PloS One*, 7(2):e31203, 2012.

L. R. Manfredi, H. P. Saal, K. J. Brown, M. C. Zielinski, J. F. Dammann III, V. S. Polashock, and S. J. Bensmaia. Natural scenes in tactile texture. *Journal of Neurophysiology*, 111(9):1792–1802, 2014.

F. McGlone, H. Olausson, J. Boyle, M. Jones-Gotman, C. Dancer, S. Guest, and G. Essick. Touching and feeling: differences in pleasant touch processing between glabrous and hairy skin in humans. *European Journal of Neuroscience*, 35(11): 1782–1788, 2012.

F. McGlone, J. Wessberg, and H. Olausson. Discriminative and affective touch: sensing and feeling. *Neuron*, 82(4):737–755, 2014.

Ş. Mihalaş and E. Niebur. A generalized linear integrate-and-fire neural model produces diverse spiking behaviors. *Neural computation*, 21(3):704–718, 2009.

Y. Monnai, K. Hasegawa, M. Fujiwara, K. Yoshino, S. Inoue, and H. Shinoda. Haptomime: mid-air haptic interaction with a floating virtual screen. In *Proceedings of the 27th annual ACM symposium on User Interface Software and Technology*, pages 663–667, 2014.

M. Obrist, S. A. Seah, and S. Subramanian. Talking about tactile experiences. In *Proceedings of the SIGCHI Conference on Human Factors in Computing Systems*, pages 1659–1668, 2013.

M. Obrist, S. Subramanian, E. Gatti, B. Long, and T. Carter. Emotions mediated through mid-air haptics. In *Proceedings of the 33rd Annual ACM Conference on Human Factors in Computing Systems*, pages 2053–2062, 2015.

Y. Ochiai, K. Kumagai, T. Hoshi, J. Rekimoto, S. Hasegawa, and Y. Hayasaki. Fairy lights in femtoseconds: aerial and volumetric graphics rendered by focused femtosecond laser combined with computational holographic fields. *ACM Transactions on Graphics (TOG)*, 35(2):1–14, 2016.

S. Okamoto, H. Nagano, and Y. Yamada. Psychophysical dimensions of tactile perception of textures. *IEEE Transactions on Haptics*, 6(1):81–93, 2012.

C. Pacchierotti, S. Sinclair, M. Solazzi, A. Frisoli, V. Hayward, and D. Prattichizzo. Wearable haptic systems for the fingertip and the hand: taxonomy, review, and perspectives. *IEEE Transactions on Haptics*, 10(4):580–600, 2017.

M. A. Plaisier, W. M. B. Tiest, and A. M. Kappers. Salient features in 3-d haptic shape perception. *Attention, Perception, & Psychophysics*, 71(2):421–430, 2009.

A. Price and B. Long. Fibonacci spiral arranged ultrasound phased array for mid-air haptics. In *2018 IEEE International Ultrasonics Symposium (IUS)*, pages 1–4. IEEE, 2018.

A. Pusch and A. Lécuyer. Pseudo-haptics: from the theoretical foundations to practical system design guidelines. In *Proceedings of the 13th International Conference on Multimodal Interfaces*, pages 57–64, 2011.

G. Reardon, Y. Shao, B. Dandu, W. Frier, B. Long, O. Georgiou, and Y. Visell. Cutaneous wave propagation shapes tactile motion: Evidence from air-coupled ultrasound. In *2019 IEEE World Haptics Conference (WHC)*, pages 628–633. IEEE, 2019.

T. J. Royston, Z. Dai, R. Chaunsali, Y. Liu, Y. Peng, and R. L. Magin. Estimating material viscoelastic properties based on surface wave measurements: A comparison of techniques and modeling assumptions. *The Journal of the Acoustical Society of America*, 130(6):4126–4138, 2011.

I. Rutten, W. Frier, L. Van den Bogaert, and D. Geerts. Invisible touch: How identifiable are mid-air haptic shapes? In *Extended Abstracts of the 2019 CHI Conference on Human Factors in Computing Systems*, pages 1–6, 2019.

H. P. Saal, B. P. Delhaye, B. C. Rayhaun, and S. J. Bensmaia. Simulating tactile signals from the whole hand with millisecond precision. *Proceedings of the National Academy of Sciences*, 114(28):E5693–E5702, 2017.

O. Schneider, K. MacLean, C. Swindells, and K. Booth. Haptic experience design: What hapticians do and where they need help. *International Journal of Human-Computer Studies*, 107:5–21, 2017.

O. S. Schneider, A. Israr, and K. E. MacLean. Tactile animation by direct manipulation of grid displays. In *Proceedings of the 28th Annual ACM Symposium on User Interface Software & Technology*, pages 21–30, 2015.

M. Settnes and H. Bruus. Forces acting on a small particle in an acoustical field in a viscous fluid. *Physical Review E*, 85(1):016327, 2012.

G. Shakeri, E. Freeman, W. Frier, M. Iodice, B. Long, O. Georgiou, and C. Andersson. Three-in-one: Levitation, parametric audio, and mid-air haptic feedback. In *Extended Abstracts of the 2019 CHI Conference on Human Factors in Computing Systems*, pages 1–4, 2019.

Y. Shao, V. Hayward, and Y. Visell. Spatial patterns of cutaneous vibration during whole-hand haptic interactions. *Proceedings of the National Academy of Sciences*, 113(15):4188–4193, 2016.

L. Skedung, M. Arvidsson, J. Y. Chung, C. M. Stafford, B. Berglund, and M. W. Rutland. Feeling small: exploring the tactile perception limits. *Scientific Reports*, 3(1):1–6, 2013.

R. Sodhi, I. Poupyrev, M. Glisson, and A. Israr. Aireal: interactive tactile experiences in free air. *ACM Transactions on Graphics (TOG)*, 32(4):1–10, 2013.

D. Spelmezan, D. R. Sahoo, and S. Subramanian. Sparkle: Towards haptic hoverfeedback with electric arcs. In *Proceedings of the 29th Annual Symposium on User Interface Software and Technology*, pages 55–57, 2016.

A. P. Sripati, S. J. Bensmaia, and K. O. Johnson. A continuum mechanical model of mechanoreceptive afferent responses to indented spatial patterns. *Journal of Neurophysiology*, 95(6):3852–3864, 2006.

P. Strohmeier and K. Hornbæk. Generating haptic textures with a vibrotactile actuator. In *Proceedings of the 2017 CHI Conference on Human Factors in Computing Systems*, pages 4994–5005, 2017.

R. Takahashi, K. Hasegawa, and H. Shinoda. Lateral modulation of midair ultrasound focus for intensified vibrotactile stimuli. In *Proceedings of Eurohaptics: International Conference on Human Haptic Sensing and Touch Enabled Computer Applications*, pages 276–288. Springer, 2018.

M. Y. Tsalamlal, P. Issartel, N. Ouarti, and M. Ammi. Hair: Haptic feedback with a mobile air jet. In *2014 IEEE International Conference on Robotics and Automation (ICRA)*, pages 2699–2706. IEEE, 2014.

A. Vallbo, H. Olausson, J. Wessberg, and N. Kakuda. Receptive field characteristics of tactile units with myelinated afferents in hairy skin of human subjects. *The Journal of Physiology*, 483(3):783–795, 1995.

A. B. Vallbo, R. S. Johansson, et al. Properties of cutaneous mechanoreceptors in the human hand related to touch sensation. *Human Neurobiology*, 3(1):3–14, 1984.

A. B. Vallbo, K.-E. Hagbarth, and B. G. Wallin. Microneurography: how the technique developed and its role in the investigation of the sympathetic nervous system. *Journal of Applied Physiology*, 96(4):1262–1269, 2004.

Y. Vardar, B. Güçlü, and C. Basdogan. Effect of waveform on tactile perception by electrovibration displayed on touch screens. *IEEE Transactions on Haptics*, 10 (4):488–499, 2017.

R. T. Verrillo. Effect of contactor area on the vibrotactile threshold. *The Journal of the Acoustical Society of America*, 35(12):1962–1966, 1963.

R. T. Verrillo. Vibrotactile thresholds measured at the finger. *Perception & Psychophysics*, 9(4):329–330, 1971.

M. B. Wagner, M. G. J. Gerling, and J. Scanlon. Validation of a 3-d finite element human fingerpad model composed of anatomically accurate tissue layers. In *2008 Symposium on Haptic Interfaces for Virtual Environment and Teleoperator Systems*, pages 101–105. IEEE, 2008.

Q. Wang and V. Hayward. Compact, portable, modular, high-performance, distributed tactile transducer device based on lateral skin deformation. In *2006 14th Symposium on Haptic Interfaces for Virtual Environment and Teleoperator Systems*, pages 67–72. IEEE, 2006.

Q. Wang and V. Hayward. In vivo biomechanics of the fingerpad skin under local tangential traction. *Journal of Biomechanics*, 40(4):851–860, 2007.

A. I. Weber, H. P. Saal, J. D. Lieber, J.-W. Cheng, L. R. Manfredi, J. F. Dammann, and S. J. Bensmaia. Spatial and temporal codes mediate the tactile perception of natural textures. *Proceedings of the National Academy of Sciences*, 110(42): 17107–17112, 2013.

E. H. Weber and H. E. Ross. *The sense of touch*. Academic Press for [the] Experimental Psychology Society, 1978.

M. Wiertlewski and V. Hayward. Mechanical behavior of the fingertip in the range of frequencies and displacements relevant to touch. *Journal of Biomechanics*, 45 (11):1869–1874, 2012.

G. Wilson, T. Carter, S. Subramanian, and S. A. Brewster. Perception of ultrasonic haptic feedback on the hand: localisation and apparent motion. In *Proceedings of the SIGCHI Conference on Human Factors in Computing Systems*, pages 1133–1142, 2014.

J. Z. Wu, R. G. Dong, S. Rakheja, A. Schopper, and W. Smutz. A structural fingertip model for simulating of the biomechanics of tactile sensation. *Medical Engineering & Physics*, 26(2):165–175, 2004.

M. Z. Yıldız, I. Toker, F. B. Özkan, and B. Güçlü. Effects of passive and active movement on vibrotactile detection thresholds of the pacinian channel and forward masking. *Somatosensory & Motor Research*, 32(4):262–272, 2015.

M. Zhang and A. Mak. In vivo friction properties of human skin. *Prosthetics and Orthotics International*, 23(2):135–141, 1999.